NAVAL POSTGRADUATE SCHOOL
Monterey, California

THESIS

EFFECTS OF SHORT CRESTED SEAS ON THE MOTIONS OF A TROLLEY INTERFACE FOR SHIP-TO-SHIP CARGO TRANSFER

by

Chong Keng Shin

March 2003

Thesis Advisor: Fotis A. Papoulias

Approved for public release; distribution is unlimited.

THIS PAGE INTENTIONALLY LEFT BLANK

REPORT DOCUMENTATION PAGE		*Form Approved OMB No. 0704-0188*

Public reporting burden for this collection of information is estimated to average 1 hour per response, including the time for reviewing instruction, searching existing data sources, gathering and maintaining the data needed, and completing and reviewing the collection of information. Send comments regarding this burden estimate or any other aspect of this collection of information, including suggestions for reducing this burden, to Washington headquarters Services, Directorate for Information Operations and Reports, 1215 Jefferson Davis Highway, Suite 1204, Arlington, VA 22202-4302, and to the Office of Management and Budget, Paperwork Reduction Project (0704-0188) Washington DC 20503.

1. AGENCY USE ONLY *(Leave blank)*	2. REPORT DATE March 2003	3. REPORT TYPE AND DATES COVERED Master's Thesis
4. TITLE AND SUBTITLE: Effects Of Short Crested Seas On The Motions Of A Trolley Interface For Ship-To-Ship Cargo Transfer		5. FUNDING NUMBERS
6. AUTHOR (S) Chong Keng Shin		
7. PERFORMING ORGANIZATION NAME(S) AND ADDRESS(ES) Naval Postgraduate School Monterey, CA 93943-5000		8. PERFORMING ORGANIZATION REPORT NUMBER
9. SPONSORING / MONITORING AGENCY NAME(S) AND ADDRESS(ES)		10. SPONSORING/MONITORING AGENCY REPORT NUMBER
11. SUPPLEMENTARY NOTES: The views expressed in this thesis are those of the author and do not reflect the official policy or position of the U.S. Department of Defense or the U.S. Government.		
12a. DISTRIBUTION / AVAILABILITY STATEMENT Approved for public release; distribution is unlimited.		12b. DISTRIBUTION CODE

13. ABSTRACT *(maximum 200 words)*

This thesis sets out to explore the effects on the dynamic response of a hybrid trolley system employed in ship to shore cargo transfer operating in a realistic short crested irregular seaway. Compared to the uni-directional long crested waves, the multi-directional nature of short crested waves enhances the realism of the modeling. A standard cosine-squared spreading law was added to the two-parameter Bretschneider spectrum. The results provide added data on the coupled system response in all directions and moderate any overestimation that may be derived from simply using long crested waves.

14. SUBJECT TERMS Short-Crested Seas, Trolley Interface, WAMIT, Cosine Spreading Function, Wave Energy Dispersion, Bretschneider Spectrum, Motion Analysis.			15. NUMBER OF PAGES 116
			16. PRICE CODE
17. SECURITY CLASSIFICATION OF REPORT Unclassified	18. SECURITY CLASSIFICATION OF THIS PAGE Unclassified	19. SECURITY CLASSIFICATION OF ABSTRACT Unclassified	20. LIMITATION OF ABSTRACT UL

NSN 7540-01-280-5500

Standard Form 298 (Rev. 2-89)
Prescribed by ANSI Std. 239-18

THIS PAGE INTENTIONALLY LEFT BLANK

EFFECTS OF SHORT CRESTED SEAS ON THE MOTIONS OF A TROLLEY INTERFACE FOR SHIP-TO-SHIP CARGO TRANSFER

Chong Keng Shin
Major, Republic of Singapore Navy
B.S., U.S. Naval Academy, 1993

Submitted in partial fulfillment of the
requirements for the degree of

MASTER OF SCIENCE IN MECHANICAL ENGINEERING

from the

NAVAL POSTGRADUATE SCHOOL
March 2003

Author: Chong Keng Shin

Approved by: Fotis A. Papoulias
                Thesis Advisor

                Young W. Kwon
                Chair, Department of Mechanical Engineering

THIS PAGE INTENTIONALLY LEFT BLANK

ABSTRACT

This thesis sets out to explore the effects on the dynamic response of a hybrid trolley system employed in ship to shore cargo transfer operating in a realistic short crested irregular seaway. Compared to the uni-directional long crested waves, the multi-directional nature of short crested waves enhances the realism of the modeling. A standard cosine-squared spreading law was added to the two-parameter Bretschneider spectrum. The results provide added data on the coupled system response in all directions and moderate any overestimation that may be derived from simply using long crested waves.

THIS PAGE INTENTIONALLY LEFT BLANK

TABLE OF CONTENTS

THIS PAGE INTENTIONALLY LEFT BLANK

LIST OF FIGURES

Simulation Results:

Higher Order Spreading Function : Cosine^6 Spreading

Higher Order Spreading Function : Cosine[8] Spreading

Comparison Between Cosine2 And Cosine8 Dispersion.

<u>Transfer Rate Reduction.</u>

LIST OF TABLES

xvi

ACKNOWLEDGEMENTS

I.   INTRODUCTION

A.   OVERVIEW OF SHIP TO SHORE CARGO TRASFER USING THE TROLLEY SYSTEM

The US Marine Corp doctrine of Operational Maneuver from the Sea(OMFTS) uses the sea as maneuver space to bring the troops as close as possible to the objective. Exploiting the sea as battle space, the enemy is force to defend a vast area, providing the MAGTF an opportunity for deeper power projection, ref (1). A key tenet to OMFTS is the conduct of Ship-To-Objective-Maneuver(STOM), which refers to the direct movement of personnel and equipment from the ship to the objective without requiring a beachhead to be established. STOM aims at thrusting combat units in a fighting formation in sufficient strength against the objective to successfully accomplish the mission. It bridges the capability gap by facilitating rapid and unfettered access for the US military to advance from the sea to shore without significant build up of a large logistic footprint ashore in the absence of friendly ports and airfields.

The new era of global uncertainties impose continual demands on the forward presence and force projection of the US military to operate in any place on the globe. While doctrinal concepts such as OMFTS and STOM are fundamental pillars to facilitate this, Joint Logistics-Over-Shore(JLOTS) doctrine is the Combat Service Support and Logistic equivalent to support this.

Key measure of effectiveness in the conduct of STOM include the mobility and responsiveness of the system to

deploy large concentration of forces from the sea to shore within a specified time period and in the most demanding operating environment. While transporting and delivering of logistical support by air remains the most expeditious option, current aerial lift capabilities limit the amount of logistics that can be transfer by this means. Deploying combat support and logistics via specially configured ships such as the CAPE-D Class, Large Medium Support Roll-On/Roll-Off(LMSR) ships retain higher transport factor that makes ship to shore transfer a comparatively more efficient option within the near future.

The process of loading and unloading of combat and logistic equipment onto interconnected floating causeway which are also known as the Roll-On/Roll-Off Discharge Facility (RRDF) is one of the most challenging and time demanding part of the ship to shore cargo transfer operation. The Roll-On/Roll-Off Discharge Facility (RRDF) is a series of connected floating causeway sections that is moored to the CAPE D ship. The RRDF serves as the floating platform and roadway from which heavy military equipment such as, HMMVs, trucks, wheel containers etc are moved from the ship's cargo hold via the ramp to the lighterage.

The ship to shore cargo transfer process typically takes place within 50nm from the coastline. In the normal mode of operation, the ramp of the ships open onto the RRDF and connection of the RRDF and the vehicles are driven from the ship onto the RRDF and then ferried to shore via the lighters. A schematic of the mooring plan layout is shown in figure (1). The entire ship to shore transfer system of using CAPE D's stern ramp connected to the floating RRDF

results in a physical system that is coupled mechanically and hydro-dynamically.
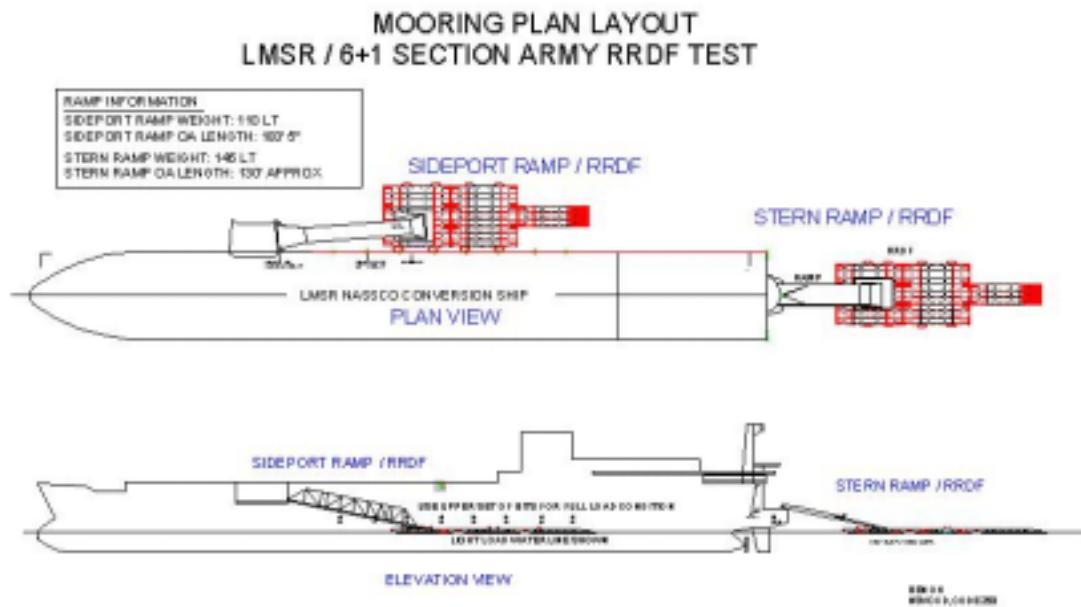
Figure 1.   LMSR and RRDF interface (After: NAVSEA, David Taylor)

This mode of operation has several limitations in that the coupled system response in seaway is high due to the lack of passive damping and severe motion of the RRDF and ship in high sea states. Excessive relative motions due to the effect of wind and waves may lead to delays or inefficiencies in the transfer from ship to RRDF causing undue operational pause that may seriously affect the larger operational outcome. Chaffing and wear between the RRDF to ship connections occurs and must be insulated by fendering material. Thus operational efficiency and transfer rates of cargo to shore can be severely affected. The maximum operating conditions is sea state three and throughput capacity of the transfer suffers greatly from

sea states two onwards. A motion compensation/mitigation interface system is needed between sealift ship ramps and the causeway Roll-On Roll-Off Discharge Facility (RRDF) platform.

In the design of complex coupled marine systems operating in the real world ocean environment, it is vital that the dynamic 6 degrees of freedom motion, surge, sway, heave, roll, pitch and yaw which governs the movement of the system should be evaluated in an accurate representation of the actual operating environment.

Under a study conducted by Carderock, NAVSEA, a motorized trolley system that connects to the RRDF and Stern Ramp is under development to provide "passive" isolation from the relative motions of the RRDF and CAPE D. A schematic drawing of the trolley unit is shown in figure (2). The trolley is powered by a motor and has the ability to compensate for motions between the two bridge structures that serve as physical linkages to the CAPE D stern ramp and the RRDF.
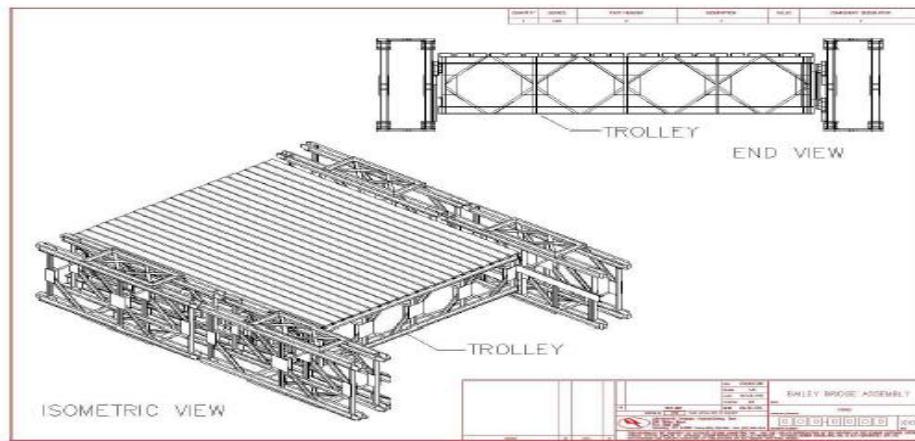
Figure 2.   Isometric drawing of the Trolley Interface mounted on top of CAPE D's stern ramp. (From: NAVSEA)

4

The Roll on Roll off Trolley Interface system allows the ship-to-platform RO/RO vehicle offload operation to continue in heavy weather by precluding torsion, bending and acceleration loads on the ramp for which it was not designed. The entire physical linkages that makes up the ship to shore transfer from the CAPE D to the RRDF will henceforth be refer to as the 'system' in this thesis.

Following work done by Higgins ref(2) which modeled the system operating in long crested seaway, this thesis will augment the degree of realism in modifying the environmental modeling to simulate the system operating in a multi-directional uni-modal short crested seaway.

THIS PAGE INTENTIONALLY LEFT BLANK

I. WAVE SPECTRA

A. WAVE SPECTRA ANALYSIS

The response of the system floating in the seaway is dependent on the wave environment and its motion characteristics. This chapter will provide a brief overview of wave spectrum as a representation of the distribution of the wave energy as a function of the wave frequency. It will address the significance of the realism afforded by modeling the system operating in a realistic environment comprising of short crested seaway where a directional spreading function is introduced.

Waves in nature are caused by disturbances to the ocean media, these disturbances are generally categorized into wind generated, earthquakes or via the gravitational forces from the planetary motions of the sun and moon. While planetary forces drives tides and creates long period waves on the order of 12 to 24 hours, a significant segment of ocean waves are wind generated waves. The figure (3) shown below illustrate the typical wave energy due to the different modes of wave generation, it also indicates restoring forces which tends to dampen out the waves and tries to restores the ocean to equilibrium.
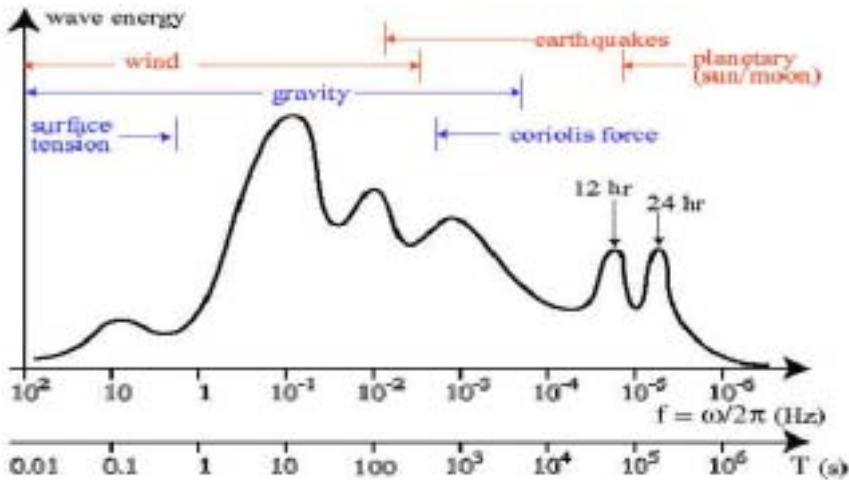
Figure 3.   Wave energy spectra. Red text indicates wave generation forces while Blue text indicates damping/restoring forces. (From: Techet)

The occurrence and severity of winds are random in nature and wind generated waves can be further categorized into seas and swell. A sea is a series of wave trains that are produced as a result of the prevailing local wind field acting on the wave surface and a swell is compose of waves that have traveled out of their propagating area. The wave periods are in the order of 5 to 15 seconds and they are highly irregular and multi directional. During the course of traveling the shorter waves are overtaken by the larger waves and this result in trains of longer and more regular waves of wavelengths 6-7 times larger than in irregular seas. While realizing that wind generated wave falls into both regimes of seas and swell, within the context of the operating environment of the trolley interface, this thesis will focus on the modeling of wind generated short crested waves and compare the dynamic response of the system to that observed in long crested seas.

The solution to the Laplace potential flow equation
$\dfrac{\partial \phi^2}{\partial x^2} + \dfrac{\partial \phi^2}{\partial y^2} = 0$ provides the basis for the Linear Wave Theory, subject to the boundary conditions imposed by uniform atmospheric pressure exerted on the fluid at the free surface and zero vertical velocity water particle velocity at the bottom. A depiction of the 2-dimensional wave theory is shown in figure (4).
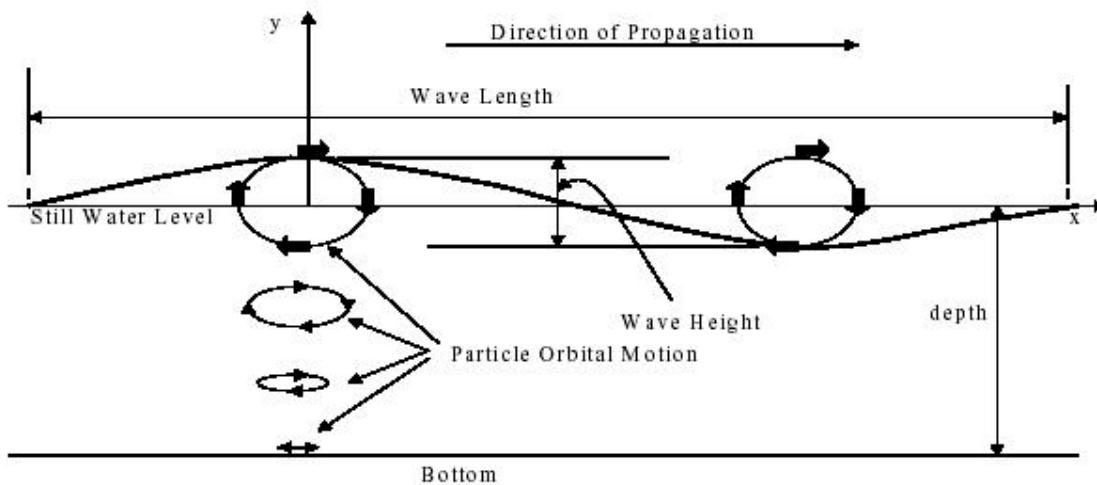
 Figure 4.   Depiction of 2-D Linear Wave Theory (From: Holmes P.)

The solution for the potential function in equation(1) is satisfied by the 2D velocity potential expression derived in ref (3):

$$\phi(x,y,t) = \left(\frac{gHT}{4\pi}\right) \left[\frac{\cosh\left[(\frac{2\pi}{L_w})(y+d) \right].\sin\left[2\pi(\frac{x}{L_w} - \frac{t}{T}) \right]}{\cosh(\frac{2\pi d}{L_w})} \right] \qquad (1)$$

where the horizontal, u_x and vertical water particle, v_y velocities for irrotational flow can be further expanded

9

$$u_x = \frac{d\phi}{dx} = \left(\frac{\pi H}{T}\right) \left[\frac{\cosh\left[\left(\frac{2\pi}{L_w}\right)(y+d)\right].\cos\left[2\pi\left(\frac{x}{L_w}-\frac{t}{T}\right)\right]}{\sin\left(\frac{2\pi d}{L_w}\right)} \right] \tag{2}$$

$$v_y = \frac{d\phi}{dy} = \left(\frac{\pi H}{T}\right) \left[\frac{\sinh\left[\left(\frac{2\pi}{L_w}\right)(y+d)\right].\sin\left[2\pi\left(\frac{x}{L_w}-\frac{t}{T}\right)\right]}{\sinh\left(\frac{2\pi d}{L_w}\right)} \right] \tag{3}$$

such that the surface profile is simplified to its basic form shown in equation (4). This represents that simplified sinusoidal equation of the wave surface.

$$\zeta = v_y = \zeta_a \cos k\left(x - \frac{L_w t}{T}\right) \tag{4}$$

It is noted that water particle under linear waves reaches their maxima at the surface elevation and reduces in magnitude as depth increases and the two dimensional wave forms can also be described by

$$\zeta(x,y,t) = \zeta_a \cos\left[k\left(x\cos\beta + y\sin\beta\right) - \omega t + \varepsilon\right] \tag{5}$$

Where; ε = phase angle

β = wave direction in global coordinates

ω = wave frequency

Wave Number: $k = \frac{2\pi}{L_w} = \frac{\omega^2}{g}$

Wave Length: $L_w = 2\pi\frac{V_c^2}{g}$

10

Wave Period: $\quad T_w = \sqrt{\left(\dfrac{2\pi L_w}{g} \right)}$

Wave Variance: $\quad \langle \zeta^2 \rangle = \dfrac{1}{2} \zeta_a^2$

Wave celerity: $\quad V_c = \dfrac{L_w}{T} = \sqrt{\dfrac{g}{k}}$

Modeling our ocean environment using short term statistics; the total wave system that makes up an irregular seaway can be imagined as a composition of an infinite number of regular progressive waves each having its own definitive frequency, amplitude and random phase relationship to each other. The elevation of the surface sea surface can then be described as a superposition of an infinite amount of sinusoidal component waves is described by the equation (6). This is often equated to the more familiar form of a point spectrum for long crested seas as shown in equation (7).

$$\zeta(t) = \sum_i \zeta_a \cos(-\omega_i t + \varepsilon_i) \qquad (6)$$

$$\langle \zeta^2 \rangle = S(\omega) d\omega \qquad (7)$$

Hydrodynamic theory suggests that the total energy per wave per unit width of crest is a summation of the potential and kinetic of the wave as described below.

$$E = \dfrac{1}{8} \rho g \zeta^2 L_w \qquad (8)$$

The total energy of the wave spectra $\overline{E}$ is then the integral of the point spectrum over the range of wave frequencies:

$$\overline{E} = \int_0^\infty S(\omega)d\omega \qquad (9)$$

Over the years, numerous mathematical models describing different spectra have been formulated. Some of the more influential spectra include the single parameter Pierson Moskowitz Spectrum developed by the offshore industry for fully developed seas in the North Seas generated by local winds and the three parameters JONSWAP Spectrum developed for a limited fetch in the North Seas.

Another spectrum used extensively in the marine industry is the Bretshneider, $S_{BS}^+(\omega)$ two parameters wave spectrum. The Bretschneider Spectrum is chosen for this thesis following the recommendations of the 15th International Towing Tank Conference for it's relevance for use in modeling average sea conditions. Short crested seas are composed of many wave groups that represent a broad spectrum. In the ocean environment, theses waves are three-dimensional with different components traveling in different directions. Corrections to the uni-directional 2D long crested spectra by energy spreading will have to be made to achieve a more accurate 3D modeling of the wave spectra. The Bretschneider spectra shown in equation (10) is an empirical formula derived from the spectral analysis of the North Atlantic Ocean and it is a spectrum valid for fully developed seas that have a broader spectra peak that

12

caters for a wide range of single peaked wave spectra, it is therefore suitable for use in our modeling simulation. The spectrum is define by the significant wave height, the modal period(peak period) and the spectral type. Figure (5) shows a representation of the JONSWAP spectrum with the Bretschneider Spectrum, the former is akin to a distortion of the Bretschneider spectra but with sharper spectra peak and steeper wave slope.

$$S_{BS}^{+}(\omega) = \frac{1.25}{4} \frac{\omega_m^{4}}{\omega^{5}} \zeta^{2} e^{-1.25\left(\frac{\omega_m}{\omega}\right)^{4}}$$

(10)

Where,

Significant wave height, $H^{1/3} = \zeta$

Modal frequency, $\omega_m = 0.4\sqrt{\left(\frac{g}{\zeta}\right)}$
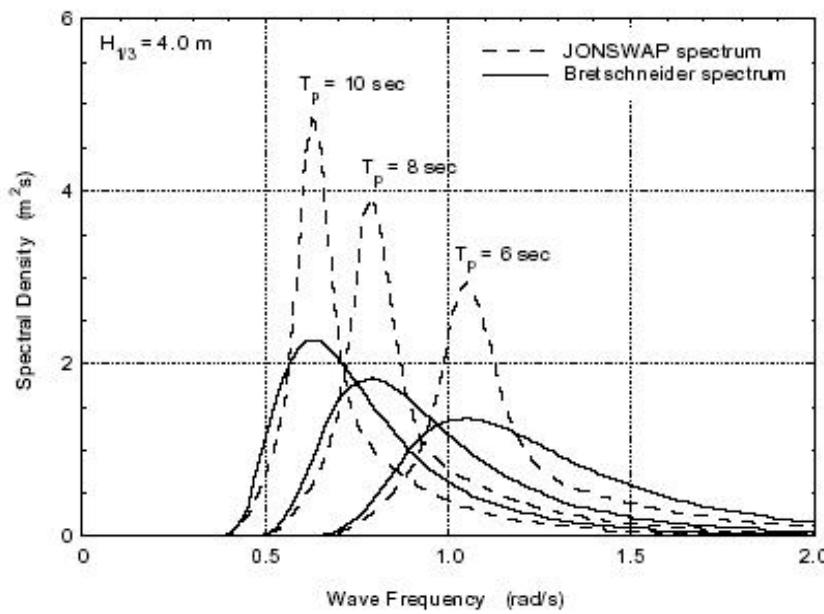
Figure 5.   Comparison of Jonswap and Bretschneider Spectra with significant wave height of 4 m (From. Journee)

13

Analysis of the natural seaway and the development of seaway responses as a non-steady, irregular process by means of stochastic process can be view as a higher level of approximation to reality than purely using the relevant deterministic form as described in ref(4). The sea surface is an ergodic and Gaussian random process with zero mean and the coupled response of the system can be represented as the superposition of linear wave systems. One way to analyze the whole process is to divide it into short time stationary processes and to assess the motions in these short time periods. Such a short time period is described by a seaway energy spectrum and is characterized by the average value of 1/3-highest wave elevation $H_{1/3}$ and an average wave period, T. Consequently, the response becomes statistic values. For the modeling in this report, wave heights from 0.5ft to 30ft(representing sea state 1 to 7) in increments of 0.5ft will be used to determine the system response.

B. SIGNIFICANCE OF SHORT CRESTED SEAS

Short crested seas like long crested seas are wind generated waves. Short crested waves are surface water waves, periodic in both the direction of propagation and in the transverse direction. However, wind generated wave energy do not necessarily propagate in just a unidirectional mode as suggested by long crested waves. Instead of a wave spectra simply represented by an accumulation of energy from all waves as a point spectrum, the wave energy is spread over various directions although the majority of the energy resides in the prominent wind direction. This gives rise to short crested waves that

14

provide a more accurate representation of a realistic seaway that is multi-directional and random in nature.

The modeling of the system operating a realistic short crested seaway bears significant importance because of the directionality aspect of real waves in the open oceans. Responses of complex and coupled marine system operating in seaway using just the unidirectional produce results, which tend to overestimate the response of the system. This may lead to significant over design and add to the overall cost and complexity of design of marine systems. In some cases, it may even result in the death knell of a project at the early design exploration stage. As a follow on to work done by ref(2), the wave trains in the MATLAB code in appendix A is modeled as moving in slightly different directions give a resultant pattern composed of "short-crested" waves as distinct from the "long-crested" waves when a single train is present.

Furthermore, simulations and modeling of marine systems in short crested seas using a directional spreading function also provides added data on the coupled dynamical responses of the system in non-prominent wind directions, which is inherently neglected in long crested wave modeling.

THIS PAGE INTENTIONALLY LEFT BLANK

III. MODELLING

A.   PHYSICAL MODELLING OF THE TROLLEY INTERFACE

The physical modeling of the trolley interface is similar to that used by Higgins in order to facilitate comparison of the motion effects in short crested and long crested seas. The RRDF and CAPE D will serve as the platform models for this analysis.

The connection of the ramp to the ship is modeled as a simple pin connection with 3 DOF in heave, pitch and roll motions. The trolley is mounted on the ramp and attached to the side bridge structure that dictates the plane angle on the surface of the trolley. Four points demarcating the extreme corners of the trolley interface at both the CAPE D and RRDF ends have been specified. For the purpose of the simulation, a trolley length of 100ft is assumed. The distance athwart ship from the CAPE D's center of gravity to the near end at point (1) of the trolley interface is 300 ft while from point(2) to the RRDF end is 20ft. Transversely, point(1) and point(2) is 10ft from the centerline of the trolley interface as shown in figure(6).
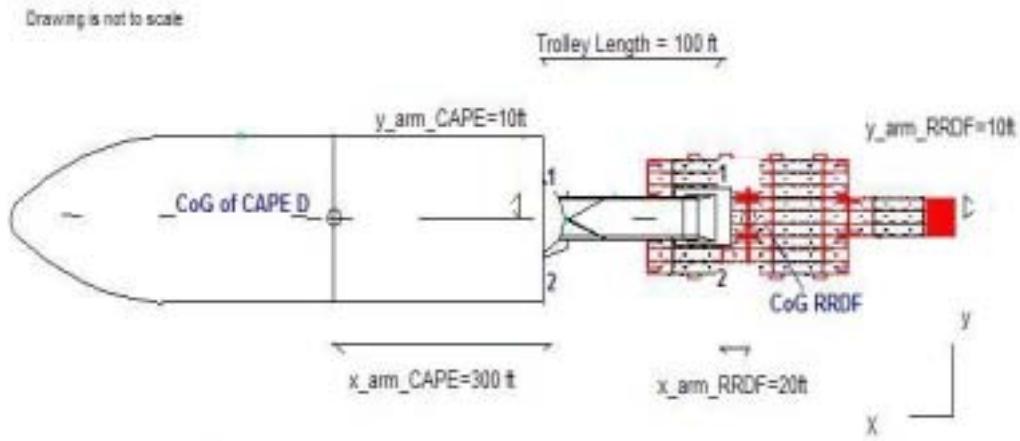
Figure 6.   Physical Dimensions of the moment arms of the trolley from the center of gravity of the CAPE D and the RRDF.
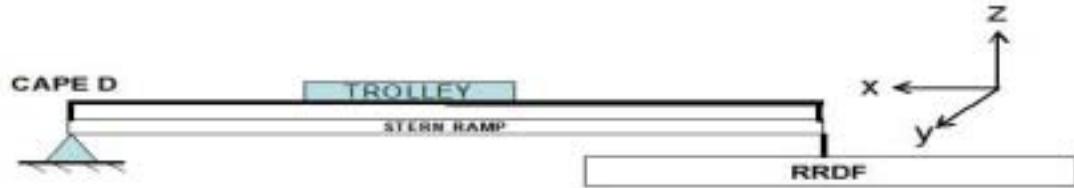
Figure 7.   Physical Model of Trolley Interface

Through the six degree of freedom motions of the CAPE D and RRDF and using simple geometry, the motions of the trolley system define by the four points on the ends of the CAPE D and the RRDF can be determined. This is accomplished by extracting the complex modulus magnitude of the motions fro each frequency vector and multiplying them by the appropriate moment arms for both points (1) and (2). The three principal motions affecting the vertical motions are heave, roll and pitch. From the response amplitude operators, the vertical motion of point (1) and (2) can be determined as described in equation (11). Other critical

18

parameters such as the trolley's relative vertical angular displacement, the average trolley angle and average trolley twist shown in equation (12) and (13) respectively can also be determined.

$$
\begin{aligned}
VerticalMotion_{Trolleyangle}^{Point1}(i) = \{ & abs(Heave\_CAPED(i) - x\_armCAPED^{Point1}) \times abs(pitch\_CAPED(i)) - \\
& y\_arm\_CAPED^{Point1} \times abs(roll - CAPED(i)) - \{abs(heave\_RRDF(i) - \\
& x\_arm\_RRDF^{Point1} \times abs(pitch\_RRDF(i)\} - (y\_arm\_RRDF^{Point1} \\
& \times abs(roll\_RRDF(i)))\} / trolley_{length}
\end{aligned}
\tag{11}
$$

$$
AverageTrolleyAngle(i) = \frac{\left\{ VerticalMotion_{TrolleyangleRRDF}^{Point1}(i) + VerticalMotion_{TrolleyangleCAPED}^{Point1}(i) \right\}}{2}
\tag{12}
$$

$$
AverageTrolleyTwist(i) = \left\{ VerticalMotion_{TrolleyangleRRDF}^{Point1}(i) - VerticalMotion_{TrolleyangleCAPED}^{Point2}(i) \right\}
\tag{13}
$$

B. HYDRODAYNAMIC MODELLING OF TROLLEY INTERFACE

In general a spring-mass-damper system is able to model the hydrodynamic characteristics of a rigid body floating in a fluid medium. Ship motions are assessed based on the determination of the coefficients, exciting forces and moment amplitudes. For the case of the ship at sea, the standard description for the equations of motions for a vessel can be express as six simultaneous linear equations in the frequency domain as shown below in the form of equation (14).

$$
\sum_{k=1}^{6}(M_{jk} + A_{jk})\ddot{\eta}_k + \sum_{k=1}^{6} B_{jk}\dot{\eta}_k + \sum_{k=1}^{6} C_{jk}\eta_k = F_j^{H} e^{i\omega_o t} \qquad \text{j=1,2,..6} \tag{14}
$$

Where

A_{jk} = Hydrodynamic added mass terms

B_{jk} = Hydrodynamic damping terms

C_{jk} = Restoring forces and moments due to the net hydrostatic buoyancy effects of the ship motions.

$F_j^H = F_j^I + F_j^D$ = Hydrodynamic wave exciting forces and moments where;

F_j^I = complex amplitude of the wave exciting force and moments due to incident waves,

F_j^D = complex amplitude of the wave exciting force and moments due to diffracted waves.

The hydrodynamic coupling of the ship's stern ramp and RRDF with the trolley interface can be represented as a series of linear system of equations in 12x12 matrix whose solutions correspond to the amplitudes and phase lags for the heave and pitch movements and for the sway, yaw and roll motions of the coupled system as shown in equation (15), where upon solving for $\{\bar{\eta}\}$ leads to equation (17) where $\{\bar{\eta}\}$ is the solution vector to the 6 DOF motion.

$$\sum_{k=1}^{12}\left[-\omega_o^2(M_{jk}+A_{jk})+i\omega_o B_{jk}+C_{jk}\right]\bar{\eta}_k = F_j^H \tag{15}$$

$$\left(-\omega_o^2[M+A]+i\omega_o[B]+[C]\right)\{\bar{\eta}\}=\{F\} \tag{16}$$

$$\{\bar{\eta}\}=\left(-\omega_o^2[M+A]+i\omega_o[B]+[C]\right)^{-1}\{F\} \tag{17}$$

The Response Amplitude Operator(RAO) can be extracted to determine the, RAO that defines the six-degree of motions of CAPE D and the RRDF from their respective centers of gravity. Each 6x6 off-diagonal block represents the acceleration and velocity coupling that is interacting between the RRDF and CAPED. Via simple geometry elaborated

20

in the previous section, the motions of the trolley interface or any point on the aboard the ship and RRDF can be determined by the complex local amplitude of the motion of the given point.

To facilitate the modeling of the system coupled response and acquire the RAOs, the full three dimensional solver, Wave Analysis MIT(WAMIT) was used to determine the interaction effects of the floating bodies and account for wave diffraction of each individual body for 30 frequency vectors ranging from 0.3 to 2.5 rad/sec. The frequency range covers the scope of sea spectra energy. Further elaboration of the hydrodynamic modeling using WAMIT can be found in Ref(2).

C. ENVIRONMENTAL MODELLING OF SHORT CRESTED SEAS

The prediction of 2-D random long crested irregular seas using a probabilistic approach is represented in equation (6). Expanding on this, a 3-D short crested wave model that encompasses the random wave fields propagating simultaneously from widely different directions, giving rise to a directional wave spectrum is described by the following equation:

$$\zeta(x,y,t) = \sum_i \sum_j \zeta_a \cos\left[k_i \left(x\cos\beta_j + y\sin\beta_j \right) - \omega_i t + \varepsilon_{ij} \right] \tag{18}$$

And

$$\left\langle \zeta(t)^2 \right\rangle \equiv \overline{E} = \int_0^\infty \int_0^{2\pi} S(\omega, \beta) d\beta d\omega \tag{19}$$

21

Directional Energy Dispersion

The directional wave spectra $S(\omega,\theta)$ can be articulated as a product of the point spectrum $S(\omega)$ with the function representing the energy dispersion function, $D(\omega,\theta)$. Using Fourier series the new wave spectra $S(\omega,\theta)$ can be expressed as a summation of series of sines and cosines functions as shown in equation (20).

$$S(\omega,\theta) = \frac{a_o}{2} + \sum_{n=1}^{\infty}(a_n\cos n\theta + b_n\sin n\theta) = S(\omega)D(\omega,\theta) \tag{20}$$

Where

$$a_n = \frac{1}{\pi}\int_{-\pi}^{\pi} S(\omega,\theta)\cos n\theta d\theta$$
$$b_n = \frac{1}{\pi}\int_{-\pi}^{\pi} S(\omega,\theta)\sin n\theta d\theta \tag{21}$$

$$D(\omega,\theta) = \frac{1}{\pi}\left\{\frac{1}{2} + \sum_{n=1}^{\infty}(A_n\cos n\theta + B_n\sin n\theta)\right\} \tag{22}$$

The directional energy spreading function $D(\omega,\theta)$ in equation (22) now represents a state of wave energy as it is dispersing and does not correlate to a probability density function because of negative values. However for a given specified wave frequency, ω, the spreading function becomes a non-negative integral function, $D(\theta|\omega)$, such that $\int_{-\pi}^{\pi} D(\omega,\theta)d\theta = 1$ and $D(\theta|\omega)$ can be approximated as a probability density function. This correlation thus allows a probabilistic approach to estimating the effects due to the spreading functions.

The predominant operating environment where the ship to shore cargo trolley interface is envisaged to operate in is likely to experience insignificant swell as it will be

employed in an environment within 50 nm from the sheltered coastline. The Cosine Power Distribution (23) introduced by [Longuet-Higgins 1963][1] uses two free parameters to describe the uni-modal distribution of wave energy,

$$D(\theta) = A\cos^{2s}(\frac{\theta - \theta_o}{2})$$ (23)

Where,

θ_o = Angle of propagation of predominant wave energy

s = parameter associated with the width of distribution

A = normalization coefficient

A simplistic form of equation (24) with s=2 is recommended for estimation of the energy dispersion of the short crested seas is appropriate for this scenario.

$$D(\theta) = \frac{2}{\pi}\cos^2(\theta - \theta_o) \qquad \text{for} \quad -\frac{\pi}{2} < \theta < \frac{\pi}{2}$$ (24)

$D(\theta)$ is the cosine spreading function and represents moderate spreading of wave energy due to normal wave speed without the occurrence of swell. The short crested nature of natural random waves is modeled by distributing the energy over +/- 90° around the mean direction of wave propagation, θ_o. as shown in the figure below.

---

[1] Longuet-Higgins, M.S. , Ocean wave Spectra, Prentice Hall 1963
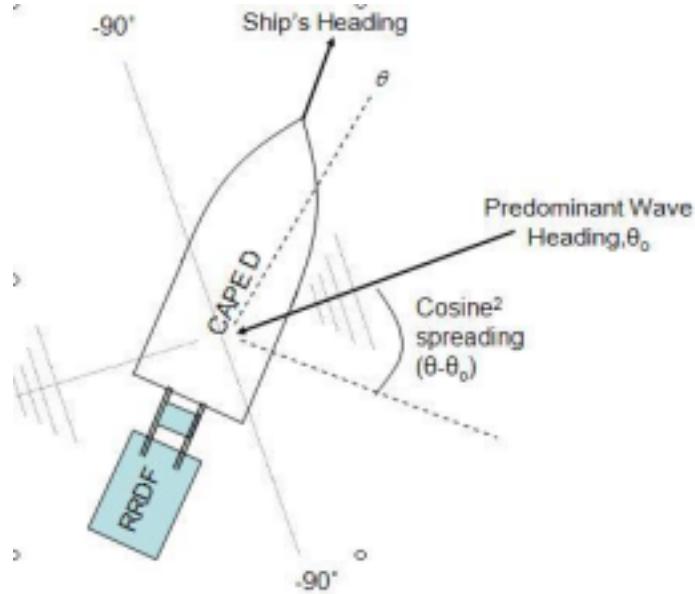
Figure 8.   Schematic of Short Crested wave with cosine squared energy spreading acting on the trolley interface.

A study conducted by the HR Wallingford Limited to determine the "FPSO response in long crested and short crested seas" suggest the used of the higher order cosine spreading functions as described in Table (1) for the following seaway description thus changing the width of distribution in shallow waters. These higher order cosine functions were incorporated into the MATLAB coding for simulation and the normalizing coefficient, A was modified to ensure that the integral of the energy spreading remains at the same throughout i.e. equal to one.

Spreading function	Description	Energy Dispersion
Short Crested $\cos^2(\theta-\theta_o)$	θ_o represents the mean wave direction. Such a spreading is appropriate for open wave generation.	$\int_{\frac{-\pi}{2}}^{\frac{\pi}{2}} D(\theta)d\theta = \int_{\frac{-\pi}{2}}^{\frac{\pi}{2}} A\cos^2(\frac{\theta-\theta_o}{2})d\theta = 1$ where $A = \frac{2}{\pi} = 0.6367$

Short Crested $\cos^6(\theta - \theta_o)$	Conditions for higher order cosine-spreading represents waves in shallower water, or narrower fetches.	$\int_{\frac{-\pi}{2}}^{\frac{\pi}{2}} D(\theta)d\theta = \int_{\frac{-\pi}{2}}^{\frac{\pi}{2}} A\cos^6(\frac{\theta - \theta_o}{2})d\theta = 1$ where $A = 1.0186$
Short Crested $\cos^8(\theta - \theta_o)$	For shallow water or narrow fetches.	$\int_{\frac{-\pi}{2}}^{\frac{\pi}{2}} D(\theta)d\theta = \int_{\frac{-\pi}{2}}^{\frac{\pi}{2}} A\cos^6(\frac{\theta - \theta_o}{2})d\theta = 1$ where $A = 1.1641$
Long Crested	Swell in long waves in shallow water.	

Table 1. Description of Spreading functions adopted for MATLAB simulations(After: HR Wallingford Limited)

For areas where swell and frequent wind changes are present, complex energy spreading functions such as *Misutyasu* formula which characterize a clover leaf spreading pattern and *Borgmann's* formula shown in equation (25) which describe a circular normal distribution of the energy, should be used

$$D(\omega, \theta) = \frac{1}{2\pi I_o(a)} \exp\{a\cos(\theta - \bar{\theta}\} \qquad (25)$$

Where

a = positive constant

$\bar{\theta}$ = angle of propagation of predominant wave energy

$I_o(\_)$ = modified Bessel function of the zero[th] order;

As pointed out, the Cosine Power Distribution is limited to uni-modal short crested seas, bi-modal sea states depicting multi directional seas during wind veering events or swell arriving from different sources can be

modeled using the Maximum Entropy Method as proposed by Healey. Wave energy dispersion due to the diffraction of the short crested waves around the RRDF and stern of the CAPED D is also not address. Both limitations in the environmental modeling are possible areas for future work.

Since the ship to shore transfer using the trolley interface is conducted in zero speed with no headway. The equation for wave directionality estimations can be directly applied without the need to determine the encounter frequency using the Doppler equation.

With the spreading function defined, the two parameter Bretschneider wave spectra in equation (10) is now combine with the energy dispersion modeling to derive the propagation and transformation of random, short-crested, wind generated waves;

$$S^+(\omega,\theta) = S^+_{BS}(\omega)D(\theta|\omega) \qquad (26)$$

$$S^+(\omega,\theta) = S^+_{BS}(\omega)D(\theta) = S^+_{BS}(\omega)\frac{2}{\pi}\cos^{2s}(\theta-\theta_o) \qquad (27)$$

This formulation is utilized in the MATLAB simulation. It allows the total amount of energy in the wave system, E to be preserved and remain unchanged from simply integrating a point spectrum using long crested waves and therefore serves to add realism to the modeling as elaborated in the previous section. This report will focus only on the cosine squared and higher order spreading functions applied to the Bretschneider and Pierson Moskowitz spectra.

D.   FORMULATION OF MATLAB SIMULATION

The linear system assumption allows the spectral density of any given response to be determined by multiplying the incident wave spectrum by the square of the response amplitude operator(RAO) of the desired response. The RAO can be thought of as a transfer function of the system, describing the amplitude and phase of the desired system response to regular incident waves acting on the system at the specific frequency. In practice, the RAO can be obtained experimentally via model testing in regular waves or analytically. As described in earlier sections, an analytical approach using WAMIT simulations was used to determine the RAO's for the system and the results incorporated into the MATLAB simulations to determine the system response in irregular short crested seas. Figure (9) illustrates the control theory representation of system response to irregular wave spectra input, while Figure (10) shows a similar representation in time domain.
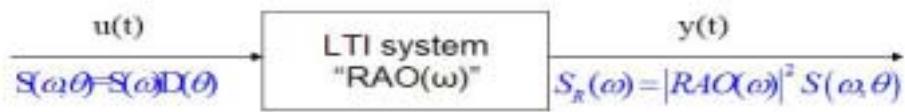
 Figure 9.   Control theory representation of transfer of wave spectra to dynamic system response.

27
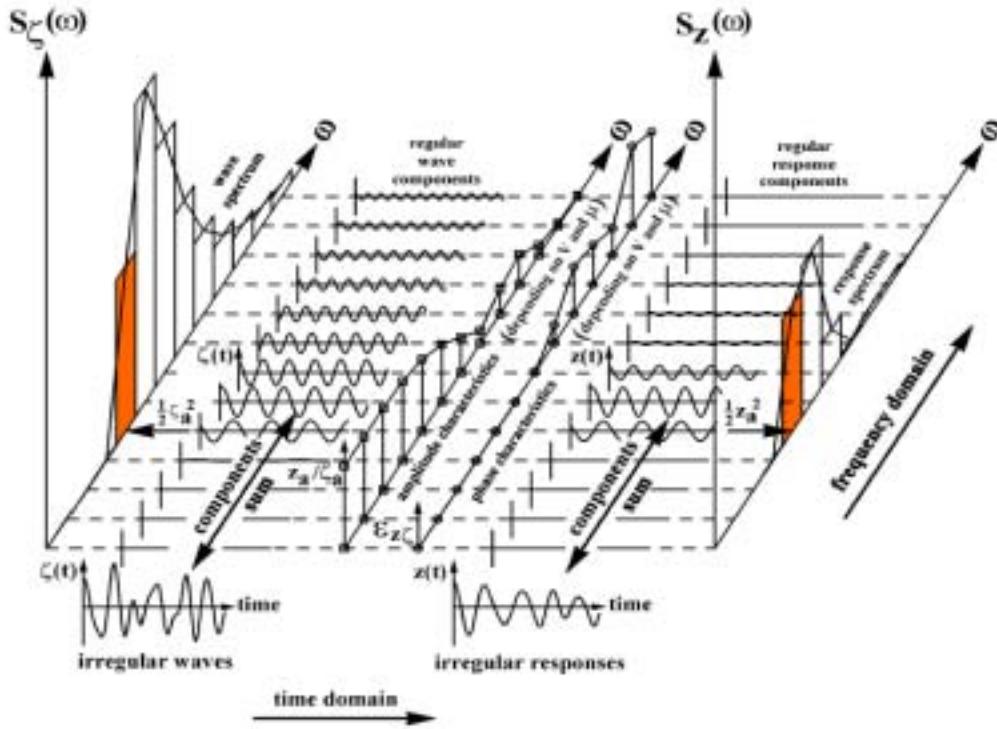
Figure 10.   Time domain representation of transfer of wave
spectra to dynamic system response (From Journee)

The wave amplitude at a series of discrete frequencies
defines the excitation wave spectrum. For each combination
of significant wave height, hence frequency, the systems
dynamic response amplitude operator is determined and used
as the ship excitation frequency.

In short crested sea spectra, the frequency domain
response of the coupled system is a random variable. The
system response statistics and wave statistics are similar
and can be computed by multiplying the wave spectra, $S^+(\omega,\theta)$
with the square of the RAO. The system dynamic response(S_R),
for a given input sea spectra at specific frequency is
represented by;

$$S_R(\omega) = \left|RAO(\omega)\right|^2 S_{BS}^+(\omega)D(\theta) = \left|RAO(\omega)\right|^2 S^+(\omega,\theta) \qquad (28)$$

The statistical prediction of the amplitudes of the system's response is determined by integrating over the entire frequency period given by the equation:

$$RMS^2 = \int\limits_{\theta}\int\limits_{\omega} S_R d\omega d\theta \qquad (29)$$

While the Root Mean Square(RMS) values of the response amplitudes is the square root of the area under the spectrum response curve indicated on the far right of figure (10).

Having developed the physical, hydrodynamic and environmental models necessary to shape the computer simulation of the ship to shore cargo transfer using the trolley interface, a flowchart schematic was formulated to guide the logical flow in MATLAB. The flow chart is enclosed in figure (11).

Obtained amplitude characteristics of system from WAMIT for 30 frequency vector 0.3 to 2.5 rad/s

ω_i

Select Pierson Moskowitz / Bretschneider Response S(ω)

Select order of Cosine Spreading Function

Select Significant Wave Ht, $H_{1/3}$ from 0.5ft to 30ft in increments of 0.5ft

$S(\omega_i),H_{1/3i}$

For each $\omega_i,H_{1/3}$

Select Ship's Heading, β

For each $\omega i,\beta i,\theta i,H_{1/3}$

Spreading angle, θ
(θ =i_beta= -90˚+ β to β+90˚)

Calculate Wave spectra with Spreading function S(ω ,θ)

Determine 6 DOF non-dimensional frequency domain response, RAO(ω)

Calculate system response
$S_R(\omega) = |RAO(\omega)|^2 S(\omega)D(\theta)$

Integrate Spectra response $S_R(\omega)$

Determine RMS response
$RMS^2 = \iint_{\theta\ \omega} S_R d\omega d\theta$

Obtained Polar Plots for the System Dynamic Response in Short Crested Seas

Figure 11.   Flow Chart of MATLAB Modeling to determine the system response to short crested seas.

In accordance with the flow chart describing the formulation of the MATLAB program, the amplitude characteristics of the coupled system were derived using WAMIT for 30 sets of frequencies vector from 0.3 to 2.5 rad/s. The MATLAB program extracted the amplitudes for the 6 DOF motions encountered by the system. Three sub-loop routines are embedded into each significant wave height calculation that increments from 0.5ft to 30ft, which is representative of sea states 1 to 7. For each wave height, the first sub-routine determines a wave heading, β ranging from 0° to 360° for 25 increments i.e. 15° per increment. Within this sub-loop, the energy dispersion routine is embedded within the β routine where it is spread over $-\dfrac{\pi}{2}$ to $\dfrac{\pi}{2}$ from each β heading. The response spectra calculated were integrated in 15° steps for 13 increments. The calculations are repeated for Pierson Moskowitz spectra and Bretschneider spectra with Modal periods of 5, 7.5, 10 and 12.5 seconds and for lower order, cosine squared to higher order cosine[8] spreading. Crucial parameters such as the average trolley angle and trolley twist were extracted for plotting as well as to determine the reduction in the rate of transfer of a single trolley pass in different sea states with different seaway spectra.

THIS PAGE INTENTIONALLY LEFT BLANK

IV. RESULTS

A.   SYSTEM RESPONSE TO SHORT CRESTED SEAS

The dynamic system response pertaining to the trolley roll motion and twist angle are the most critical initial parameters in assessing the viability of the trolley design. From the MATLAB simulations some of the more noteworthy observations are:

1.   Pierson Moskowitz Spectra

The differences in magnitudes of the trolley angle and trolley twist are higher in long crested seas compared to short crested seas. In particular, for the 90°-120° and 240°-270° quadrants i.e incident seas from the port and starboard beam, the trolley angles in long crested seas experience up to a maximum of 10% more motion than short crested seas. Similarly trolley twist magnitudes in short crested seas were in the region from 0-1.2° for all incident sea directions while long crested seas experience trolley twist up to 2° for sea directions 30° off the port/starboard bow and quarters.

2.   Bretschneider Spectra, Modal Period 5 seconds

The highest level of trolley angles and twist were experienced in long crested seas in a 30°-50° sector concentrated at the starboard beam. The asymmetry of the RRDF structure is likely to be the cause of the variation in port and starboard response. The highest difference in trolley twist for both seaways is approximately 35% in beam seas. A

comparison of cosine square and higher order cosine spreading functions indicates that although the shape and form of the dispersion was similar, higher Order cosine distribution encountered slightly higher magnitudes of level of trolley angle and trolley twist. The trolley angle motions were evenly disperse over all angles in short crested seas.

3.   Bretschneider Spectra, Modal Period 7.5 seconds.

As the modal period is increased to 7.5 seconds, the magnitude of the trolley angle is reduce, however there is almost doubling of the absolute magnitude of angular twist experienced by the trolley in both seaways at this modal period, indicating proximity to resonant frequency of the trolley interface. Comparatively, long crested seas encountered higher trolley twist up to a maximum of 4.56° in sea state 7 and this is confine to similar directional quadrants as described above. Maximum trolley twist angles up to 2.89° at sea state 7 were experienced in short crested seas but this was spread out over a large sector.

4.   Bretschneider Spectra, Modal Period 10 and 12.5 seconds.

It is observed that the magnitude of trolley responses for modal period of 10 seconds were similar to those observed for 5 seconds. There is only a maximum of 0.908° difference between the trolley twist angle in 5 and 10 seconds in short crested seas. As the modal period increases to 12.5 seconds, the shape of response in trolley twist and angle in short crested seas becomes increasingly circular.

Average Vertical Trolley Angle for Cosine² Spreading Function (deg)

Short Crested Seas - Pierson Moskowitz Spectra
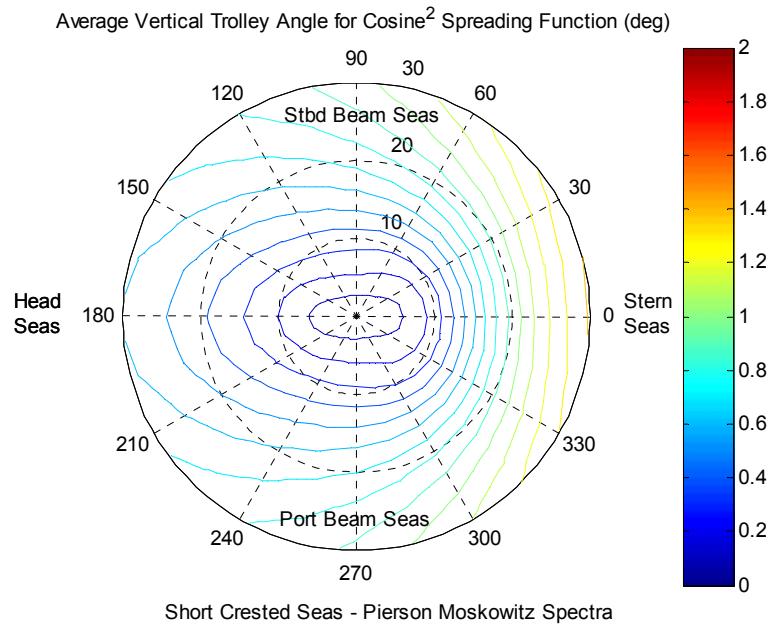
Figure 12.   Average Vertical Trolley Angle for Short Crested
Seas in Pierson Moskowitz Spectra

Average Vertical Trolley Angle (deg)

Long Crested Seas - Pierson Moskowitz Spectra
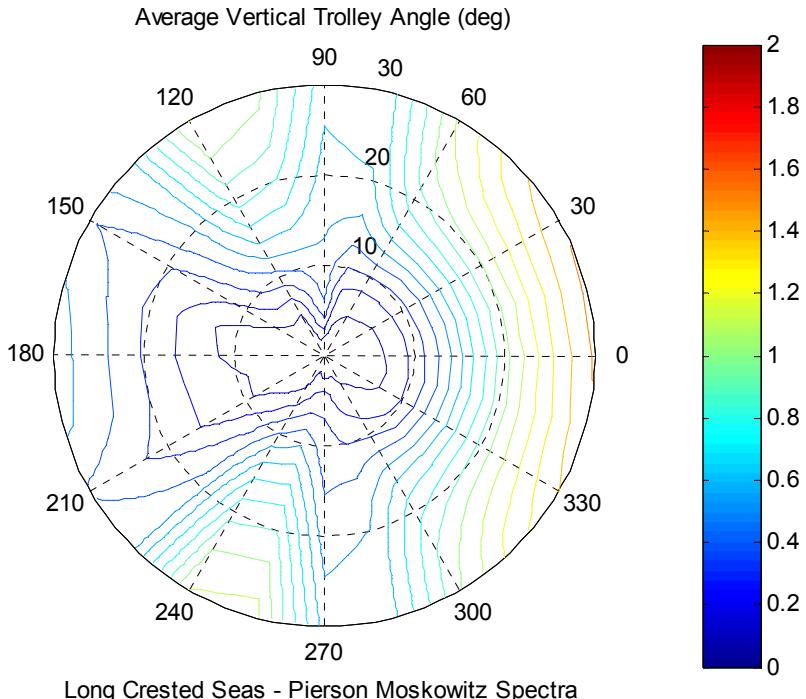
Figure 13.   Average Vertical Trolley Angle for Long Crested
Seas with Pierson Moskowitz Spectra

35

Average Vertical Trolley Twist for Cosine² Spreading Function (deg)

Short Crested Seas - Pierson Moskowitz Spectra
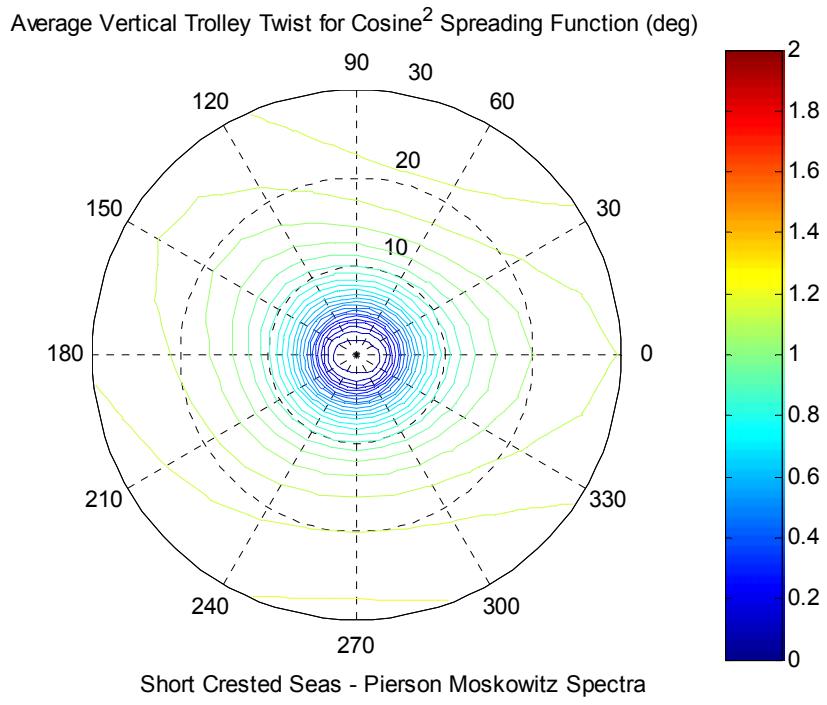
Figure 14.   Average Vertical Trolley Twist for Short Crested
Seas with Pierson Moskowitz Spectra

Average Vertical Trolley Twist (deg)

Long Crested Seas - Pierson Moskowitz Spectra
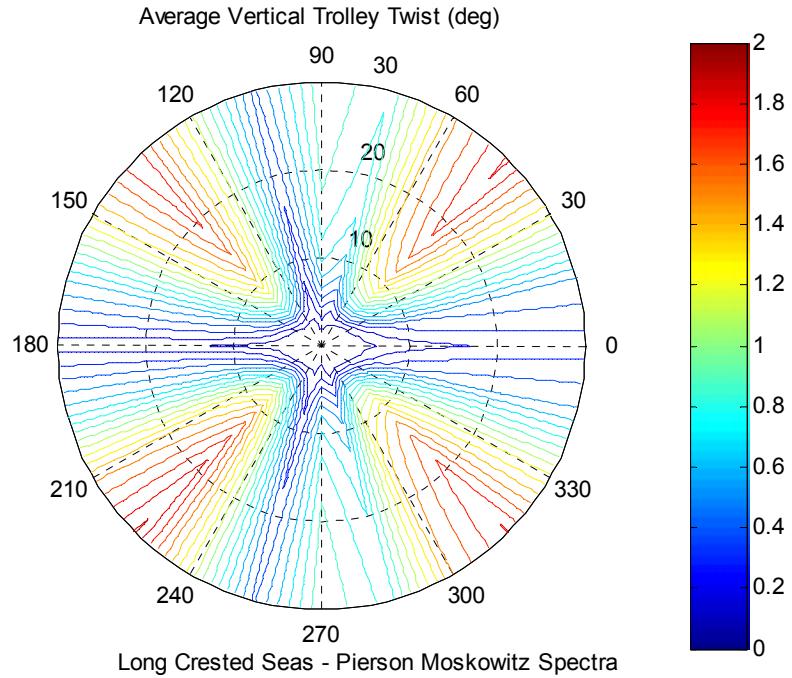
Figure 15.   Average Vertical Trolley Twist for Long Crested
Seas with Pierson Moskowitz spectra

36
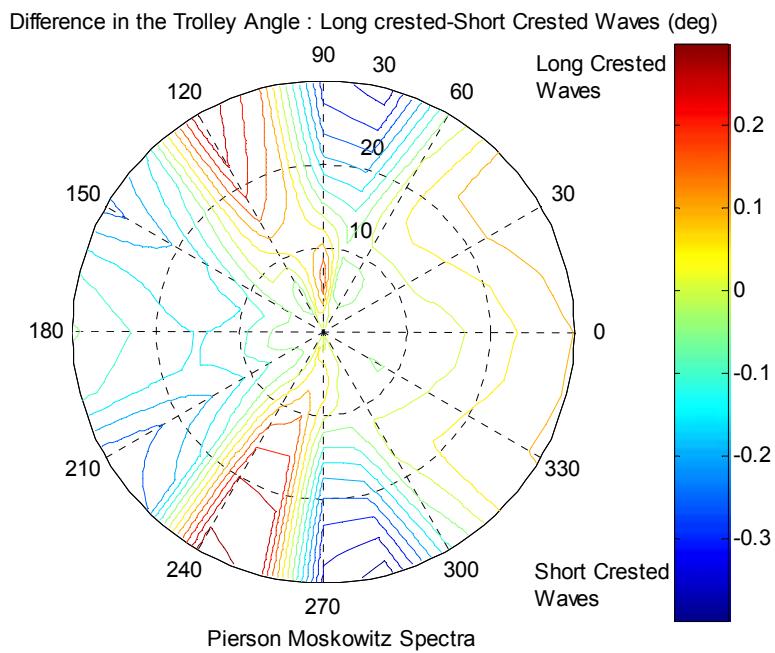
Figure 16.   Comparison of Average Vertical Trolley Angle for
Long Crested and Short Crested Seas with Pierson Moskowitz
spectra.
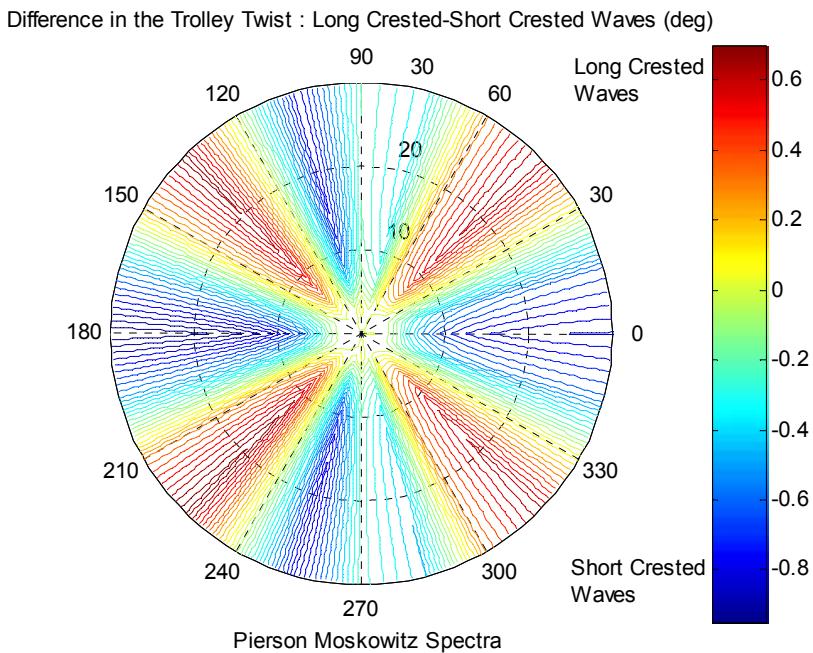
Figure 17.   Comparison of Average Vertical Trolley Twist for
Long Crested and Short Crested Seas with Pierson Moskowitz
spectra.

Average Vertical Trolley Angle for Cosine² Spreading Function (deg)

Short Crested Seas - Bretschneider Spectra Modal Period 5 secs
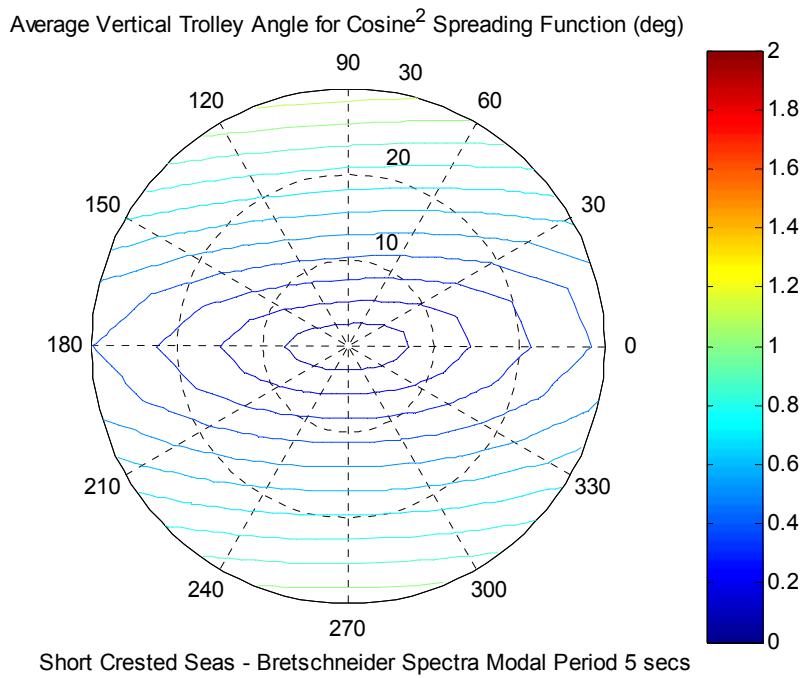
Figure 18.   Average Vertical Trolley Angle for Short Crested
Seas with Bretschneider Spectra and Modal Period 5 seconds

Average Vertical Trolley Angle (deg)

Long Crested Seas - Bretschneider Spectra, Modal Period 5 secs
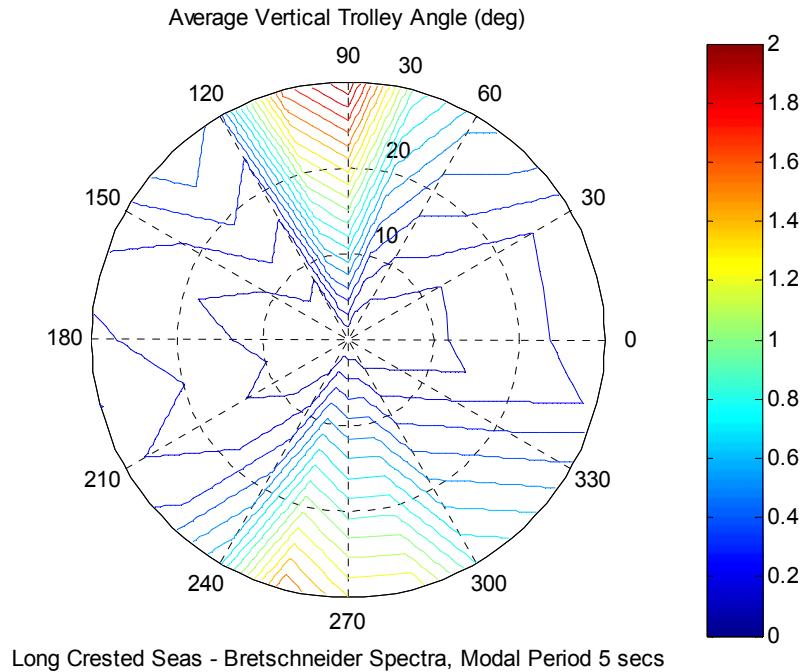
Figure 19.   Average Vertical Trolley Angle for Long Crested
Seas with Bretschneider Spectra and Modal Period 5 seconds

Average Vertical Trolley Twist for Cosine² Spreading Function (deg)

Short Crested Seas - Bretschneider Spectra, Modal Period 5secs
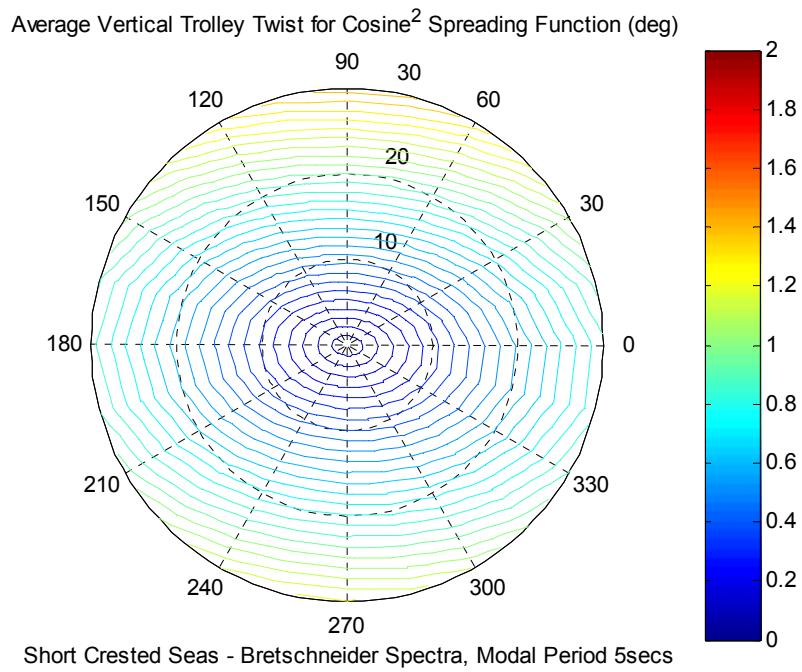
Figure 20.   Average Vertical Trolley Twist for Short Crested
Seas with Bretschneider Spectra and Modal Period 5 seconds

Average Vertical Trolley Twist (deg)

Long Crested Seas - Bretschneider Spectra, Modal Period 5 secs
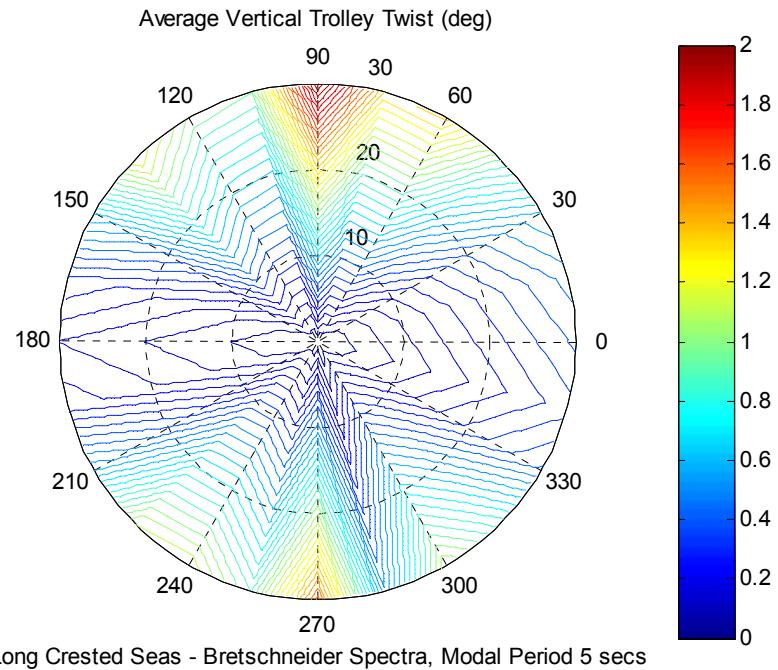
Figure 21.   Average Vertical Trolley Twist for Long Crested
Seas with Bretschneider Spectra and Modal Period 5 seconds

39

Difference in the Trolley Angle : Long Crested-Short Crested Waves (deg)

Bretschneider Spectra - Modal Period 5 sec
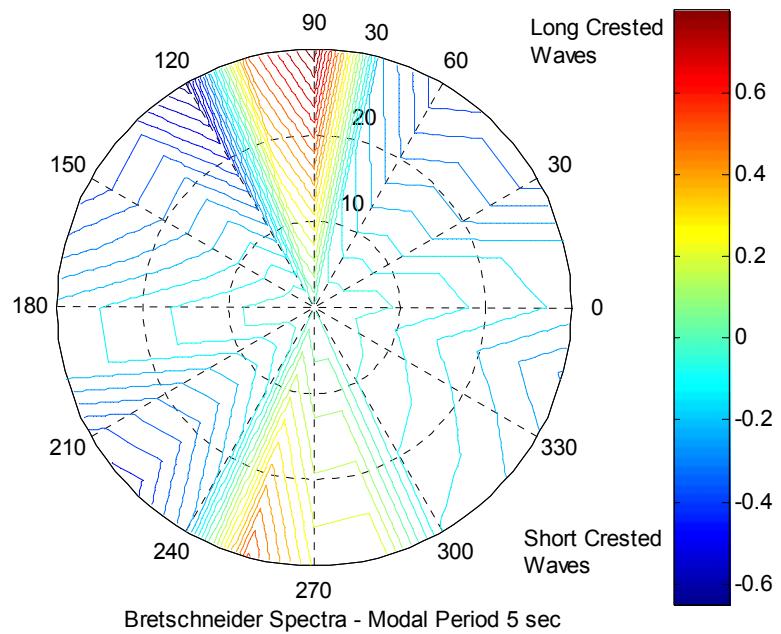
Figure 22.   Comparison of Average Vertical Trolley Angle for
Long Crested and Short Crested Seas with Bretschneider Spectra of
Modal Period 5 seconds

Difference in the Trolley Twist : Long Crested-Short Crested Waves (deg)

Brestchneider Spectra - Modal Period 5 sec
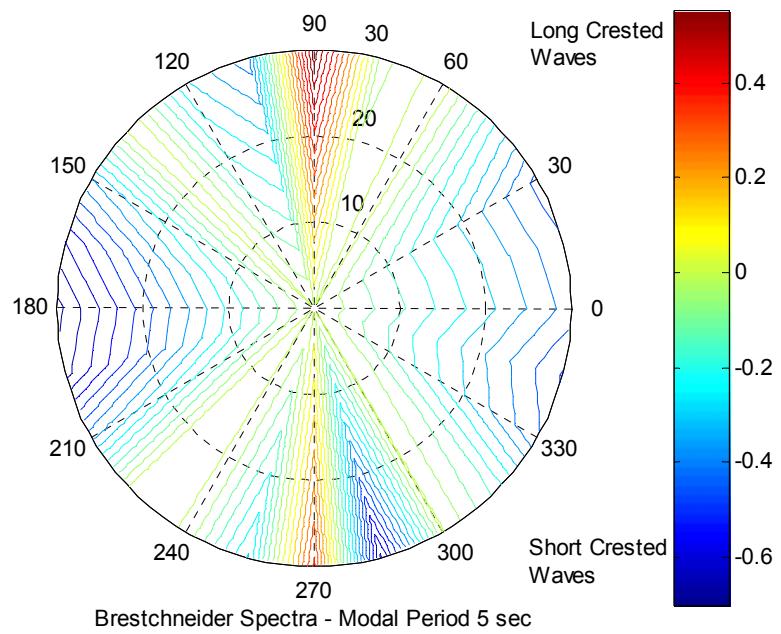
Figure 23.   Comparison of Average Vertical Trolley Twist for
Long Crested and Short Crested Seas with Bretschneider Spectra of
Modal Period 5 seconds

40

Average Vertical Trolley Angle for Cosine^2 Spreading Function (deg)

Short Crested Seas - Bretschneider Spectra, Modal Period 7.5 sec
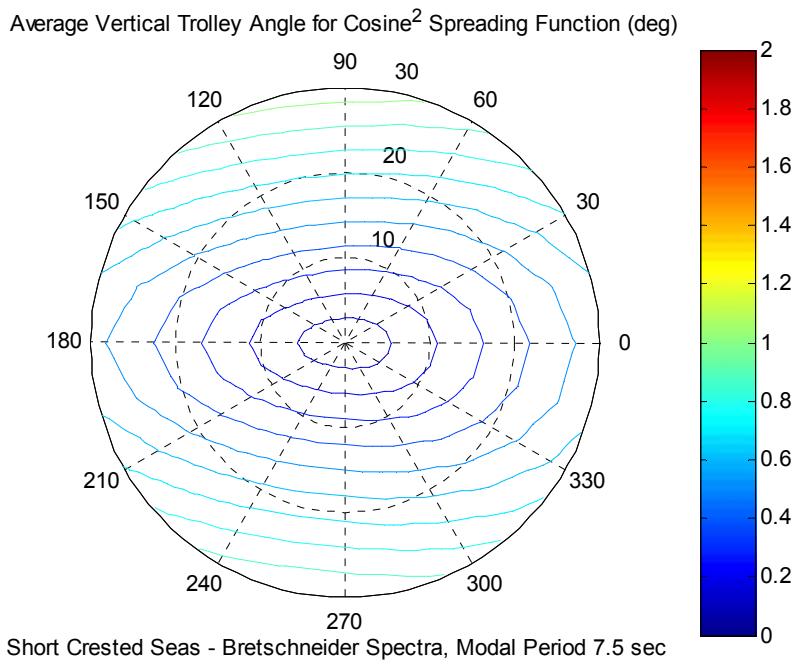
Figure 24.   Average Vertical Trolley Angle for Short Crested Seas with Bretschneider Spectra and Modal Period 7.5 seconds

Average Vertical Trolley Angle (deg)

Long Crested Seas - Bretschneider Spectra, Modal Period 7.5 secs
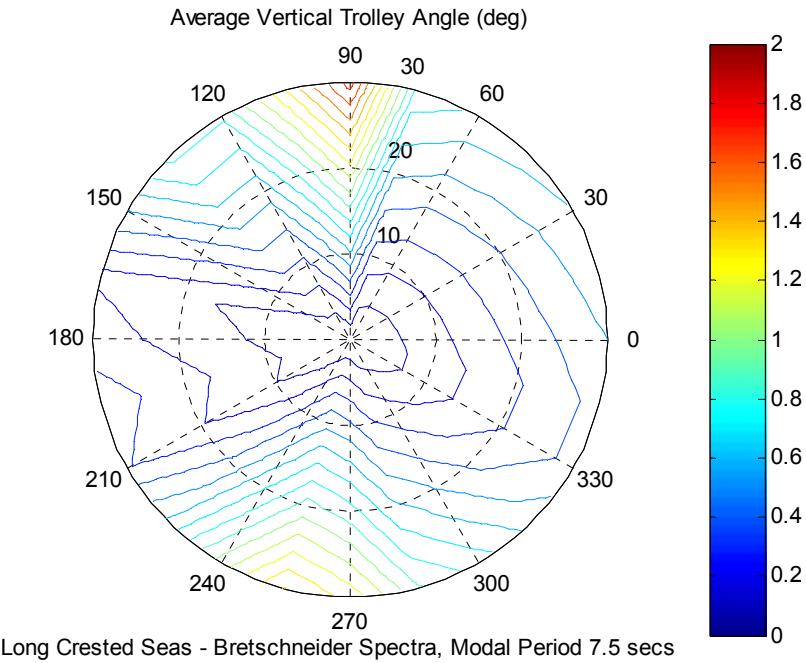
Figure 25.   Average Vertical Trolley Angle for Long Crested Seas with Bretschneider Spectra and Modal Period 7.5 seconds

41
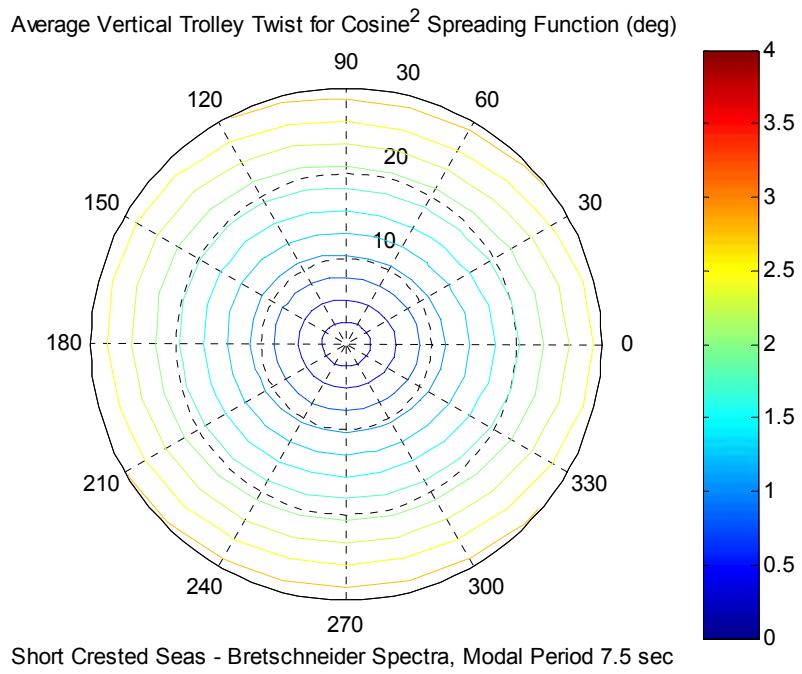
Figure 26.   Average Vertical Trolley Twist for Short Crested
Seas with Bretschneider Spectra and Modal Period 7.5 seconds
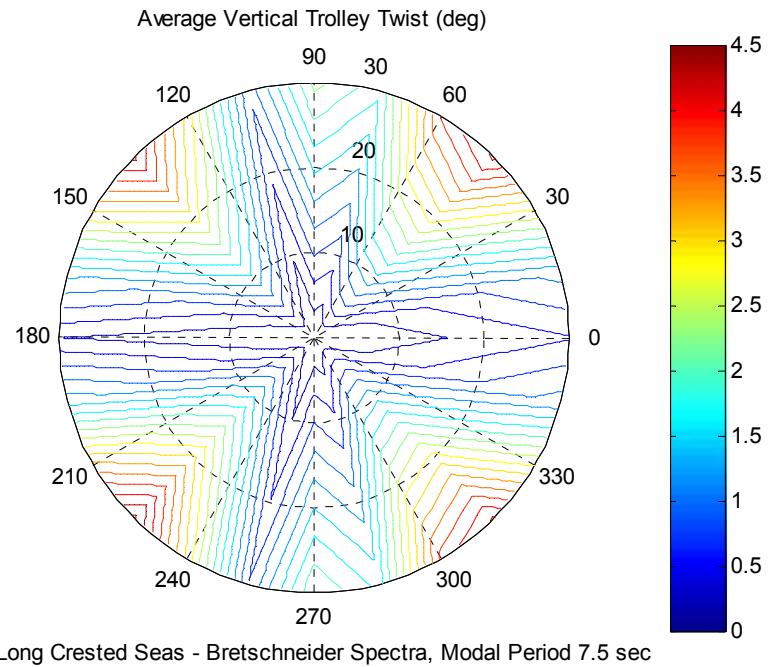
Figure 27.   Average Vertical Trolley Twist for Long Crested
Seas with Bretschneider Spectra and Modal Period 7.5 seconds.

Difference in the Trolley Angle : Long Crested-Short Crested Waves (deg)
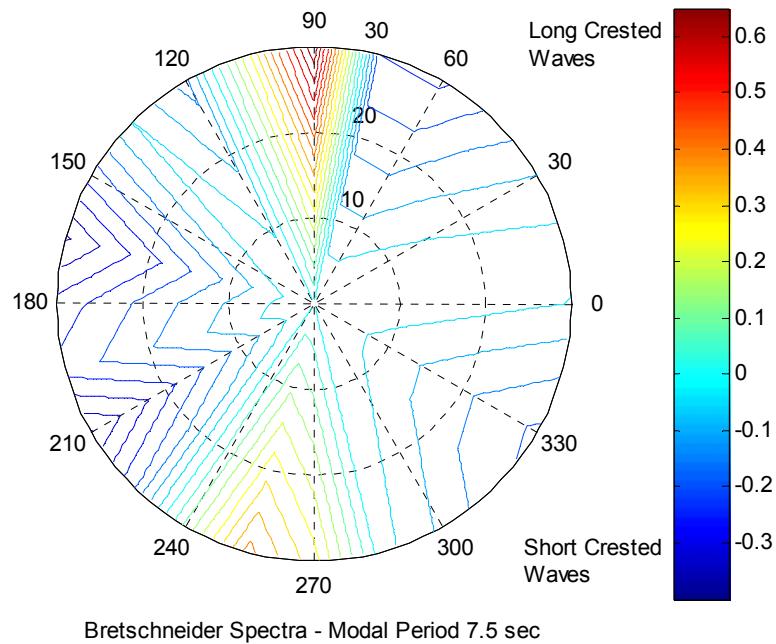
Bretschneider Spectra - Modal Period 7.5 sec

Figure 28.   Comparison of Average Vertical Trolley Angle for
Long Crested and Short Crested Seas with Bretschneider Spectra of
Modal Period 7.5 seconds.

Difference in the Trolley Twist : Long Crested-Short Crested Waves (deg)
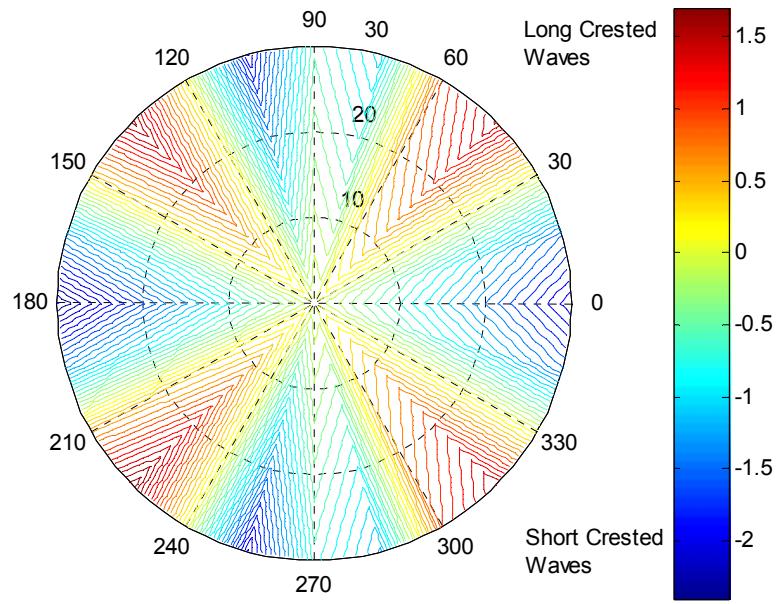
Bretschneider Spectra - Modal Period 7.5 sec

Figure 29.   Comparison of Average Vertical Trolley Twist for
Long Crested and Short Crested Seas with Bretschneider Spectra of
Modal Period 7.5 seconds.

43

Average Vertical Trolley Angle for Cosine² Spreading Function (deg)

Short Crested Seas - Bretschneider Spectra, Modal Period 10 sec
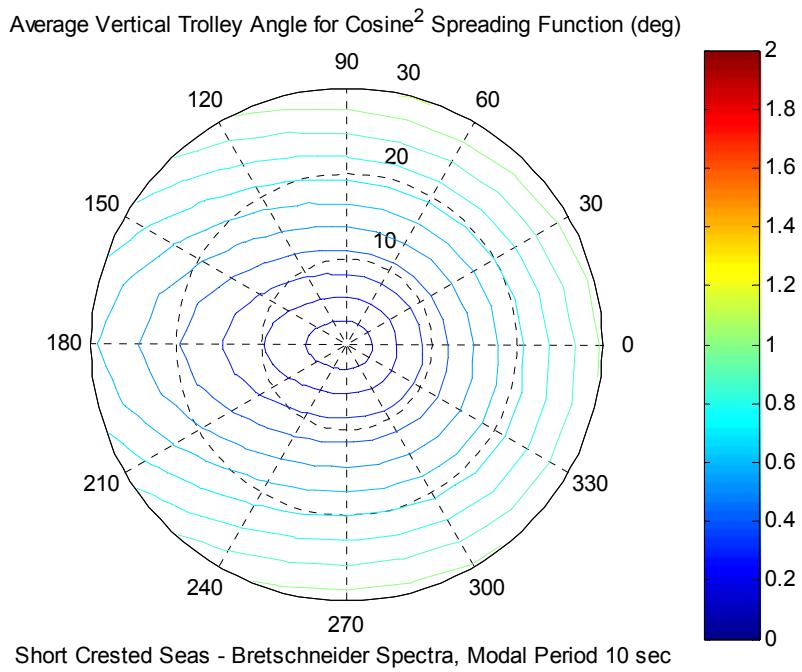
Figure 30.   Average Vertical Trolley Angle for Short Crested
Seas with Bretschneider Spectra and Modal Period 10 seconds.

Average Vertical Trolley Angle (deg)

Long Crested Seas - Bretschneider Spectra , Modal period 10 sec
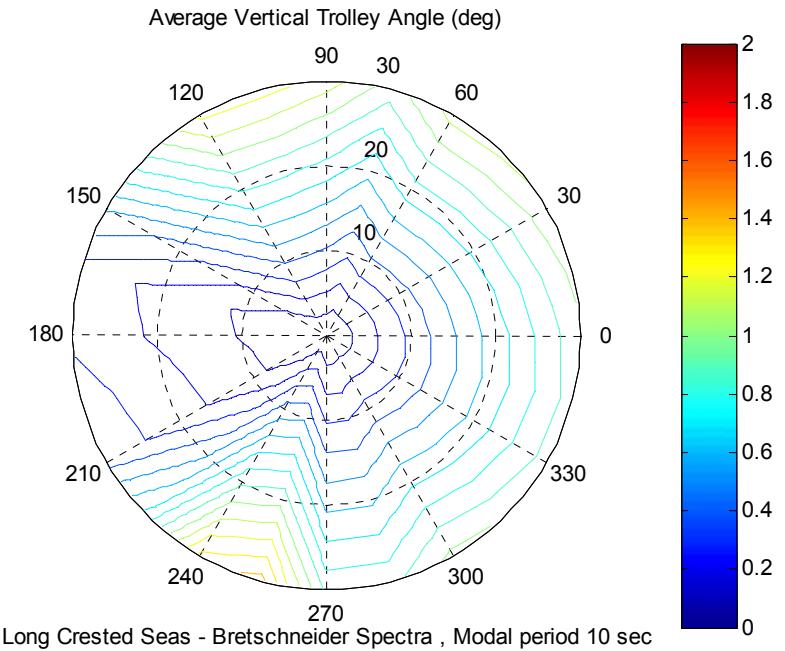
Figure 31.   Average Vertical Trolley Angle for Long Crested
Seas with Bretschneider Spectra and Modal Period 10 seconds.

44

Average Vertical Trolley Twist for Cosine² Spreading Function (deg)

Short Crested Seas - Bretschneider Spectra, Modal Perido 10 sec
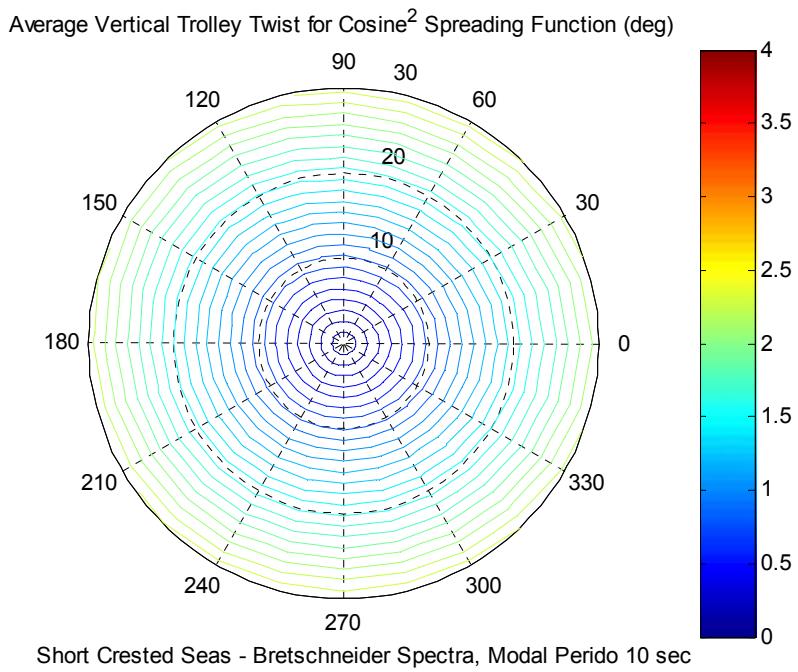
Figure 32.   Average Vertical Trolley Twist for Short Crested
Seas with Bretschneider Spectra and Modal Period 10 seconds.

Average Vertical Trolley Twist (deg)

Long Crested Seas - Bretschneider Spectra, Modal Period 10 sec
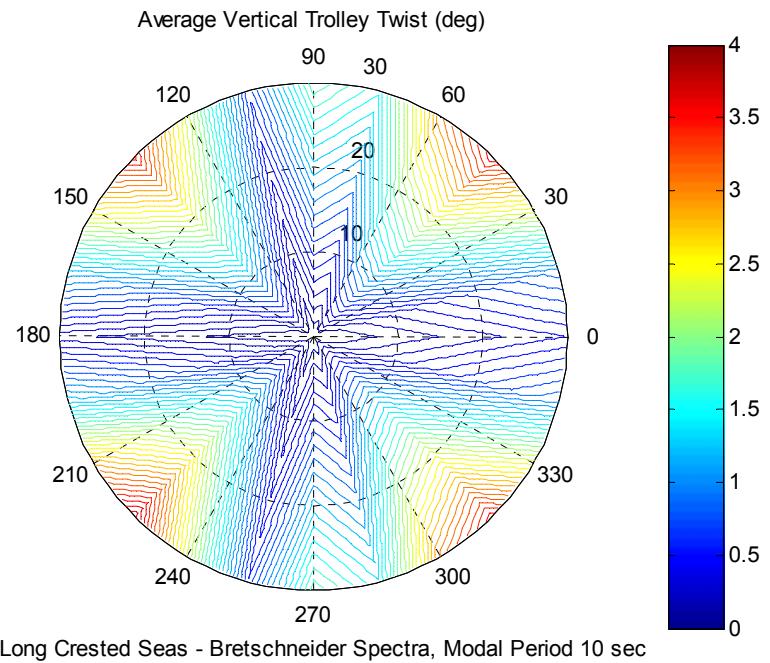
Figure 33.   Average Vertical Trolley Twist for Long Crested
Seas with Bretschneider Spectra and Modal Period 10 seconds.

45
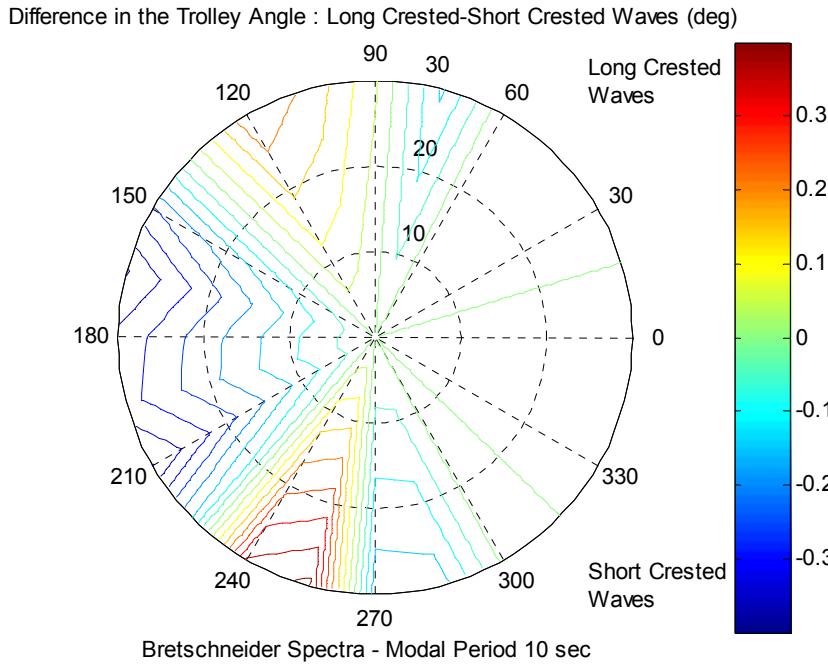
Figure 34.   Comparison of Average Vertical Trolley Angle for
Long Crested and Short Crested Seas with Bretschneider Spectra of
Modal Period 10 seconds.
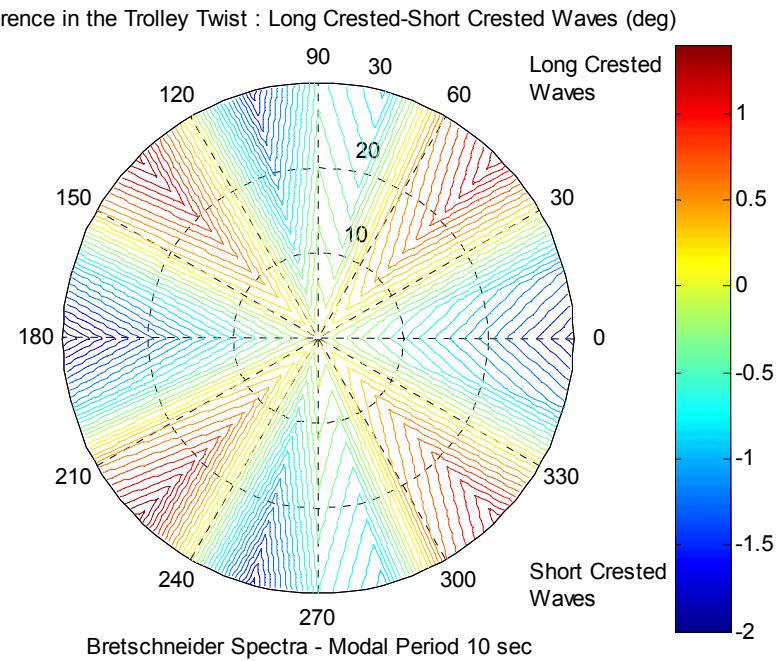
Figure 35.   Comparison of Average Vertical Trolley Twist for
Long Crested and Short Crested Seas with Bretschneider Spectra of
Modal Period 10 seconds.
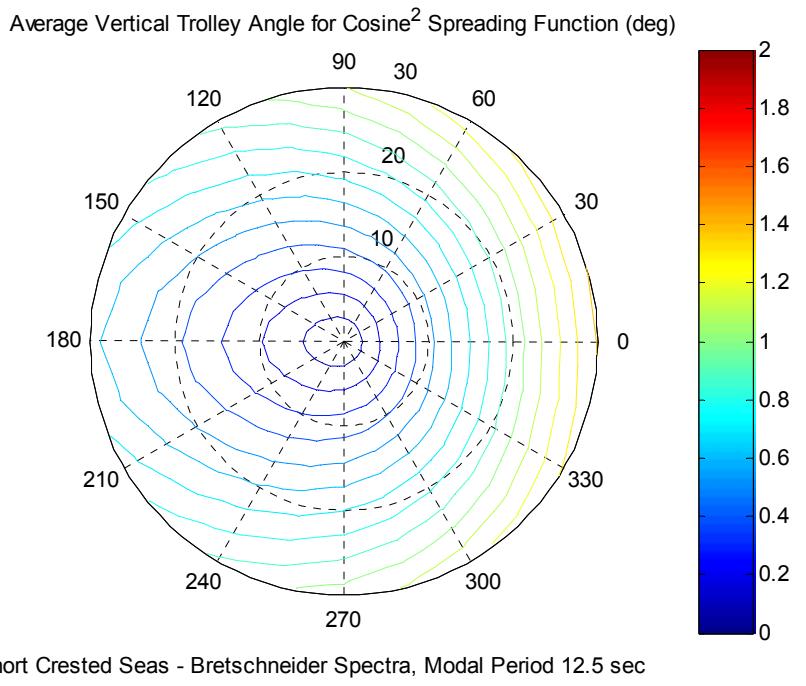
Figure 36.   Average Vertical Trolley Angle for Short Crested Seas with Bretschneider Spectra and Modal Period 12.5 seconds.
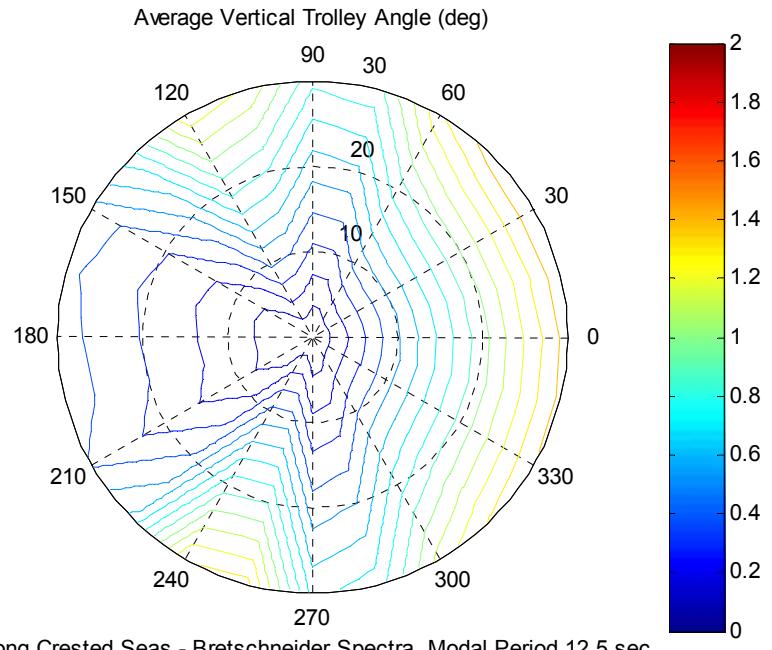
Figure 37.   Average Vertical Trolley Angle for Long Crested Seas with Bretschneider Spectra and Modal Period 12.5 seconds.

Average Vertical Trolley Twist for Cosine² Spreading Function (deg)

Short Crested Seas - Bretschneider Spectra, Modal Period 12.5 sec
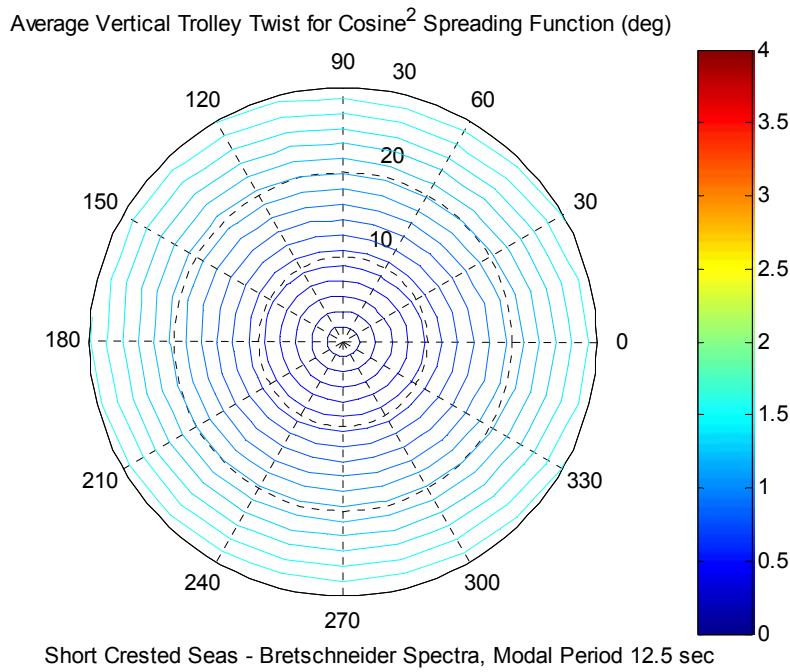
Figure 38.   Average Vertical Trolley Twist for Short Crested
Seas with Bretschneider Spectra and Modal Period 12.5 seconds.

Average Vertical Trolley Twist (deg)

Long Crested Seas - Bretschneider Spectra, Modal Period 12.5 sec
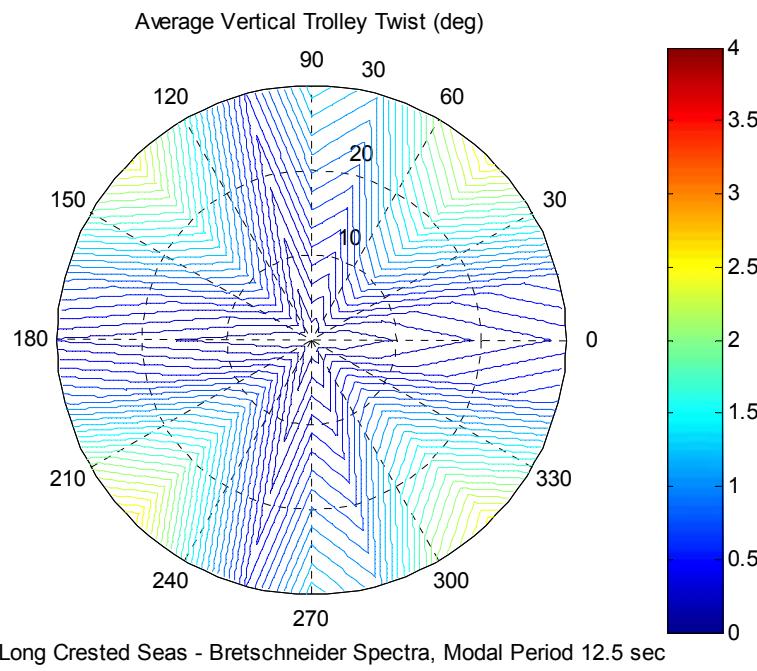
Figure 39.   Average Vertical Trolley Twist for Long Crested
Seas with Bretschneider Spectra and Modal Period 12.5 seconds.
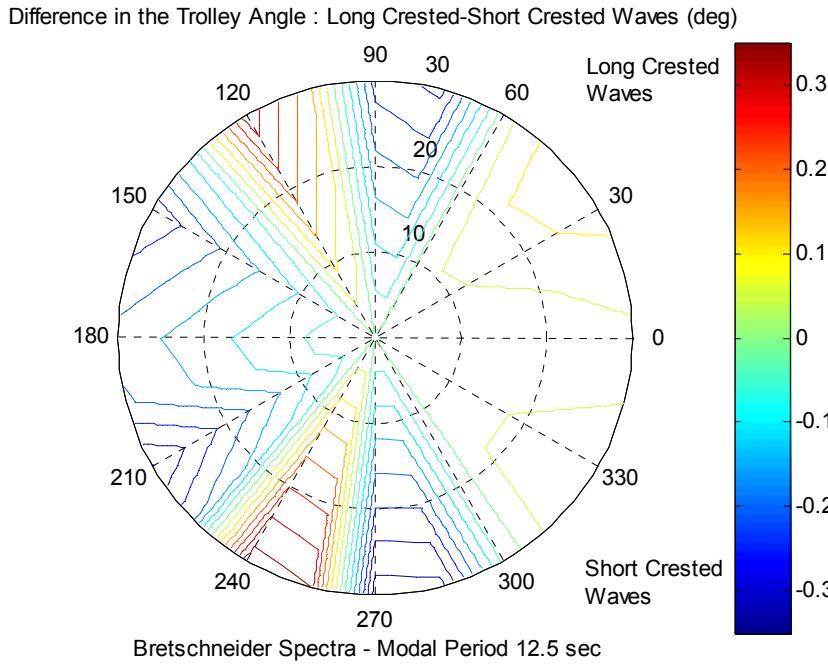
Figure 40.   Comparison of Average Vertical Trolley Angle for
Long Crested and Short Crested Seas with Bretschneider Spectra of
Modal Period 12.5 seconds.
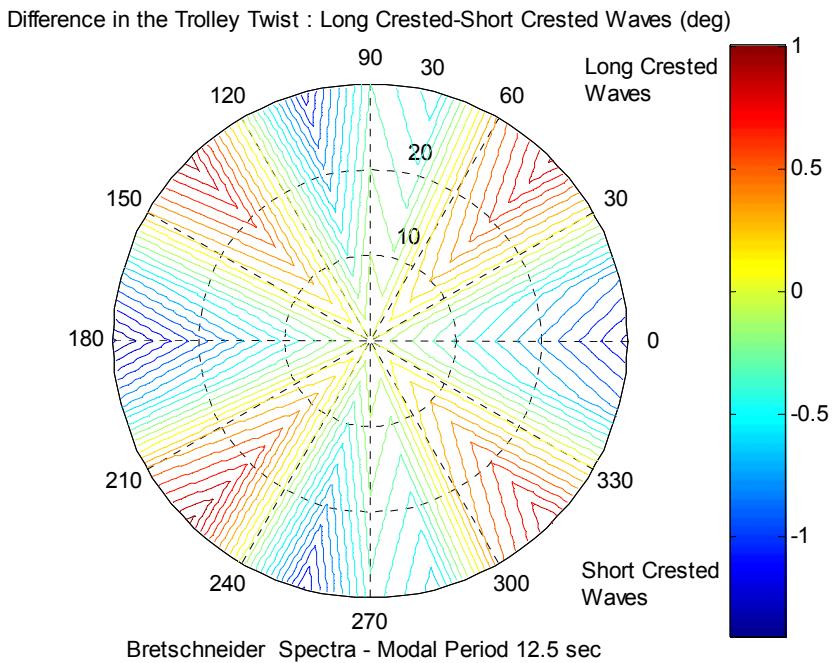
Figure 41.   Comparison of Average Vertical Trolley Twist for
Long Crested and Short Crested Seas with Bretschneider Spectra of
Modal Period 12.5 seconds.

Average Vertical Trolley Angle for Cosine[6] Spreading Function (deg)

Short Crested Seas - Pierson Moskowitz Spectra
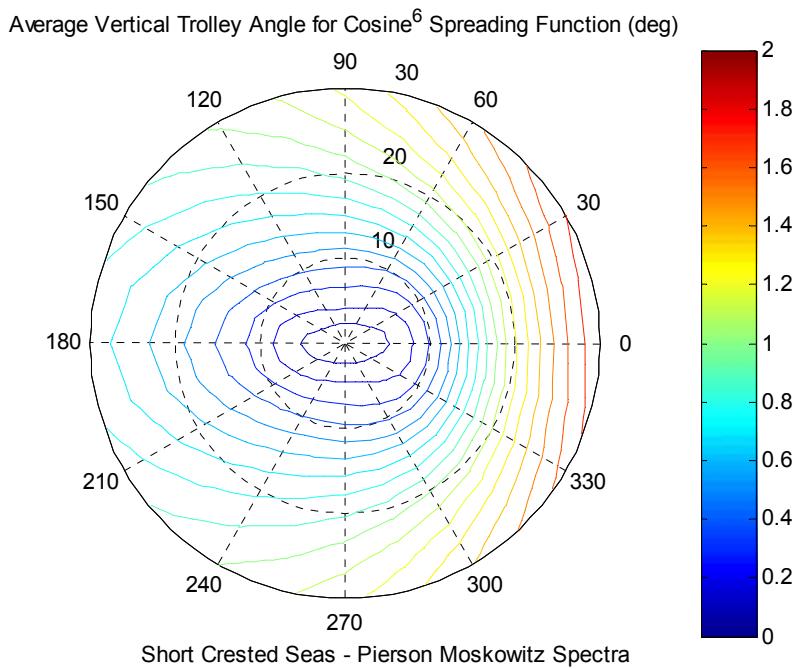
Figure 42.   Average Vertical Trolley Angle for Short Crested Seas with Pierson Moskowitz Spectra.

Average Vertical Trolley Twist for Cosine[6] Spreading Function (deg)

Short Crested Seas - Pierson Moskowitz Spectra
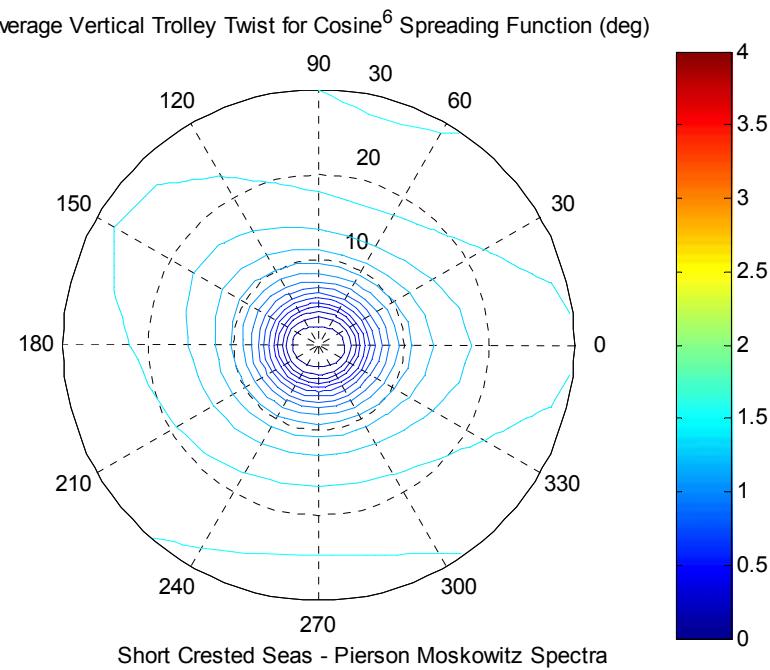
Figure 43.   Average Vertical Trolley Twist for Short Crested Seas with Pierson Moskowitz spectra.

50

Average Vertical Trolley Angle for Cosine⁶ Spreading Function (deg)

Short Crested Seas - Bretschneider Spectra, Modal Period 5 sec
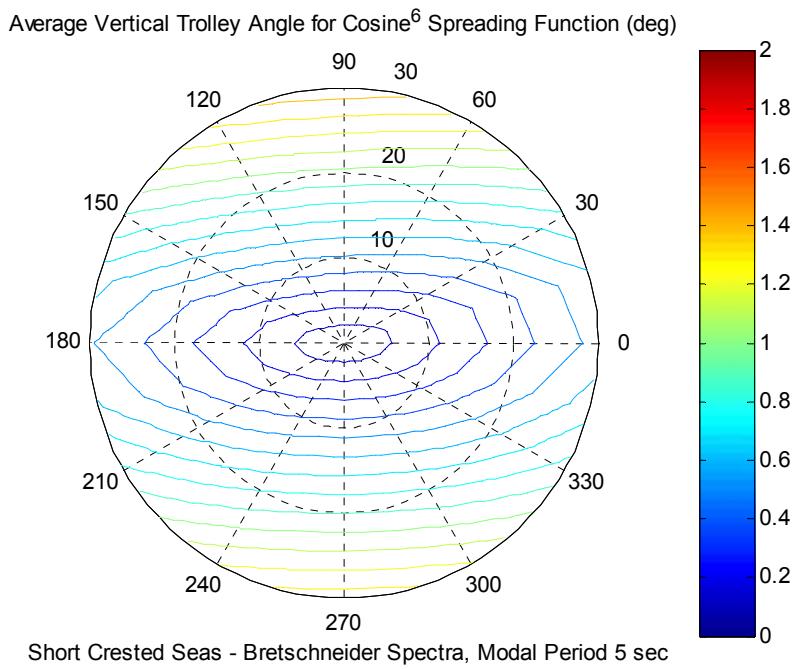
Figure 44.   Average Vertical Trolley Angle for Short Crested
Seas with Bretschneider Spectra of Modal Period 5 seconds.

Average Vertical Trolley Twist for Cosine⁶ Spreading Function (deg)

Short Crested Seas - Bretschneider Spectra, Modal Period 5 sec
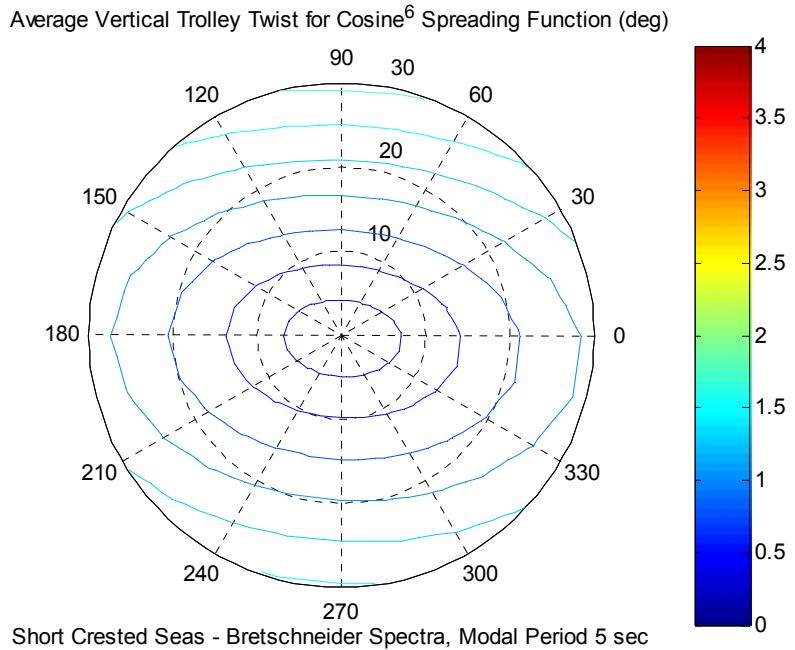
Figure 45.   Average Vertical Trolley Twist for Short Crested
Seas with Bretschneider Spectra of Modal Period 5 seconds.

Average Vertical Trolley Angle for Cosine[6] Spreading Function (deg)

Short Crested Seas - Bretschneider Spectra, Modal Period 7.5 sec
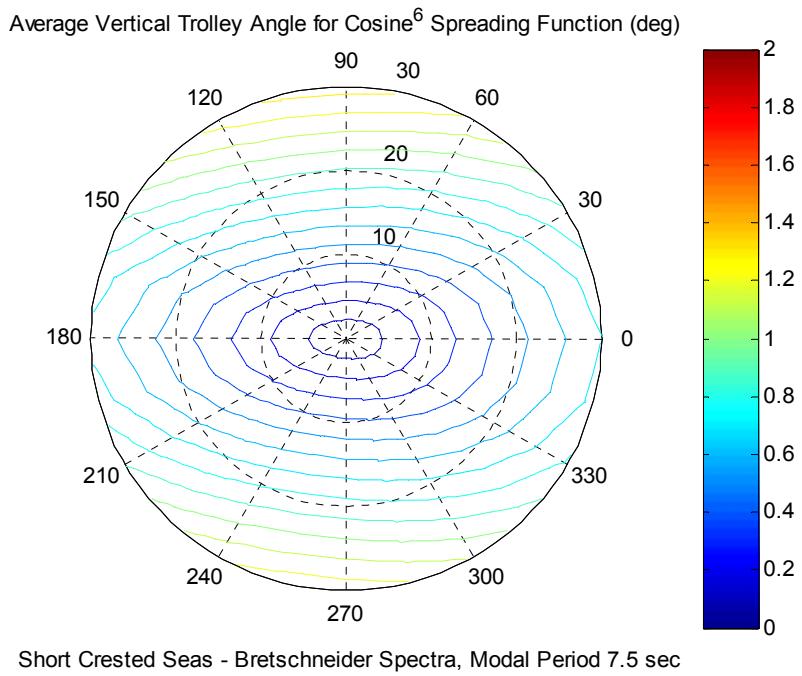
Figure 46.   Average Vertical Trolley Angle for Short Crested
Seas with Bretschneider Spectra of Modal Period 7.5 seconds.

Average Vertical Trolley Twist for Cosine[6] Spreading Function (deg)

Short Crested Seas - Bretschneider Spectra, Modal Period 7.5 sec

Figure 47.   Average Vertical Trolley Twist for Short Crested
Seas with Bretschneider Spectra of Modal Period 7.5 seconds.

52

Average Vertical Trolley Angle for Cosine[6] Spreading Function (deg)

Short Crested Seas - Bretschneider Spectra, Modal Period 10 sec

Figure 48.   Average Vertical Trolley Angle for Short Crested
Seas with Bretschneider Spectra of Modal Period 10 seconds.

Average Vertical Trolley Twist for Cosine[6] Spreading Function (deg)

Short Crested Seas - Bretschneider Spectra, Moal Period 10 sec
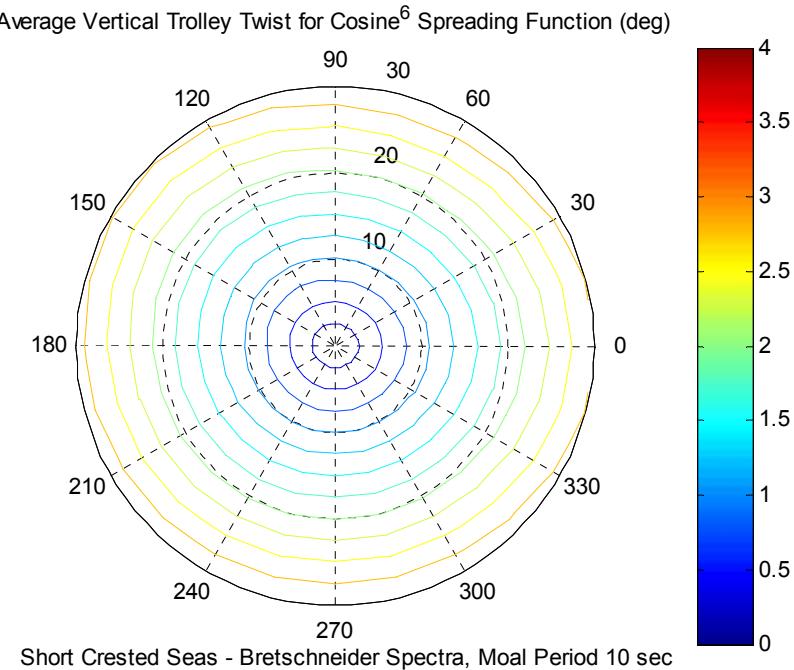
Figure 49.   Average Vertical Trolley Twist for Short Crested
Seas with Bretschneider Spectra of Modal Period 10 seconds.

53

Average Vertical Trolley Angle for Cosine[6] Spreading Function (deg)

Short Crested Seas - Bretschneider Spectra, Modal Period 12.5 sec
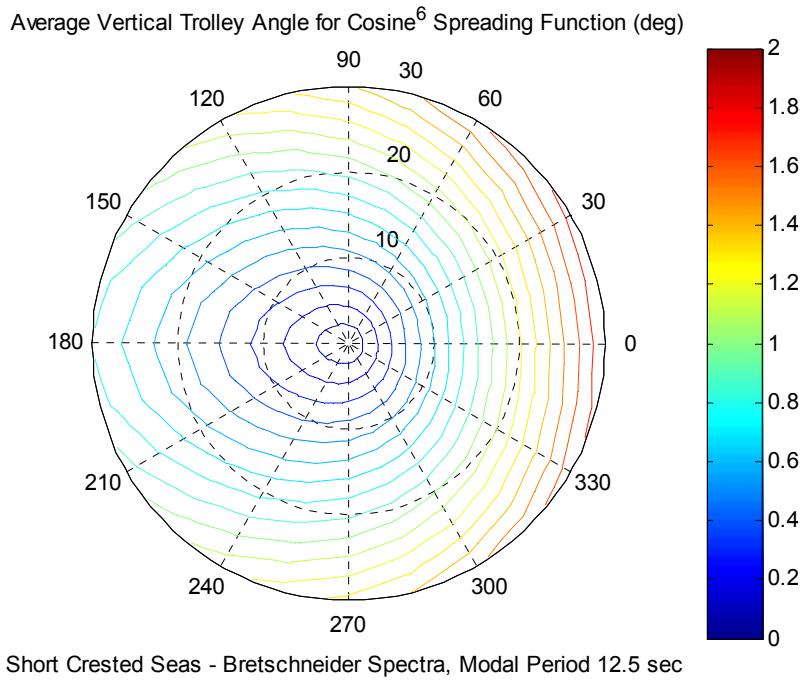
Figure 50.   Average Vertical Trolley Angle for Short Crested
Seas with Bretschneider Spectra of Modal Period 12.5 seconds.


Average Vertical Trolley Twist for Cosine[6] Spreading Function (deg)

Short Crested Seas - Bretschneider Spectra, Modal Period 12.5 sec
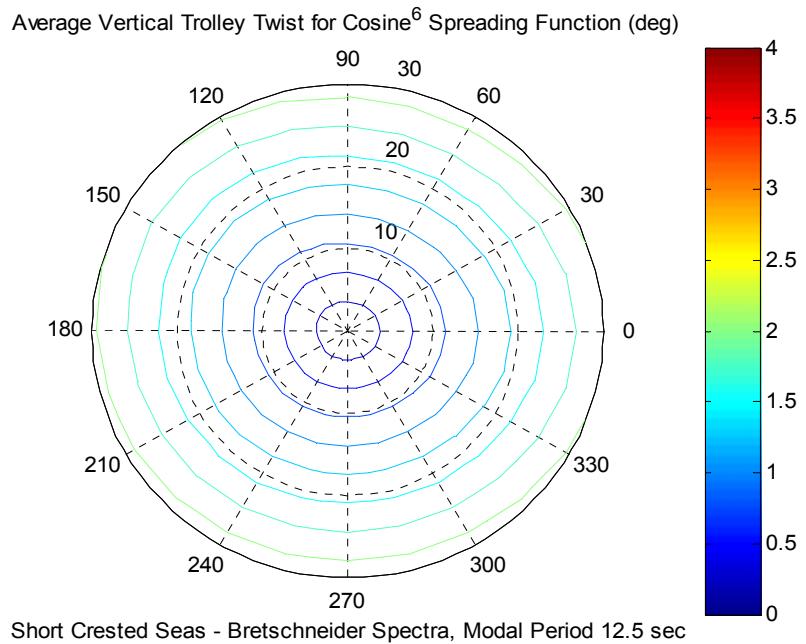
Figure 51.   Average Vertical Trolley Twist for Short Crested
Seas with Bretschneider Spectra of Modal Period 12.5 seconds.

Average Vertical Trolley Angle for Cosine[8] Spreading Function (deg)

Short Crested Seas - Pierson Moskowitz Spectra

Figure 52.　　　Average Vertical Trolley Angle for Short Crested Seas with Pierson Moskowitz Spectra.

Average Vertical Trolley Twist for Cosine[8] Spreading Function (deg)
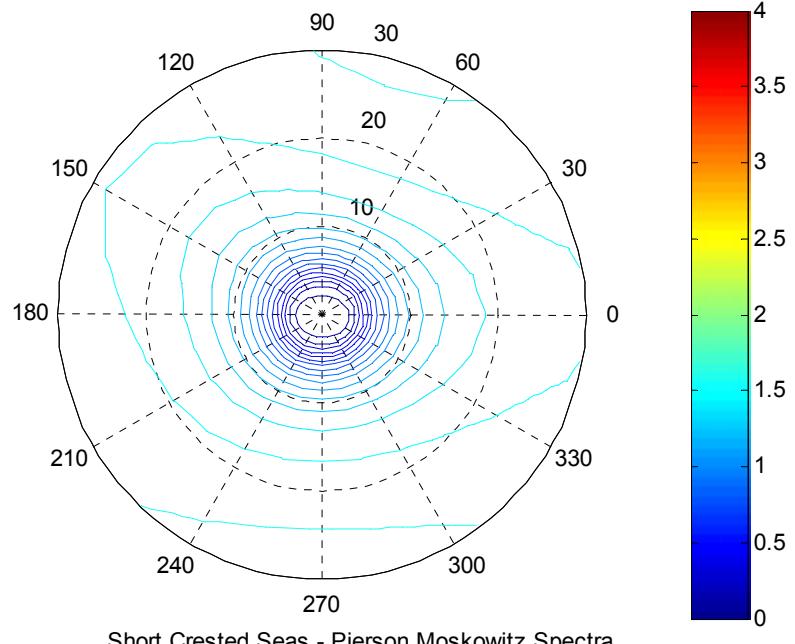
Short Crested Seas - Pierson Moskowitz Spectra

Figure 53.　　　Average Vertical Trolley Twist for Short Crested Seas with Pierson Moskowitz spectra.

Average Vertical Trolley Angle for Cosine[8] Spreading Function (deg)

Short Crested Seas - Bretschneider Spectra, Modal Period 5 sec
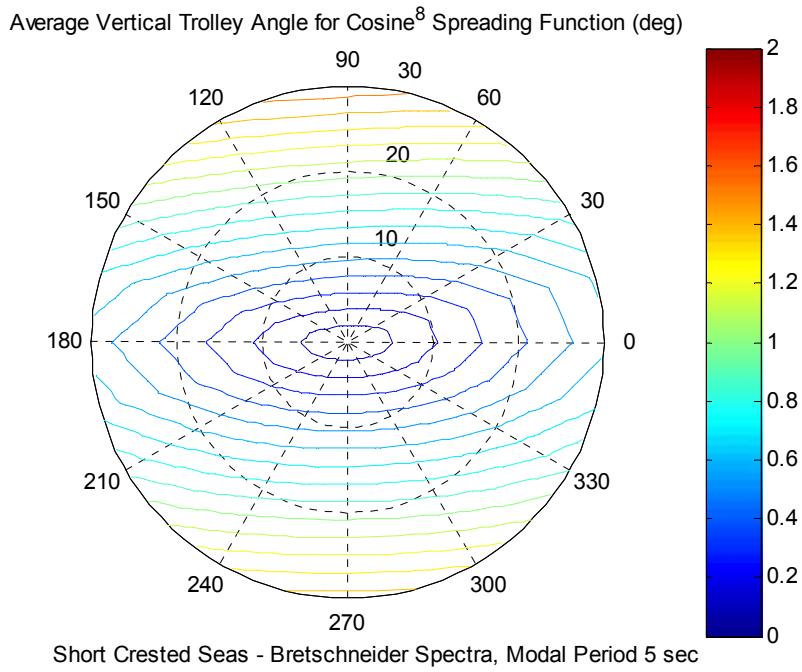
Figure 54.   Average Vertical Trolley Angle for Short Crested
Seas with Bretschneider Spectra of Modal Period 5 seconds.

Average Vertical Trolley Twist for Cosine[8] Spreading Function (deg)


Short Crested Seas - Bretschneider Spectra, Modal Period 5 sec
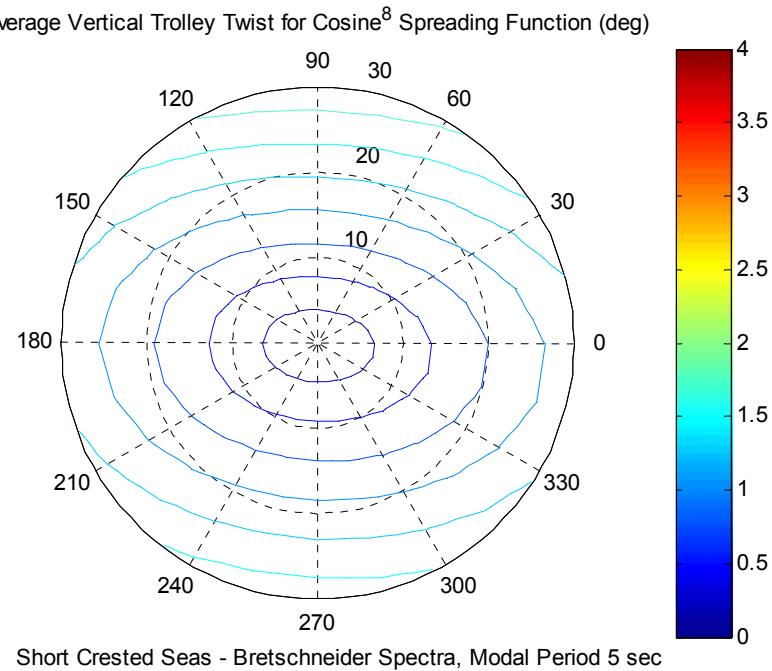
Figure 55.   Average Vertical Trolley Twist for Short Crested
Seas with Bretschneider Spectra of Modal Period 5 seconds.

Average Vertical Trolley Angle for Cosine[8] Spreading Function (deg)
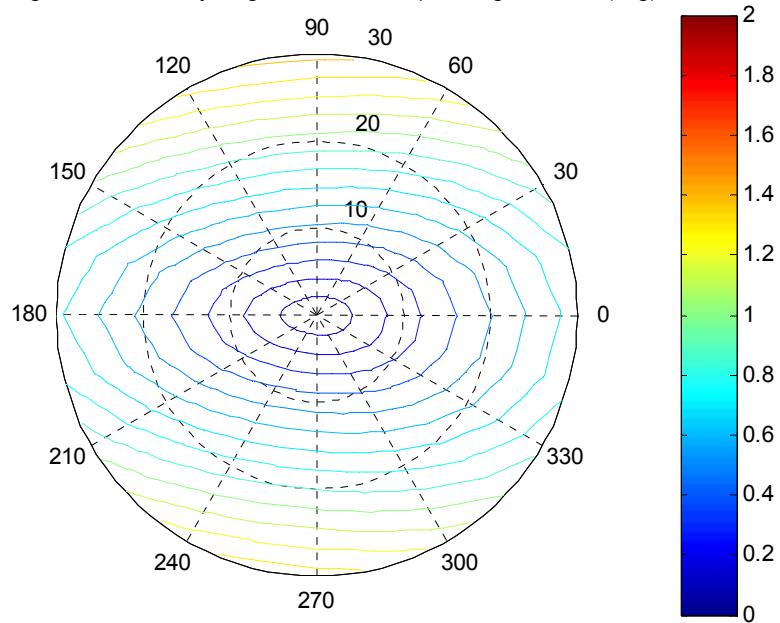
Short Crested Seas - Bretschneider Spectra, Modal Period 7.5 sec

Figure 56.   Average Vertical Trolley Angle for Short Crested
Seas with Bretschneider Spectra of Modal Period 7.5 seconds.

Average Vertical Trolley Twist for Cosine[8] Spreading Function (deg)
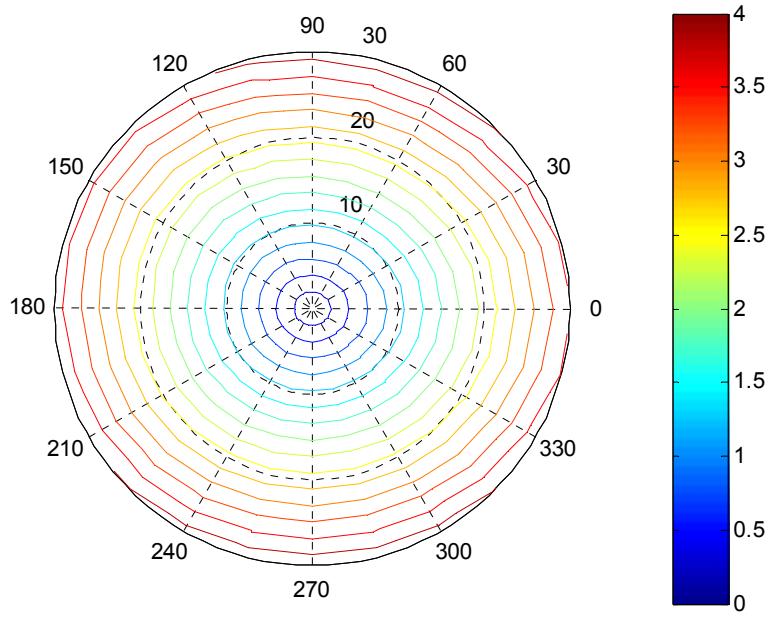
Short Crested Seas - Bretschneider Spectra, Modal Period 7.5 sec

Figure 57.   Average Vertical Trolley Twist for Short Crested
Seas with Bretschneider Spectra of Modal Period 7.5 seconds.
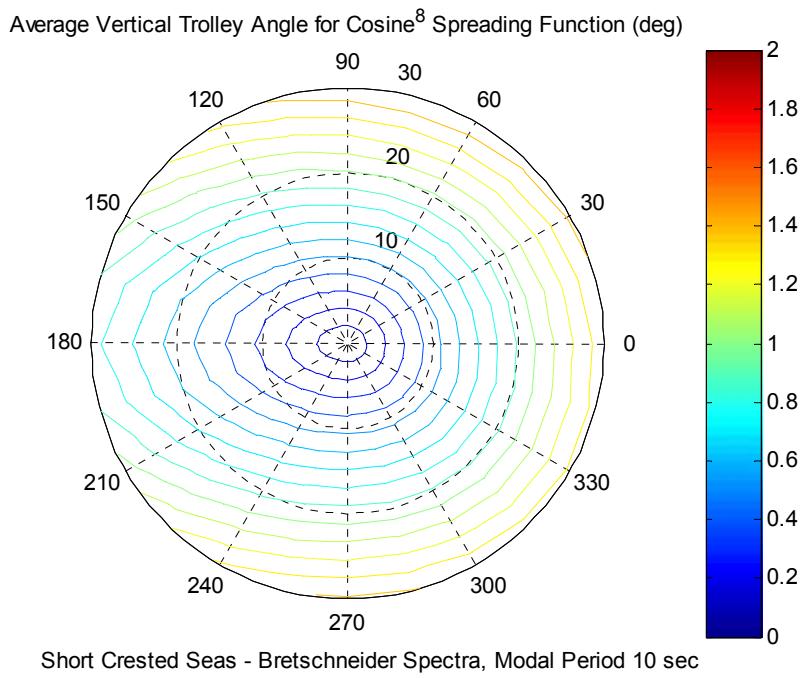
Figure 58.   Average Vertical Trolley Angle for Short Crested Seas with Bretschneider Spectra of Modal Period 10 seconds.
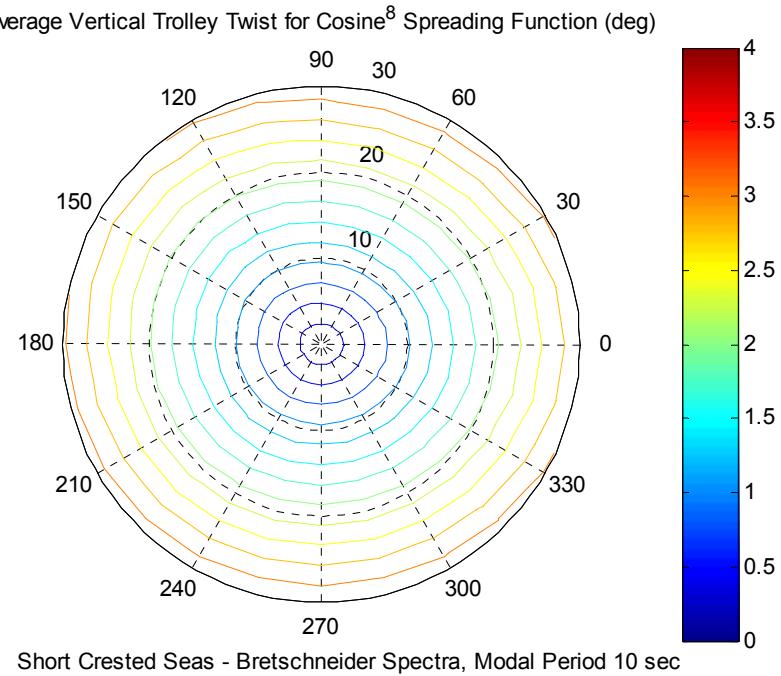

Figure 59.   Average Vertical Trolley Twist for Short Crested Seas with Bretschneider Spectra of Modal Period 10 seconds.

Average Vertical Trolley Angle for Cosine[8] Spreading Function (deg)

Short Crested Seas - Bretschneider Spectra, Modal Period 12.5 sec
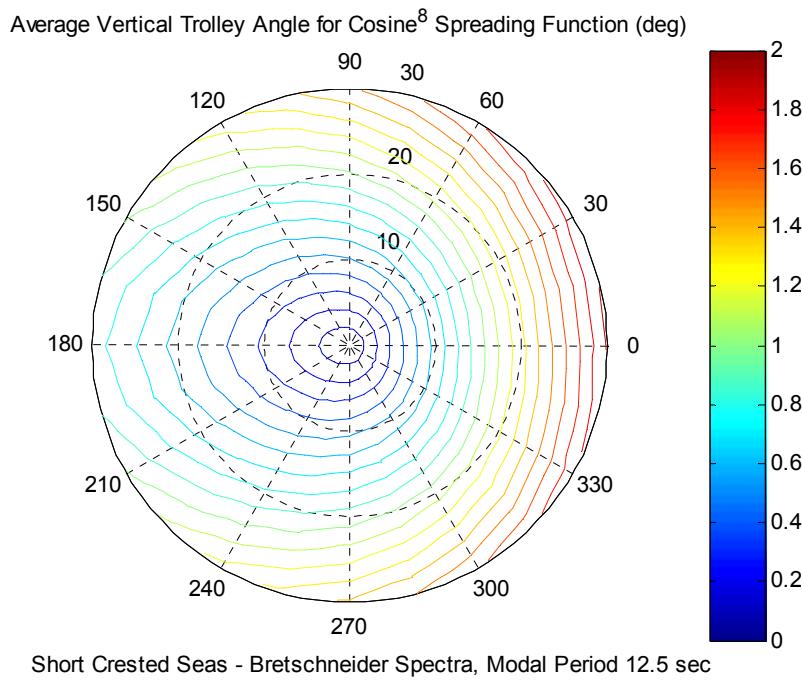
Figure 60.   Average Vertical Trolley Angle for Short Crested
Seas with Bretschneider Spectra of Modal Period 12.5 seconds.

Average Vertical Trolley Twist for Cosine[8] Spreading Function (deg)

Short Crested Seas - Bretschneider Spectra, Modal Period 12.5 sec
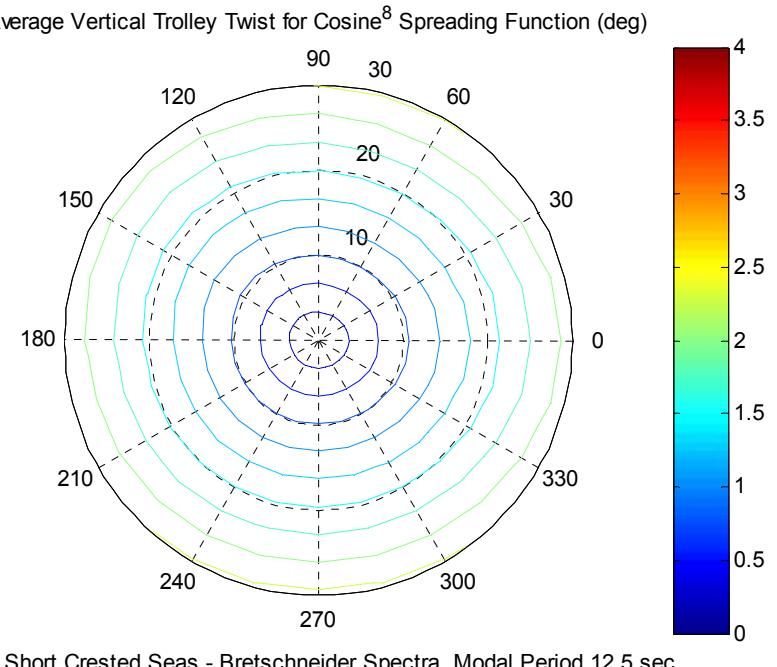
Figure 61.   Average Vertical Trolley Twist for Short Crested
Seas with Bretschneider Spectra of Modal Period 12.5 seconds.
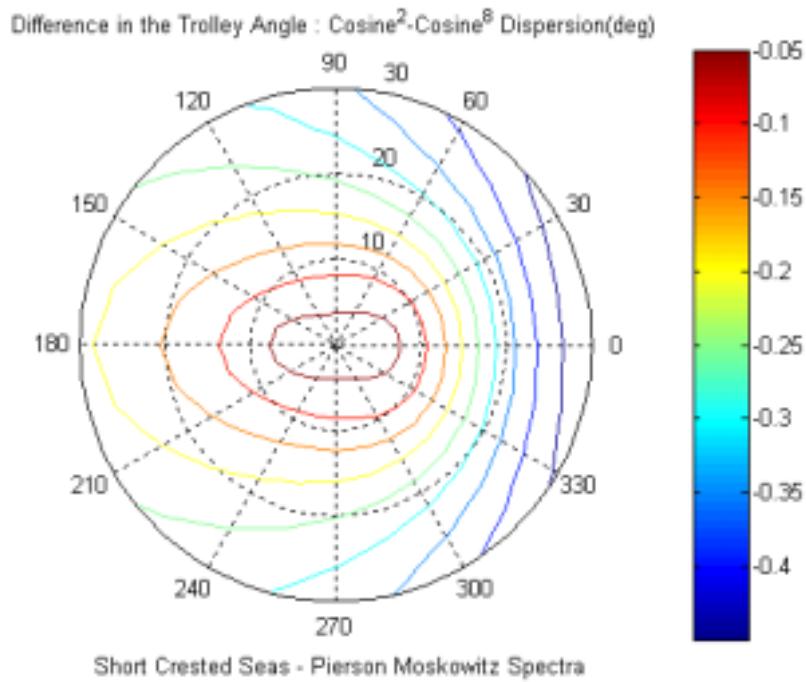
Figure 62.   Comparison of Average Vertical Trolley Angle for Short Crested Seas with Pierson Moskowitz Spectra for Cosine^2 and Cosine^8 Dispersion.
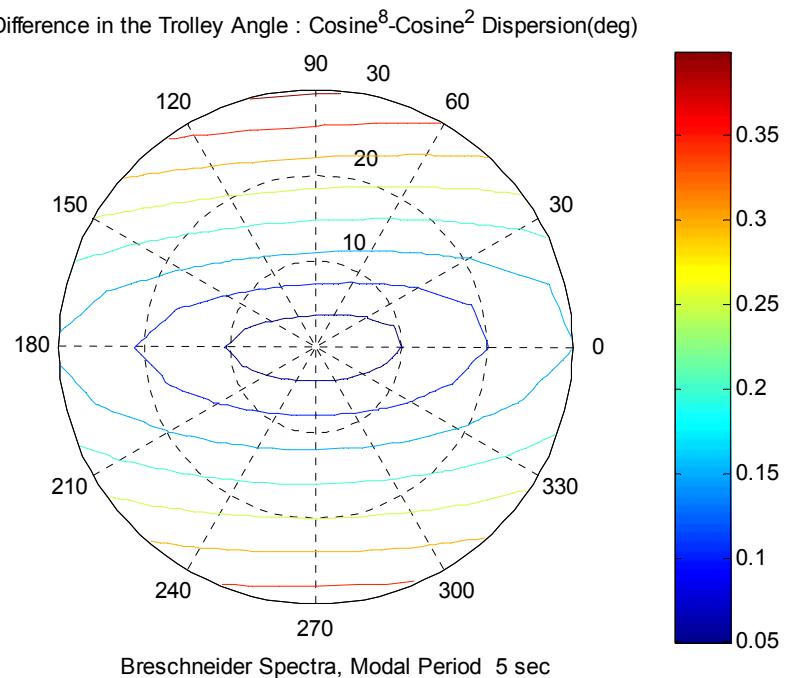
Figure 63.   Comparison of Average Vertical Trolley Angle for Short Crested Seas with Bretschneider Spectra of Modal Period 5 seconds for Cosine^2 and Cosine^8 Dispersion.

Difference in the Trolley Angle : Cosine^8-Cosine^2 Dispersion(deg)

Bretschneider Spectra, Modal Period 7.5 sec
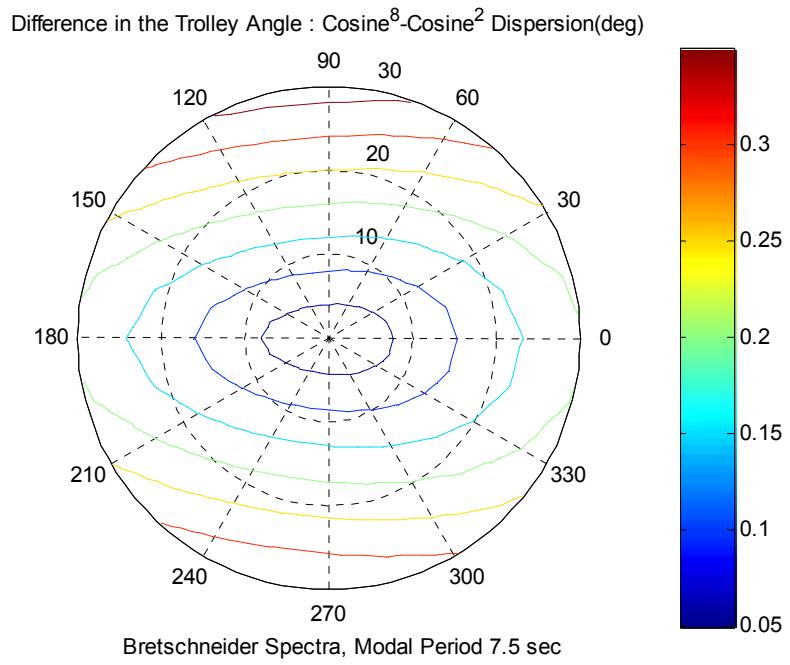
Figure 64.   Comparison of Average Vertical Trolley Angle for Short Crested Seas with Bretschneider Spectra of Modal Period 7.5 seconds for Cosine^2 and Cosine^8 Dispersion.

Difference in the Trolley Angle : Cosine^8-Cosine^2 Dispersion(deg)

Bretscheider Spectra, Modal Period 10 sec
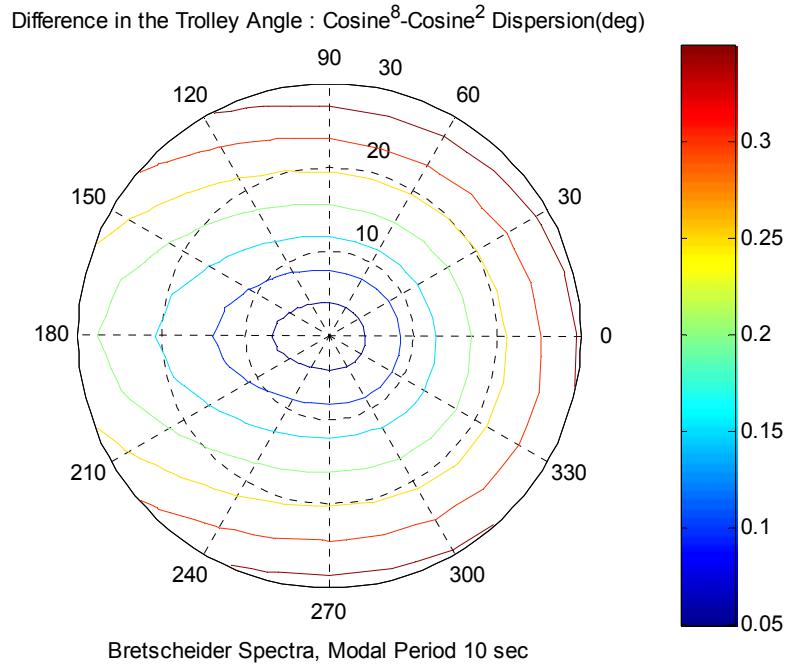
Figure 65.   Comparison of Average Vertical Trolley Angle for Short Crested Seas with Bretschneider Spectra of Modal Period 10 seconds for Cosine^2 and Cosine^8 Dispersion.

61

Difference in the Trolley Angle : Cosine^8-Cosine^2 Dispersion(deg)

Bretschneider Spectra, Modal Period 12.5 sec
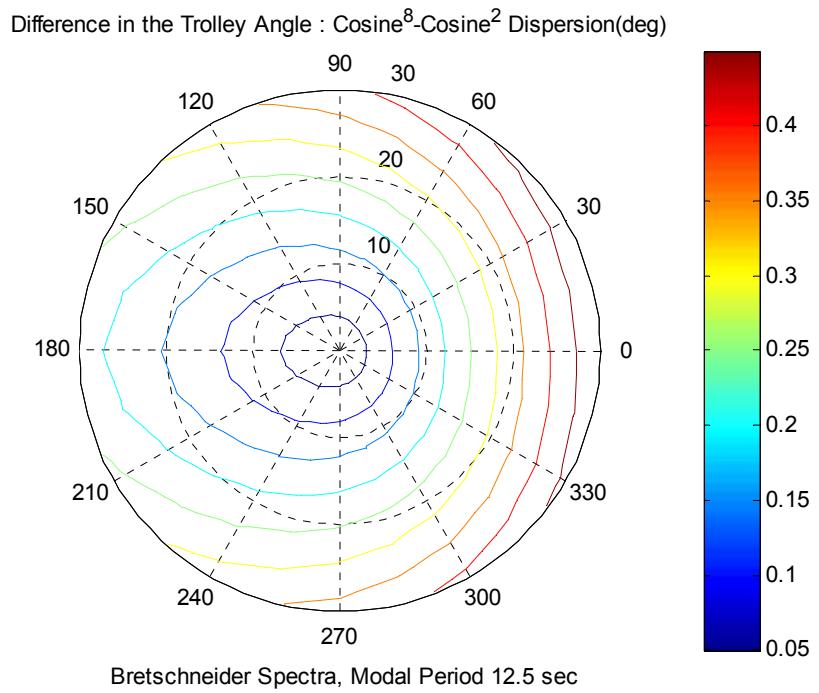
Figure 66.   Comparison of Average Vertical Trolley Angle for Short Crested Seas with Bretschneider Spectra of Modal Period 12.5 seconds for Cosine^2 and Cosine^8 Dispersion.

Difference in the Trolley Twist : Cosine^8-Cosine^2 Dispersion(deg)

Pierson Moskowitz Spectra
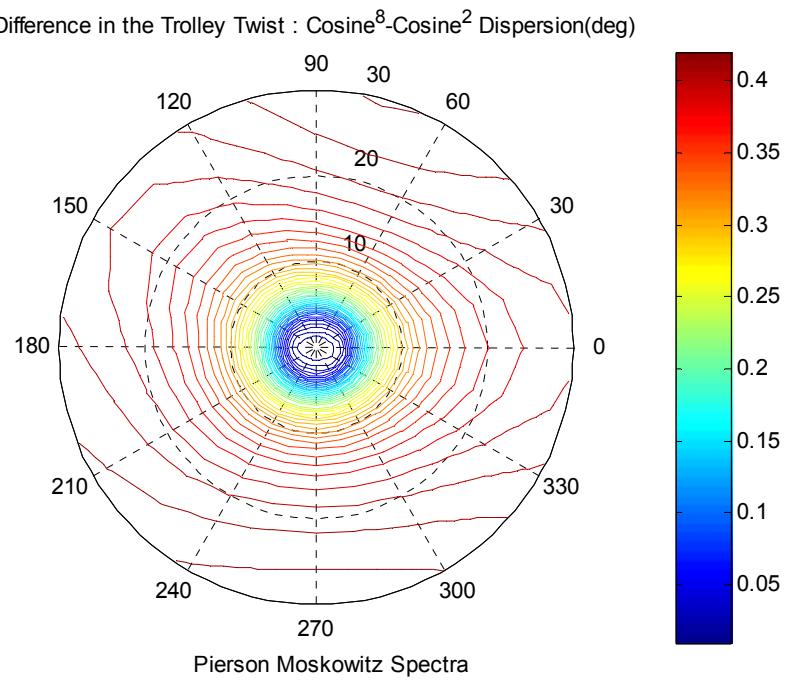
Figure 67.   Comparison of Average Vertical Trolley Twist for Short Crested Seas with Pierson Moskowitz Spectra for Cosine^2 and Cosine^8 Dispersion.
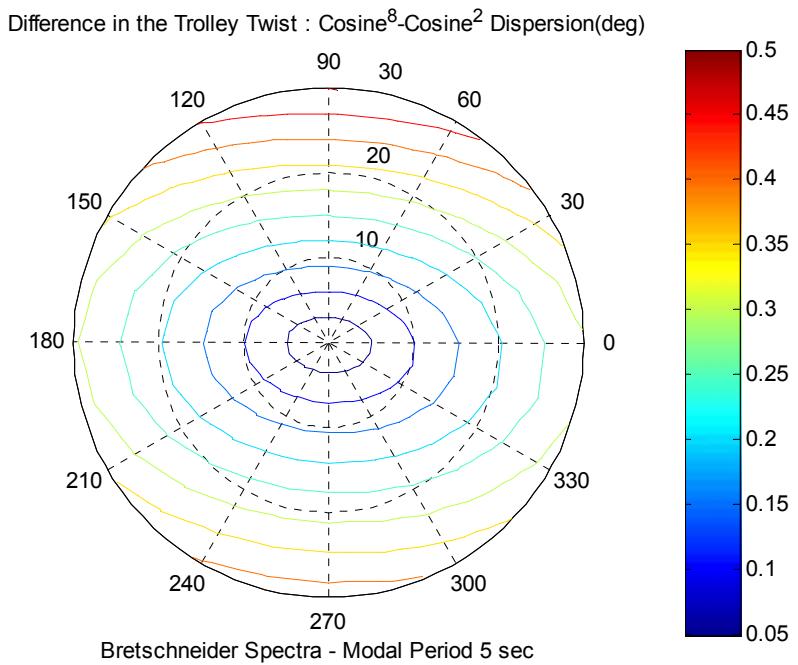
Figure 68.   Comparison of Average Vertical Trolley Twist for
Short Crested Seas with Bretschneider Spectra of Modal Period 5
seconds for Cosine^2 and Cosine^8 Dispersion.
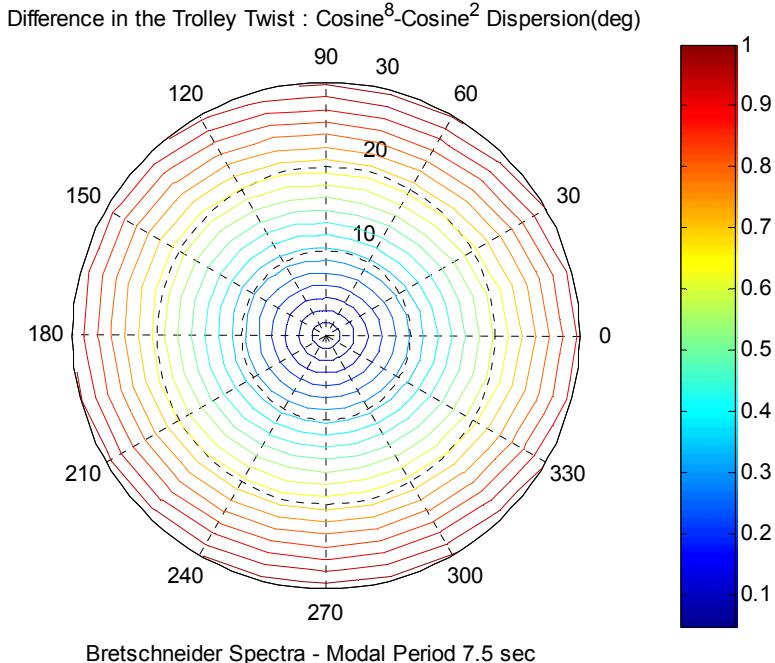
Figure 69.   Comparison of Average Vertical Trolley Twist for
Short Crested Seas with Bretschneider Spectra of Modal Period 7.5
seconds for Cosine^2 and Cosine^8 Dispersion.

63

Difference in the Trolley Twist : Cosine^8-Cosine^2 Dispersion(deg)

Bretschneider Spectra - Modal Period 10 sec
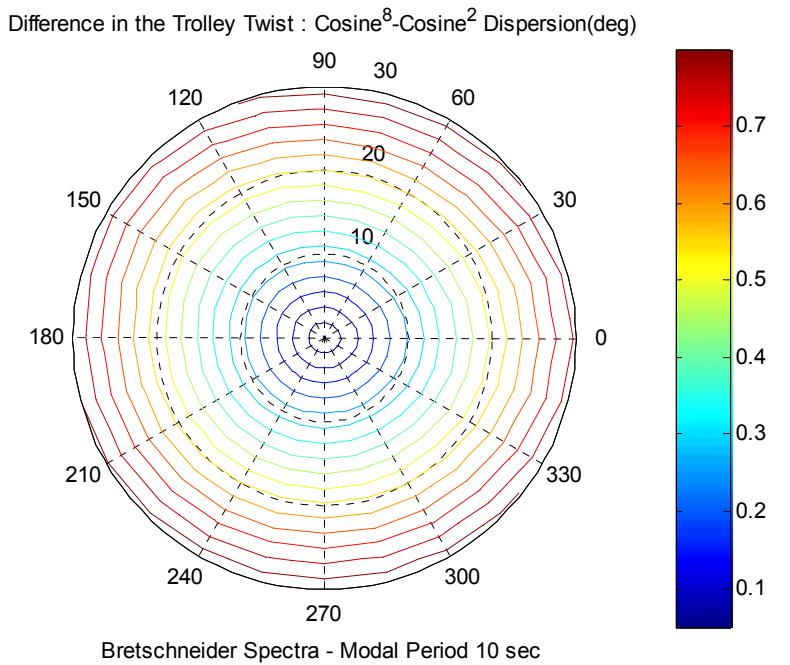
Figure 70.   Comparison of Average Vertical Trolley Twist for Short Crested Seas with Bretschneider Spectra of Modal Period 10 seconds for Cosine^2 and Cosine^8 Dispersion.

Difference in the Trolley Twist : Cosine^8-Cosine^2 Dispersion(deg)

Bretschneider Spectra - Modal Period 12.5 sec
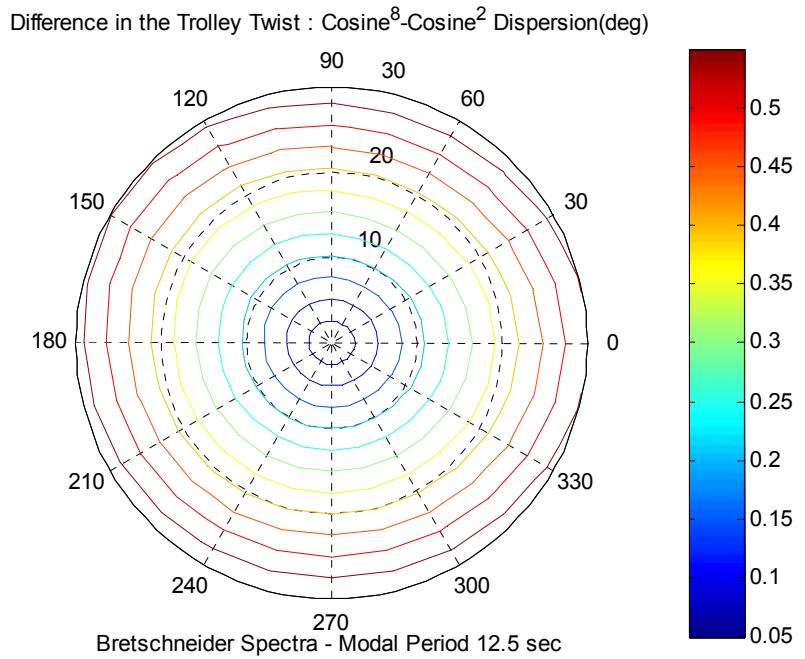
Figure 71.   Comparison of Average Vertical Trolley Twist for Short Crested Seas with Bretschneider Spectra of Modal Period 12.5 seconds for Cosine^2 and Cosine^8 Dispersion.

64

B.   EFFECTS ON RATES OF TRANSFER

Based on the NAVY RORO Project report in Ref(8) which modeled a similar trolley configuration using the CAPE D and the RRDF, the expected transfer rate of one M1A1 Tank using the trolley system power by a 300HP motor is envisaged to be approximately 2.25 minutes for every round trip with one loading sequence. The transfer rates shown in Table (2) were determined by power of the drive and the load including the trolley, trolley drive motor, 8 hours of fuel and the cargo.

TRANSFER RATES					
LOAD CONDITION	RAMP LENGTH IN FEET	DRIVE MOTOR HORSE POWER	TRANSFER RATE LOADED TIME IN MINUTES	TRANSFER RATE UNLOADED TIME IN MINUTES	ROUND TRIP WITH ONE-WAY LOAD. TIME IN MINUTES
M1A1 TANK	100	100	4.00	0.85	4.85
M1A1 TANK	100	200	3.00	0.50	3.50
M1A1 TANK	100	300	2.00	0.25	2.25
M1A1 TANK	100	400	0.85	0.19	1.04

Table 2.   Transfer Rate extracted from Navy RORO Project Phase 1 Report.

Having obtained the values of the averaged trolley angles in short crested seas for the Pierson Moskowitz and Bretschneider Spectra, a simplified model based on the angle of inclination of the trolley affected by the seaway was formed to determine the reduction on the transfer rate caused by short crested seas. A dimensionless constant called the Transfer Rate Reduction Factor(TRF) was derived as;

$$TRF = \frac{[\sin(\theta) + \mu\cos(\theta)]}{\mu} \qquad (30)$$

where θ = RMS value of the Average Trolley
Angle(deg)
μ = Coefficient of friction of the Trolley
system

The actual transfer rate(minutes) in seaway can be found by simply multiplying the TRF with the benchmark transfer rate found in table (2), i.e.,

$$TransferRate_{seaway} = TRF_{seaway} \times TransferRate_{benchmark} \qquad (31)$$

The following TRF polar plots shown in figure(72) to (81) details the effects of the reduction in transfer rates when the trolley system is modeled under various seaway with different types of wave spectra and modal periods. While figure (82) to (86) shows the difference in actual transfer rate(seconds) for one M1AI tank modeled in different seaway.

Comparing the results obtained for both short crested and long crested, the general trend suggest that the difference in magnitude of the TRF is very small, between 0% to 6% in both seaway. This is in large due to the small difference in RMS values of the trolley angle between the two seaways. However, the angular sector where the highest rate reduction occurs was vastly different. In the case of a Bretschneider Spectra with Modal period of 5 seconds shown in figure(74) , a long crested seaway predicts that the reduction is highest if the seas were from a 60° degree quadrant on starboard beam with transfer rate reduction

66

factor reducing up to 16% at sea state 7, while a short crested seaway suggest the highest reduction was felt over a larger region spread over 90° and on both the starboard and port beam. The maximum reduction is also at a lower magnitude of 10% at similar sea states.

For the Bretschneider spectra, it is also observed that at higher modal periods of 10 seconds and 12.5 seconds, the sector of where the maximum reduction in transfer factor occurs has expanded and shifted to encompass a larger region from up to 180° from beams seas through to following seas on either side of the platform.
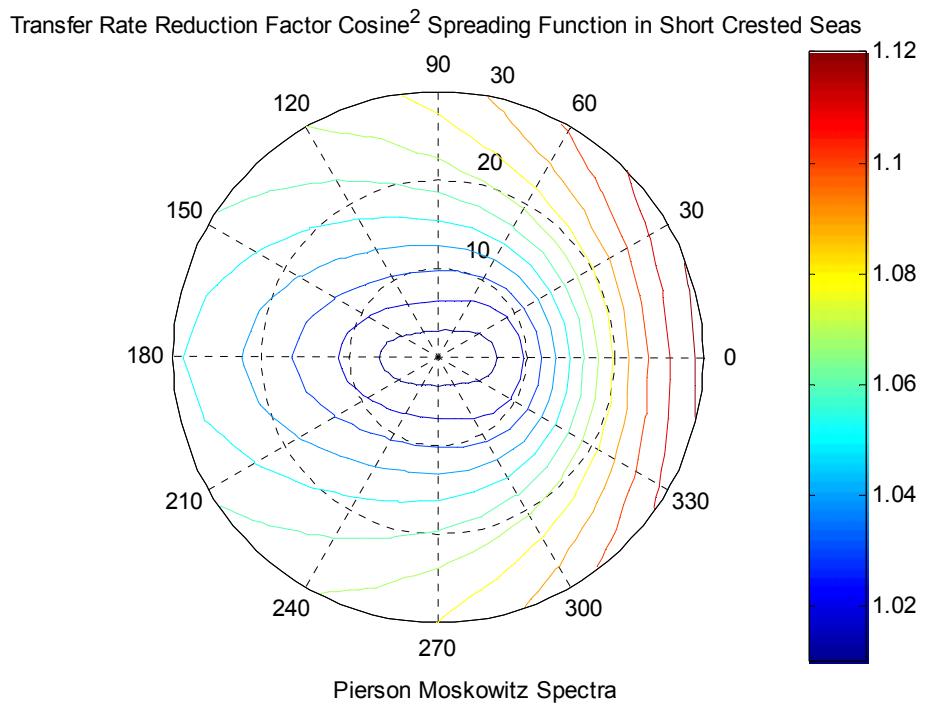
Figure 72.   Transfer Rate Reduction Factor in Short Crested Seas with Pierson Moskowitz Spectra.
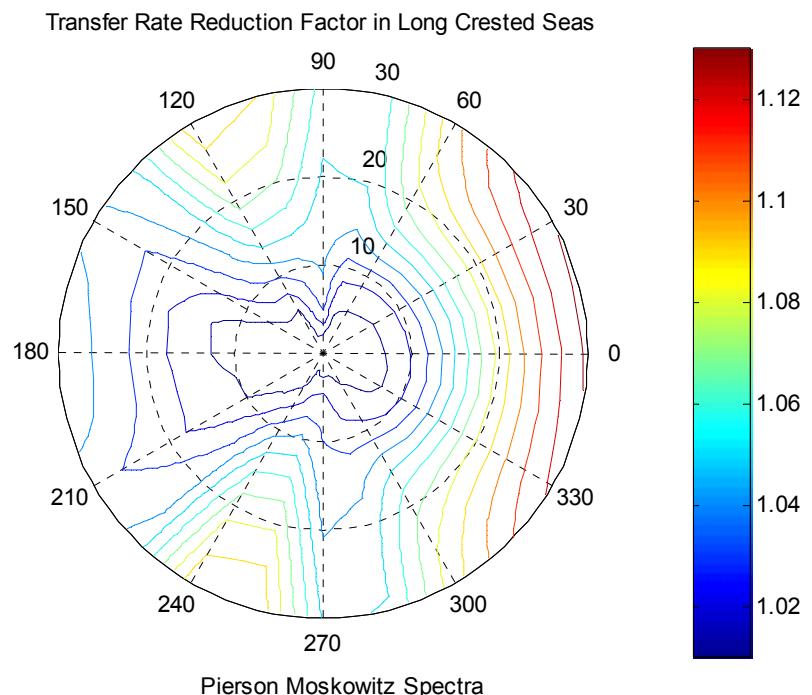
Figure 73.   Transfer Rate Reduction Factor in Long Crested Seas with Pierson Moskowitz Spectra.

Transfer Rate Reduction Factor Cosine^2 Spreading Function in Short Crested Seas

Bretschneider Spectra, Modal Period 5 sec
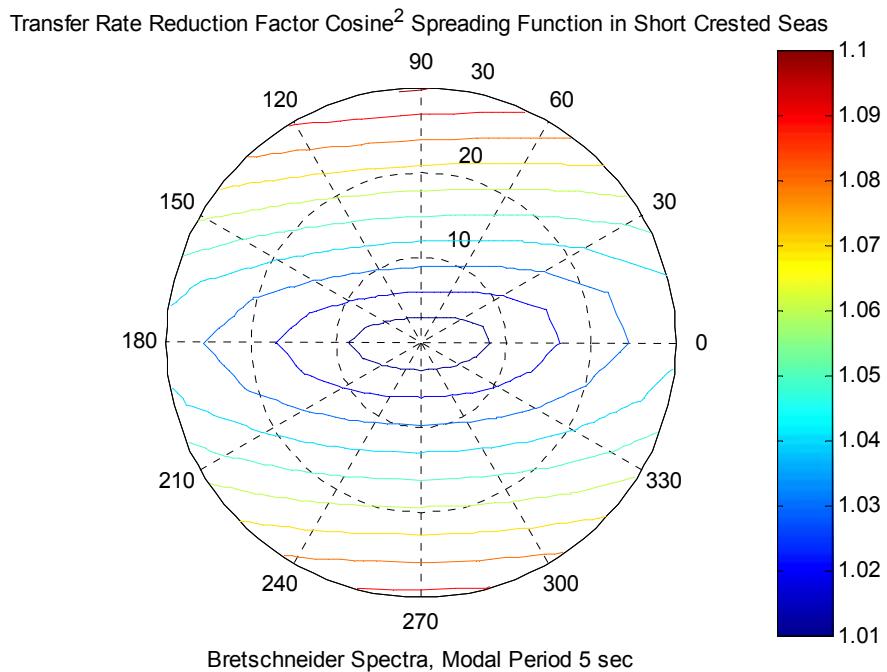
Figure 74.   Transfer Rate Reduction Factor in Short Crested Seas Bretschneider Spectra of Modal Period 5 seconds

Transfer Rate Reduction Factor in Long Crested Seas

Bretschenider Spectra , Modal Period 5 sec
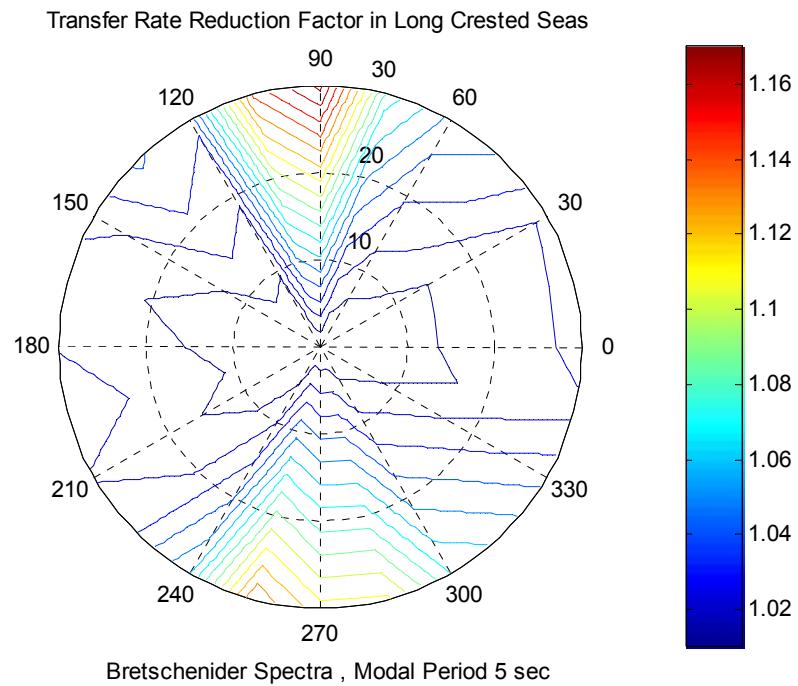
Figure 75.   Transfer Rate Reduction Factor in Long Crested Seas Bretschneider Spectra of Modal Period 5 seconds.

Transfer Rate Reduction Factor Cosine^2 Spreading Function in Short Crested Seas

Bretschneider Spectra, Modal Period 7.5 sec
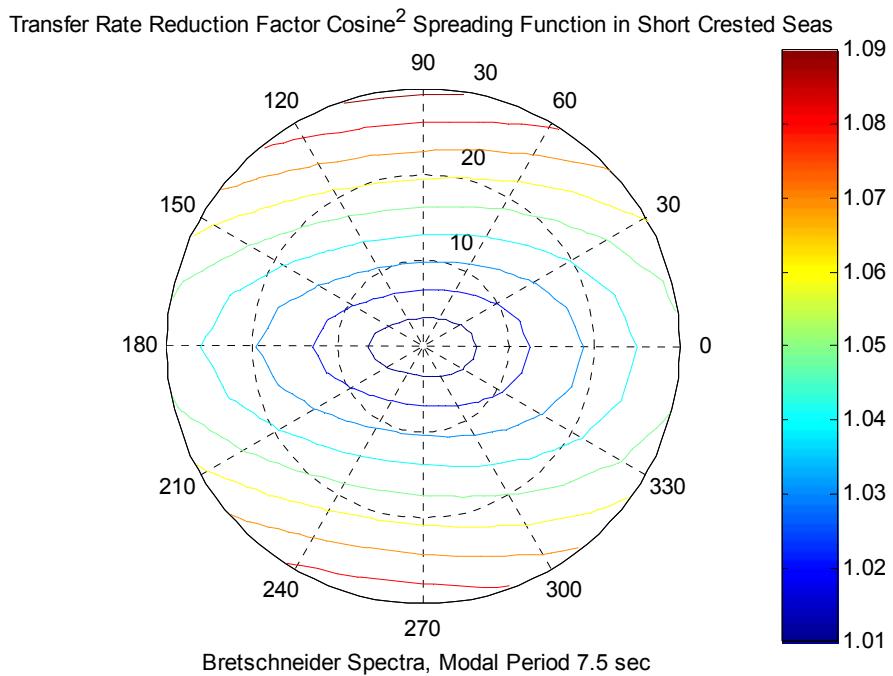
Figure 76.　　Transfer Rate Reduction Factor in Short Crested Seas Bretschneider Spectra of Modal Period 7.5 seconds

Transfer Rate Reduction Factor in Long Crested Seas

Bretschneider Spectra, Modal Period 7.5 sec
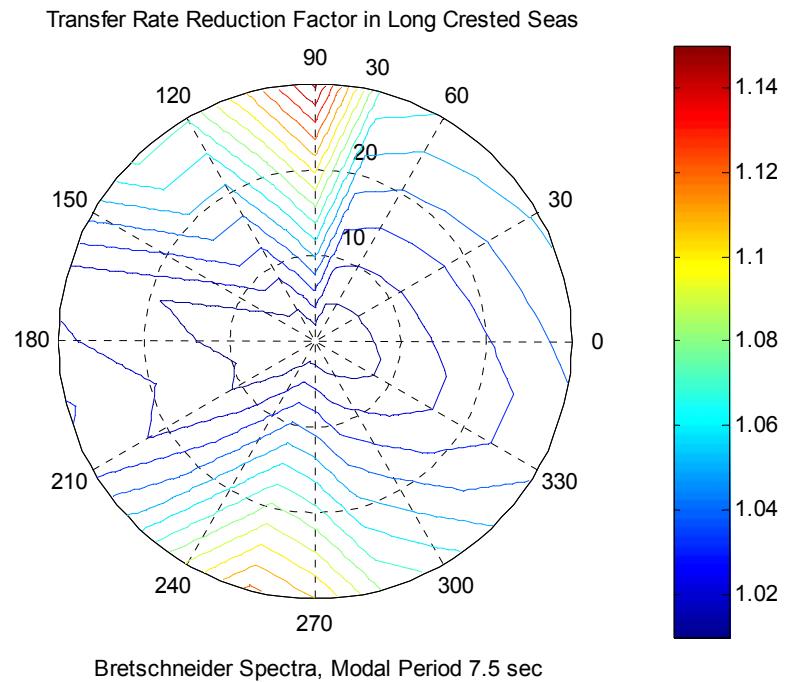
Figure 77.　　Transfer Rate Reduction Factor in Long Crested Seas Bretschneider Spectra of Modal Period 7.5 seconds.

Transfer Rate Reduction Factor Cosine² Spreading Function in Short Crested Seas
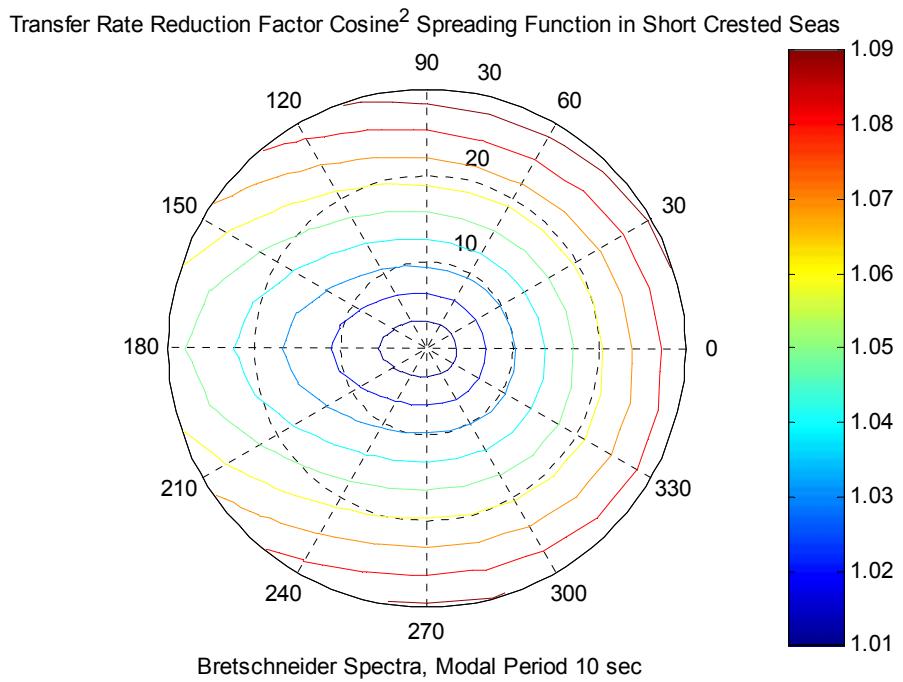
Figure 78.   Transfer Rate Reduction Factor in Short Crested Seas Bretschneider Spectra of Modal Period 10 seconds
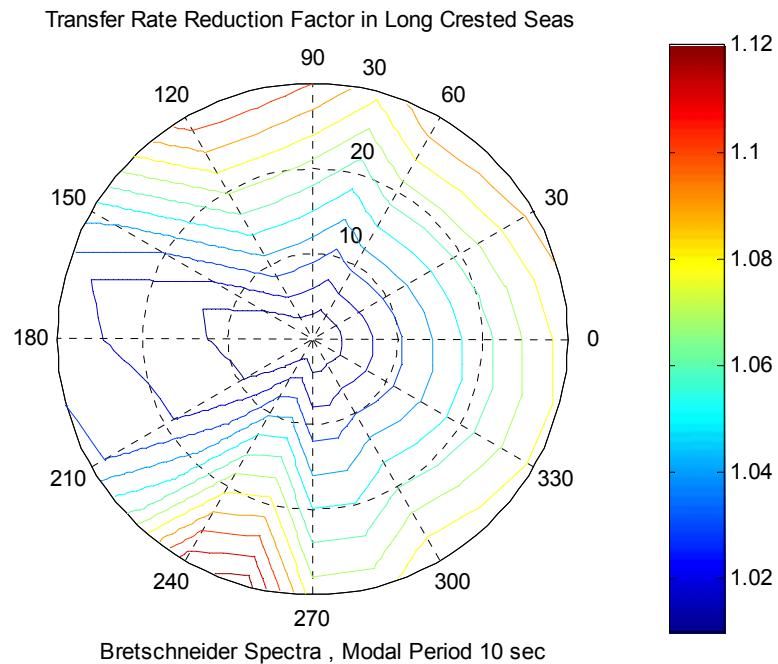
Figure 79.   Transfer Rate Reduction Factor in Long Crested Seas Bretschneider Spectra of Modal Period 10 seconds.

71
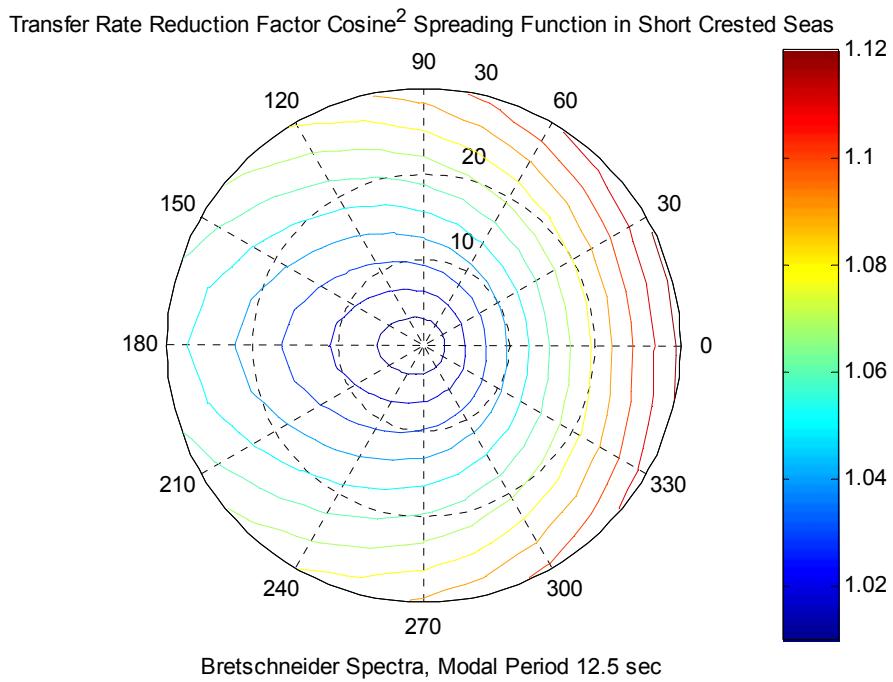
Figure 80.   Transfer Rate Reduction Factor in Short Crested
Seas Bretschneider Spectra of Modal Period 12.5 seconds
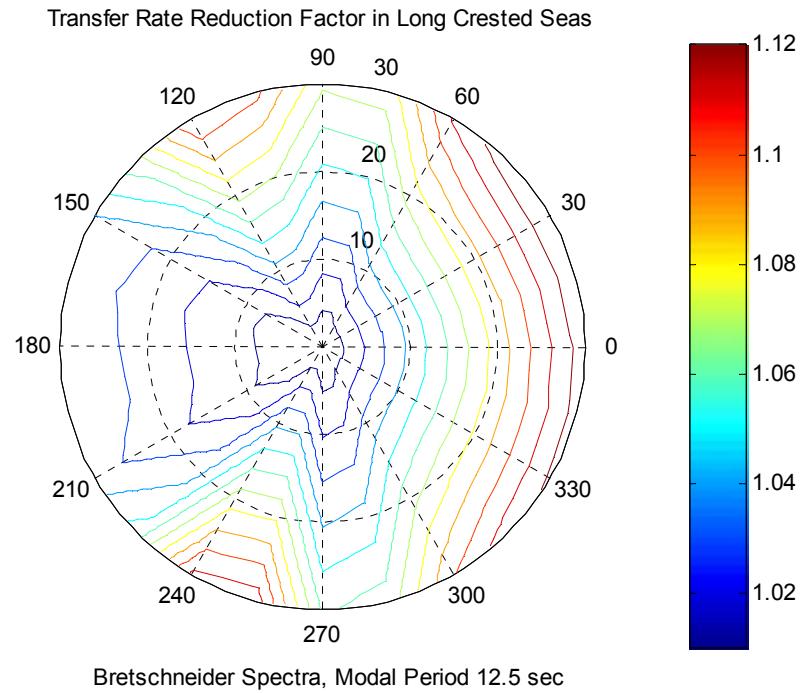
Figure 81.   Transfer Rate Reduction Factor in Long Crested
Seas Bretschneider Spectra of Modal Period 12.5 seconds.

Difference in the Transfer Time: Long Crested-Short Crested Waves (seconds)
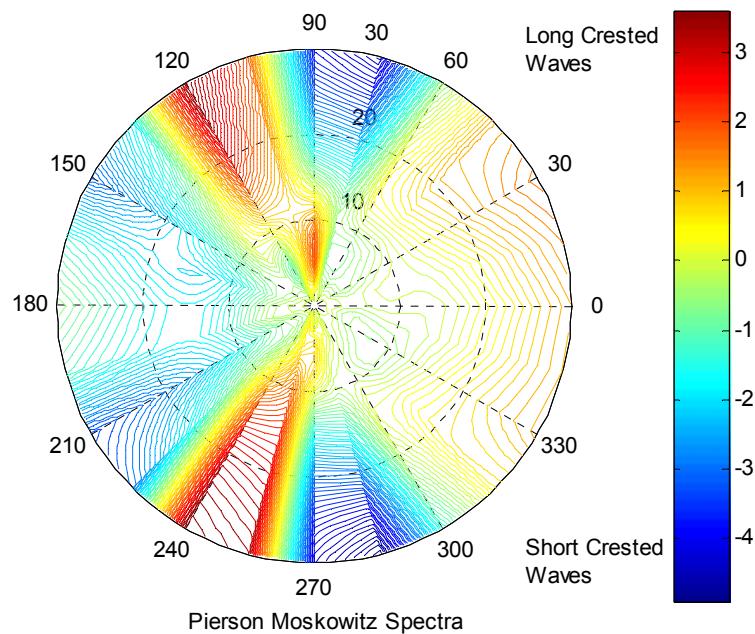
Figure 82.   Comparison of Expected Transfer Time for Long Crested and Short Crested Seas with Pierson Moskowitz Spectra.

Difference in the Transfer Time: Long Crested-Short Crested Waves (seconds)
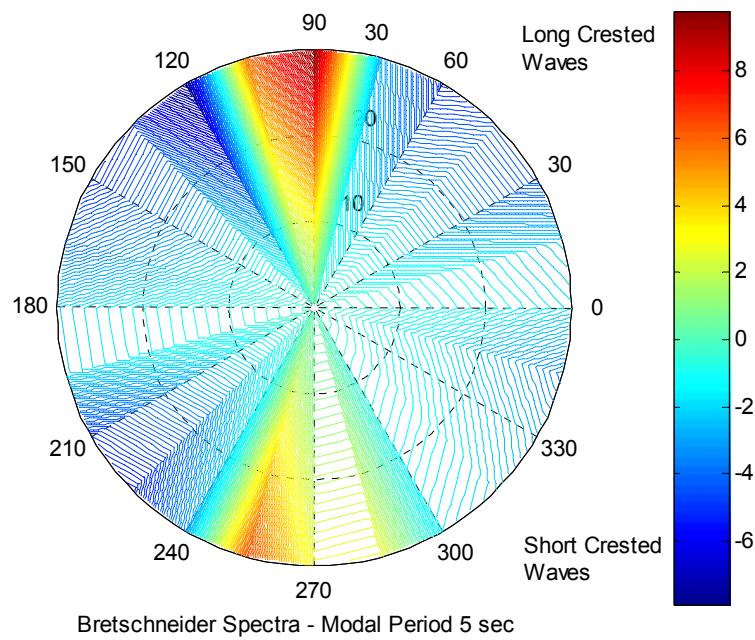
Figure 83.   Comparison of Expected Transfer Time for Long Crested and Short Crested Seas with Bretschneider Spectra of Modal Period 5 seconds.

Difference in the Transfer Time: Long Crested-Short Crested Waves (seconds)

Bretschneider Spectra - Modal Period 7.5 sec
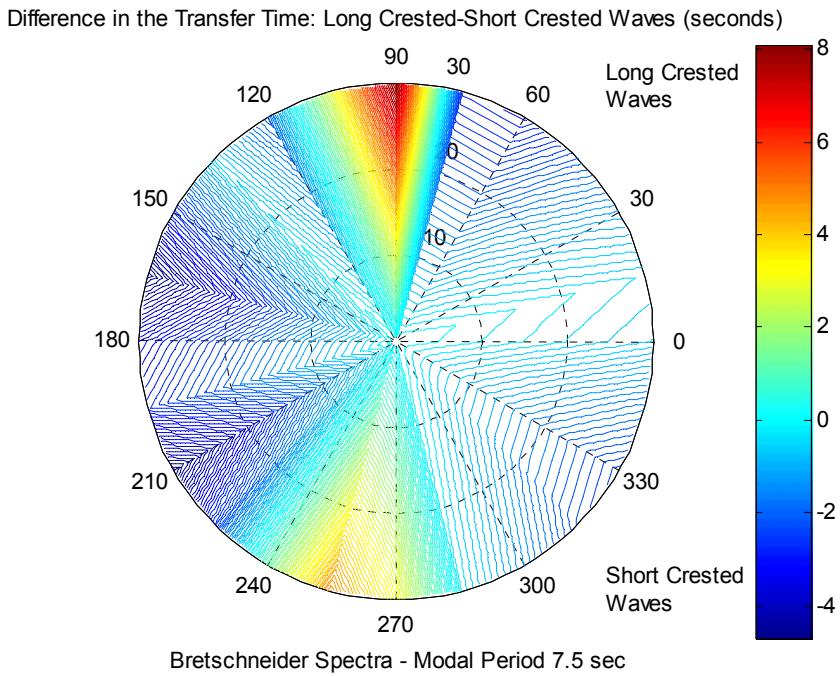
Figure 84.   Comparison of Expected Transfer Time for Long
Crested and Short Crested Seas with Bretschneider Spectra of
Modal Period 7.5 seconds.

Difference in the Transfer Time: Long Crested-Short Crested Waves (seconds)

Bretschneider Spectra - Modal Period 10 sec
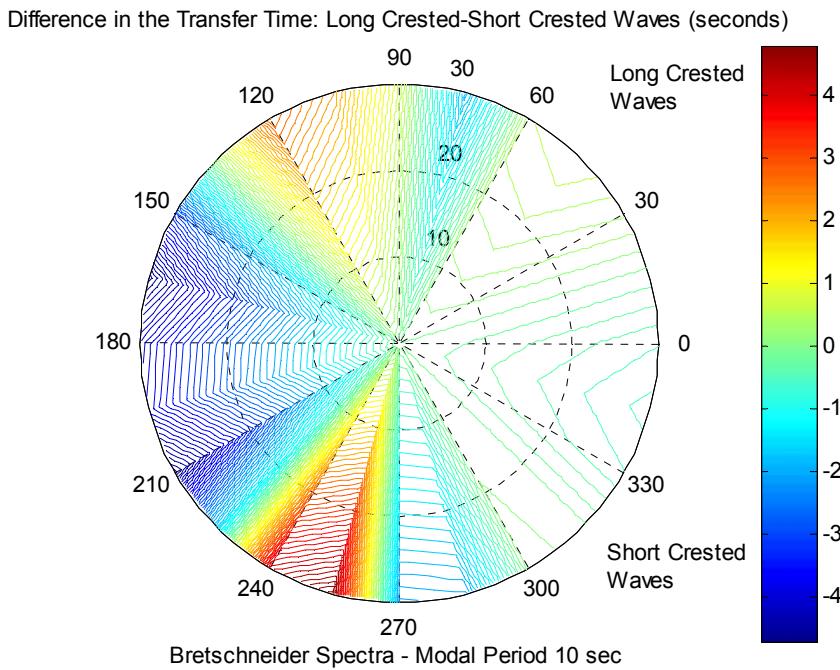
Figure 85.   Comparison of Expected Transfer Time for Long
Crested and Short Crested Seas with Bretschneider Spectra of
Modal Period 10 seconds.

74

Difference in the Transfer Time: Long Crested-Short Crested Waves (seconds)

Bretschneider Spectra - Modal Period 12.5 sec
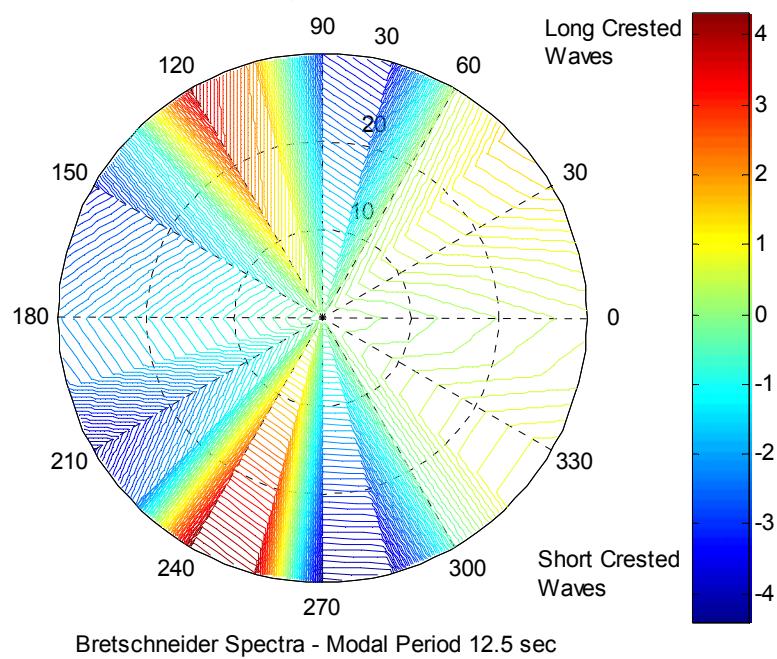
Figure 86.   Comparison of Expected Transfer Time for Long
Crested and Short Crested Seas with Bretschneider Spectra of
Modal Period 12.5 seconds.

THIS PAGE INTENTIONALLY LEFT BLANK

V. CONCLUSIONS AND RECOMMENDATIONS

A. CONCLUSIONS

In the design of the hybrid trolley interface the maximum effects on the motions of the trolley are predominantly specified by the parameters of average trolley angle and the angle of twist of the trolley. A realistic three dimension seaway representing short crested seas has been implemented in MATLAB by introducing a cosine square and higher order cosine dispersion formulation. This allows the simulation of the response of the trolley interface to be conducted in a realistic seaway. A comparison of the effect on magnitudes and directionality on the trolley in both long crested and short crested indicates the dependency on directionality typical in long crested seas is significantly reduced in short crested seas. As expected the multi-directional wave pattern of the short crested seas, spreads the available energy of the spectrum over a large range of directions, from -90 to +90 from the prominent wave heading, this has the effect of producing less trolley response over all sectors. The influence of short crested seas was significant for trolley twist angle. The largest difference in magnitudes was observed in short crested Bretschneider spectra with modal period of 7.5 seconds where the twist angle of 2.89° was encountered. Comparatively, long crested seaway predicted a response almost double the amount and confined to four 30° quadrants. Short crested seas has modest influence on the parameter of average elevation of the trolley, a 10% difference was encountered in long crested Pierson

Moskowitz spectra. The results also indicate that the difference in seaway modeling has little impact on the absolute magnitude of transfer rate because of the small difference in RMS values of the trolley angle.

In conclusion, long crested seaway modeling inherently underrates data in non-prominent wave directions while overrating data in incident wave directions. Using the results from short crested seas with a directional spreading function, information on the coupled dynamical responses of the system in all directions was obtained.

B.   RECOMMENDATIONS FOR FUTURE WORK

1.   Bimodal Wave Energy Dispersion

There may be instances where the trolley interface is employed in open waters away from the sheltering offered by coastal waters. The effects of swell and wind veering may be significant and Bi-modal modeling of directional spreading phenomenon to include these effects arriving from different sources may yield results that will affect the robustness of the design. Bi-modal spreading can be modeled using the Maximum Entropy Method.

2.   Side Trolley Placement

The CAPE D has the ability to conduct transfer at sea via a side ramp instead of a stern ramp. In this position, a trolley interface fitted onto the ramp will be faced with substantial hydrodynamic interaction from the ship and the RRDF. From the results obtained in this thesis, the effect of beam seas on trolley twist and trolley angle was found

to be most significant in short crested Bretschneider with a modal period of 7.5 seconds or less. In a side trolley placement mode, depending on the phase difference between the incident and diffracted waves, these effects can be further magnified. Future work in this area can assist in determining the scale of the effect on the motions of the trolley.

THIS PAGE INTENTIONALLY LEFT BLANK

APPENDIX A

MATLAB CODE

```
% ------------------------------------------------------------------------------------------------------------------
% Motions calculation for CapeD/RRDF/trolley interface.
% Short-crested Two Parameter Bretschneider spectrum or Pierson Moskowitz spectrum.
% ------------------------------------------------------------------------------------------------------------------
i_cosine=input('Select the power of the cosine spreading function 2, 6 or 8 = ');
i_seaway=input('Enter 0 for PM or 1 for Bretchneider spectrum = ');
if i_seaway == 1;
   T_m =input('Modal Period (sec) = ');
   omega_m=2*pi/T_m;
   disp('                    ');
   disp(['Bretschneider Sprectrum of Modal Period = ',num2str(T_m),' seconds']);
else
    disp('                    ');
    disp('Pierson Moskowitz Spectrum');
end
%Selecting the Cosine Spreading Function
if i_cosine ==8 ;
   spreadconstant= 1.1641;
   disp('Cosine^8 Spreading Function');
elseif i_cosine == 6;
   spreadconstant=1.0186;
   disp('Cosine^6 Spreading Function');
else
   spreadconstant=2/pi;
   disp('Cosine^2 Spreading Function');
end
%
mu=0.2;
time_0=2.25;
%
x_arm_CAPED_1=-330;
x_arm_CAPED_2=-330;
y_arm_CAPED_1=-10;
y_arm_CAPED_2=+10;
x_arm_RRDF_1=20;
x_arm_RRDF_2=20;
y_arm_RRDF_1=-10;
y_arm_RRDF_2=+10;1
trolley_length=100;
%
% Load processed WAMIT data file
%
load CAPED
NH=25;
i_NH=15;
beta_incr=i_NH;
```

81

```
imag_unit=sqrt(-1);
%
% Set the frequencies vector (0.3 to 2.5 rad/sec)
%
NF=(size(frequencies));
NF=NF(1,1);
w=frequencies;
%
% Set the headings vector (0 to 360 degrees in i_NH deg. =  25 increments)
%
for i=1:NH;
   heading(i)=i_NH*(i-1);
end
%
% Set added mass and damping matrices and forcing vector
%
for i=1:NF;
   i_string=num2str(i);
   A(:,:,i)=eval(strcat('admassfreq',i_string));
   B(:,:,i)=eval(strcat('addumpingfreq',i_string));
   for j=1:NH;
      j_string=num2str(j);
      if j==NH
         j_string=num2str(1);
      end
      F(:,i,j)=eval(strcat('forcfreq',i_string,'head',j_string));
   end
end
% -----------------------------------------------------------------------------------------------------
% RANDOM WAVE CALCULATIONS
% PM spectrum - weighted by the Cosine square spreading function
% -----------------------------------------------------------------------------------------------------

%------------------------------------------------------------------------------------------------------
% Level 1 :MAIN Loop on Significant Wave Height : HS
%------------------------------------------------------------------------------------------------------
iHS=0;
for HS=0.5:0.5:30,
   HS
   iHS=iHS+1;
   if i_seaway ==0
      omega_m=0.4*sqrt(32.2/HS);
   end
   A_s=(1.25/4)*(omega_m^4)*(HS^2);
   B_s=1.25*omega_m^4;
   S_main=(A_s./w.^5).*exp(-B_s./w.^4);        % Two parameter Bretschneider Spectrum
   %----------------------------------------------------------------
   %Level 2: Loop on Dominant Sea Direction, Beta
   %----------------------------------------------------------------
   ibeta=0;
   for beta=0:beta_incr:360,                % beta_incr = 15
      beta_set=beta;
      ibeta=ibeta+1;
      %
      % Spreading between (beta-90) and (beta+90)  where beta is the dominant wave angle
```

```
%
beta_spread_low  = beta_set - 90;
beta_spread_high = beta_set + 90;
ibeta_spread=0;
%------------------------------------------------------------------------------------------------------
%Level 3a: Loop on Spreading Function, Beta_spread (beta-90) and (beta+90)
%------------------------------------------------------------------------------------------------------
for beta_spread=beta_spread_low:beta_incr:beta_spread_high,
   ibeta_spread = ibeta_spread + 1;
   beta_spread_read=beta_spread;
   beta_spread_vector(ibeta_spread)=beta_spread;
   if beta_spread < 0
      beta_spread_read =360+beta_spread;
   end
   if beta_spread > 360
      beta_spread_read = beta_spread-360;
   end
   delta_beta(ibeta_spread)=beta_set-beta_spread;
   ibeta_spread_read = beta_spread_read/beta_incr + 1;
% ---------------------------------------------------------------------------------------------------------
 % Incoporate Cosine Square Spreading Function into Bretschenider Spectrum : Multiply by
(2/pi)cos^2
% ---------------------------------------------------------------------------------------------------------
   S=S_main *(spreadconstant)*(cos((beta_set-beta_spread)*pi/180))^2;
   heading_single=heading(ibeta_spread);
   % ------------------------------------------------------
   % Level 4 : Loop on Frequency Response
   % ------------------------------------------------------
   for i=1:NF,
      w_single=w(i); %Frequency domain response is given by x= [-w^2*(A+mass)+
i*w*B+C]^(-1)*F
        A_bar=-w_single*w_single*(A(:,:,i))+imag_unit*w_single*B(:,:,i)+C;
        F_bar=F(:,i,ibeta_spread_read);
        x=inv(A_bar)*F_bar;
        %
        % Extract 6 DOF CAPED RAO motions for 30 frequencies:
        %
        surge_CAPED(i) = x(1);
        sway_CAPED(i)  = x(2);
        heave_CAPED(i) = x(3);
        roll_CAPED(i)  = x(4);
        pitch_CAPED(i) = x(5);
        yaw_CAPED(i)   = x(6);
        %
        % Extract 6 DOF RRDF RAO motions for 30 frequencies:
        %
        surge_RRDF(i) = x(7);
        sway_RRDF(i)  = x(8);
        heave_RRDF(i) = x(9);
        roll_RRDF(i)  = x(10);
        pitch_RRDF(i) = x(11);
        yaw_RRDF(i)   = x(12);
        %
        %CAPED side : Motions/velocities/accelerations at trolley end
        %
```

```
m_t_CAPED_v_1(i)=heave_CAPED(i)-x_arm_CAPED_1*pitch_CAPED(i)...
    -y_arm_CAPED_1*roll_CAPED(i);
m_t_CAPED_v_2(i)=heave_CAPED(i)-x_arm_CAPED_2*pitch_CAPED(i)...
    -y_arm_CAPED_2*roll_CAPED(i);
m_t_CAPED_h_1(i)=sway_CAPED(i)+x_arm_CAPED_1*yaw_CAPED(i);
m_t_CAPED_h_2(i)=sway_CAPED(i)+x_arm_CAPED_2*yaw_CAPED(i);
v_t_CAPED_v_1(i)=imag_unit*w_single*m_t_CAPED_v_1(i);
v_t_CAPED_v_2(i)=imag_unit*w_single*m_t_CAPED_v_2(i);
v_t_CAPED_h_1(i)=imag_unit*w_single*m_t_CAPED_h_1(i);
v_t_CAPED_h_2(i)=imag_unit*w_single*m_t_CAPED_h_2(i);
a_t_CAPED_v_1(i)=-w_single*w_single*m_t_CAPED_v_1(i);
a_t_CAPED_v_2(i)=-w_single*w_single*m_t_CAPED_v_2(i);
a_t_CAPED_h_1(i)=-w_single*w_single*m_t_CAPED_h_1(i);
a_t_CAPED_h_2(i)=-w_single*w_single*m_t_CAPED_h_2(i);
%
%RRDF side : Motions/velocities/accelerations at trolley end
%
m_t_RRDF_v_1(i)=heave_RRDF(i)-x_arm_RRDF_1*pitch_RRDF(i);
m_t_RRDF_v_2(i)=heave_RRDF(i)-x_arm_RRDF_2*pitch_RRDF(i);
m_t_RRDF_h_1(i)=sway_RRDF(i)+x_arm_RRDF_1*yaw_RRDF(i);
m_t_RRDF_h_2(i)=sway_RRDF(i)+x_arm_RRDF_2*yaw_RRDF(i);
v_t_RRDF_v_1(i)=imag_unit*w_single*m_t_RRDF_v_1(i);
v_t_RRDF_v_2(i)=imag_unit*w_single*m_t_RRDF_v_2(i);
v_t_RRDF_h_1(i)=imag_unit*w_single*m_t_RRDF_h_1(i);
v_t_RRDF_h_2(i)=imag_unit*w_single*m_t_RRDF_h_2(i);
a_t_RRDF_v_1(i)=-w_single*w_single*m_t_RRDF_v_1(i);
a_t_RRDF_v_2(i)=-w_single*w_single*m_t_RRDF_v_2(i);
a_t_RRDF_h_1(i)=-w_single*w_single*m_t_RRDF_h_1(i);
a_t_RRDF_h_2(i)=-w_single*w_single*m_t_RRDF_h_2(i);
%
% Trolley relative vertical angular displacement
%
m_trolley_angle_v_1(i)=(abs(heave_CAPED(i))-
x_arm_CAPED_1*abs(pitch_CAPED(i))...
    -y_arm_CAPED_1*abs(roll_CAPED(i))-(abs(heave_RRDF(i))-
x_arm_RRDF_1*abs(pitch_RRDF(i))...
    -y_arm_RRDF_1*abs(roll_RRDF(i))))/trolley_length;
m_trolley_angle_v_2(i)=(abs(heave_CAPED(i))-
x_arm_CAPED_2*abs(pitch_CAPED(i))...
    -y_arm_CAPED_2*abs(roll_CAPED(i))-(abs(heave_RRDF(i))-
x_arm_RRDF_2*abs(pitch_RRDF(i))...
    -y_arm_RRDF_2*abs(roll_RRDF(i))))/trolley_length;
v_trolley_angle_v_1(i)=imag_unit*w_single*m_trolley_angle_v_1(i);
v_trolley_angle_v_2(i)=imag_unit*w_single*m_trolley_angle_v_2(i);
a_trolley_angle_v_1(i)=-w_single*w_single*m_trolley_angle_v_1(i);
a_trolley_angle_v_2(i)=-w_single*w_single*m_trolley_angle_v_2(i);
m_trolley_angle_v_twist(i)=m_trolley_angle_v_1(i)-m_trolley_angle_v_2(i);
m_trolley_angle_v_average(i)=0.5*(m_trolley_angle_v_1(i)+m_trolley_angle_v_2(i));
%
% Trolley relative horizontal displacement
%
m_trolley_distance_h_1(i)=(m_t_CAPED_h_1(i)-m_t_RRDF_h_1(i));
m_trolley_distance_h_2(i)=(m_t_CAPED_h_2(i)-m_t_RRDF_h_2(i));
v_trolley_distance_h_1(i)=imag_unit*w_single*m_trolley_distance_h_1(i);
v_trolley_distance_h_2(i)=imag_unit*w_single*m_trolley_distance_h_2(i);
```

```matlab
        a_trolley_distance_h_1(i)=-w_single*w_single*m_trolley_distance_h_1(i);
        a_trolley_distance_h_2(i)=-w_single*w_single*m_trolley_distance_h_2(i);
    end  %---End Level 4 : Frequency Response Loop----------
    % ----------------------------------------------------------------------------------------------------
    % Define response spectra : RAO*S_main(w)*cos^2(beta_set-beta_spread)
    % ----------------------------------------------------------------------------------------------------
    S_surge_CAPED(:,ibeta_spread) = ((abs(surge_CAPED)).^2)'.*S;
    S_surge_RRDF(:,ibeta_spread)  = ((abs(surge_RRDF)).^2)'.*S;
    S_heave_CAPED(:,ibeta_spread) = ((abs(heave_CAPED)).^2)'.*S;
    S_heave_RRDF(:,ibeta_spread)  = ((abs(heave_RRDF)).^2)'.*S;
    S_sway_CAPED(:,ibeta_spread)  = ((abs(sway_CAPED)).^2)'.*S;
    S_sway_RRDF(:,ibeta_spread)   = ((abs(sway_RRDF)).^2)'.*S;
    S_roll_CAPED(:,ibeta_spread)  = ((abs(roll_CAPED)).^2)'.*S;
    S_roll_RRDF(:,ibeta_spread)   = ((abs(roll_RRDF)).^2)'.*S;
    S_pitch_CAPED(:,ibeta_spread) = ((abs(pitch_CAPED)).^2)'.*S;
    S_pitch_RRDF(:,ibeta_spread)  = ((abs(pitch_RRDF)).^2)'.*S;
    S_yaw_CAPED(:,ibeta_spread)   = ((abs(yaw_CAPED)).^2)'.*S;
    S_yaw_RRDF(:,ibeta_spread)    = ((abs(yaw_RRDF)).^2)'.*S;
    %
    S_m_t_CAPED_v_1(:,ibeta_spread) = ((abs(m_t_CAPED_v_1)).^2)'.*S;
    S_m_t_CAPED_v_2(:,ibeta_spread) = ((abs(m_t_CAPED_v_2)).^2)'.*S;
    S_m_t_CAPED_h_1(:,ibeta_spread) = ((abs(m_t_CAPED_h_1)).^2)'.*S;
    S_m_t_CAPED_h_2(:,ibeta_spread) = ((abs(m_t_CAPED_h_2)).^2)'.*S;
    S_v_t_CAPED_v_1(:,ibeta_spread) = ((abs(v_t_CAPED_v_1)).^2)'.*S;
    S_v_t_CAPED_v_2(:,ibeta_spread) = ((abs(v_t_CAPED_v_2)).^2)'.*S;
    S_v_t_CAPED_h_1(:,ibeta_spread) = ((abs(v_t_CAPED_h_1)).^2)'.*S;
    S_v_t_CAPED_h_2(:,ibeta_spread) = ((abs(v_t_CAPED_h_2)).^2)'.*S;
    S_a_t_CAPED_v_1(:,ibeta_spread) = ((abs(a_t_CAPED_v_1)).^2)'.*S;
    S_a_t_CAPED_v_2(:,ibeta_spread) = ((abs(a_t_CAPED_v_2)).^2)'.*S;
    S_a_t_CAPED_h_1(:,ibeta_spread) = ((abs(a_t_CAPED_h_1)).^2)'.*S;
    S_a_t_CAPED_h_2(:,ibeta_spread) = ((abs(a_t_CAPED_h_2)).^2)'.*S;
    %
    S_m_t_RRDF_v_1(:,ibeta_spread)  = ((abs(m_t_RRDF_v_1)).^2)'.*S;
    S_m_t_RRDF_v_2(:,ibeta_spread)  = ((abs(m_t_RRDF_v_2)).^2)'.*S;
    S_m_t_RRDF_h_1(:,ibeta_spread)  = ((abs(m_t_RRDF_h_1)).^2)'.*S;
    S_m_t_RRDF_h_2(:,ibeta_spread)  = ((abs(m_t_RRDF_h_2)).^2)'.*S;
    S_v_t_RRDF_v_1(:,ibeta_spread)  = ((abs(v_t_RRDF_v_1)).^2)'.*S;
    S_v_t_RRDF_v_2(:,ibeta_spread)  = ((abs(v_t_RRDF_v_2)).^2)'.*S;
    S_v_t_RRDF_h_1(:,ibeta_spread)  = ((abs(v_t_RRDF_h_1)).^2)'.*S;
    S_v_t_RRDF_h_2(:,ibeta_spread)  = ((abs(v_t_RRDF_h_2)).^2)'.*S;
    S_a_t_RRDF_v_1(:,ibeta_spread)  = ((abs(a_t_RRDF_v_1)).^2)'.*S;
    S_a_t_RRDF_v_2(:,ibeta_spread)  = ((abs(a_t_RRDF_v_2)).^2)'.*S;
    S_a_t_RRDF_h_1(:,ibeta_spread)  = ((abs(a_t_RRDF_h_1)).^2)'.*S;
    S_a_t_RRDF_h_2(:,ibeta_spread)  = ((abs(a_t_RRDF_h_2)).^2)'.*S;
    %
    S_m_trolley_angle_v_1(:,ibeta_spread) = ((abs(m_trolley_angle_v_1)).^2)'.*S;
    S_m_trolley_angle_v_2(:,ibeta_spread) = ((abs(m_trolley_angle_v_2)).^2)'.*S;
    S_v_trolley_angle_v_1(:,ibeta_spread) = ((abs(v_trolley_angle_v_1)).^2)'.*S;
    S_v_trolley_angle_v_2(:,ibeta_spread) = ((abs(v_trolley_angle_v_2)).^2)'.*S;
    S_a_trolley_angle_v_1(:,ibeta_spread) = ((abs(a_trolley_angle_v_1)).^2)'.*S;
    S_a_trolley_angle_v_2(:,ibeta_spread) = ((abs(a_trolley_angle_v_2)).^2)'.*S;
    S_m_trolley_angle_v_twist(:,ibeta_spread) = ((abs(m_trolley_angle_v_twist))'.^2).*S;
    %
    S_m_trolley_angle_v_average(:,ibeta_spread) =
((abs(m_trolley_angle_v_average))'.^2).*S;
```

```
        S_m_trolley_distance_h_1(:,ibeta_spread) = ((abs(m_trolley_distance_h_1))'.^2).*S;
        S_m_trolley_distance_h_2(:,ibeta_spread) = ((abs(m_trolley_distance_h_2))'.^2).*S;
        S_v_trolley_distance_h_1(:,ibeta_spread) = ((abs(v_trolley_distance_h_1))'.^2).*S;
        S_v_trolley_distance_h_2(:,ibeta_spread) = ((abs(v_trolley_distance_h_2))'.^2).*S;
        S_a_trolley_distance_h_1(:,ibeta_spread) = ((abs(a_trolley_distance_h_1))'.^2).*S;
        S_a_trolley_distance_h_2(:,ibeta_spread) = ((abs(a_trolley_distance_h_2))'.^2).*S;
    %
end % -----End Level 3 : Loop on beta_spreading function ----------------
%
% Integral initializations
%
S_surge_CAPED_i = 0;
S_surge_RRDF_i  = 0;
S_heave_CAPED_i = 0;
S_heave_RRDF_i  = 0;
S_sway_CAPED_i  = 0;
S_sway_RRDF_i   = 0;
S_roll_CAPED_i  = 0;
S_roll_RRDF_i   = 0;
S_pitch_CAPED_i = 0;
S_pitch_RRDF_i  = 0;
S_yaw_CAPED_i   = 0;
S_yaw_RRDF_i    = 0;
S_m_t_CAPED_v_1_i = 0;
S_m_t_CAPED_h_1_i = 0;
S_v_t_CAPED_v_1_i = 0;
S_v_t_CAPED_h_1_i = 0;
S_a_t_CAPED_v_1_i = 0;
S_a_t_CAPED_h_1_i = 0;
S_m_t_RRDF_v_1_i  = 0;
S_m_t_RRDF_h_1_i  = 0;
S_v_t_RRDF_v_1_i  = 0;
S_v_t_RRDF_h_1_i  = 0;
S_a_t_RRDF_v_1_i  = 0;
S_a_t_RRDF_h_1_i  = 0;
S_m_trolley_angle_v_1_i = 0;
S_v_trolley_angle_v_1_i = 0;
S_a_trolley_angle_v_1_i = 0;
S_m_trolley_distance_h_1_i = 0;
S_v_trolley_distance_h_1_i = 0;
S_a_trolley_distance_h_1_i = 0;
S_m_t_CAPED_v_2_i = 0;
S_m_t_CAPED_h_2_i = 0;
S_v_t_CAPED_v_2_i = 0;
S_v_t_CAPED_h_2_i = 0;
S_a_t_CAPED_v_2_i = 0;
S_a_t_CAPED_h_2_i = 0;
S_m_t_RRDF_v_2_i  = 0;
S_m_t_RRDF_h_2_i  = 0;
S_v_t_RRDF_v_2_i  = 0;
S_v_t_RRDF_h_2_i  = 0;
S_a_t_RRDF_v_2_i  = 0;
S_a_t_RRDF_h_2_i  = 0;
S_m_trolley_angle_v_2_i = 0;
S_v_trolley_angle_v_2_i = 0;
```

```
    S_a_trolley_angle_v_2_i = 0;
    S_m_trolley_distance_h_2_i = 0;
    S_v_trolley_distance_h_2_i = 0;
    S_a_trolley_distance_h_2_i = 0;
    S_m_trolley_angle_v_twist_i = 0;
    S_m_trolley_angle_v_average_i = 0;
    %-------------------------------------------------------------------------------------------------------
    %Level 3b: Integration Loop : Integrate response spectra over omega and theta
    %-------------------------------------------------------------------------------------------------------
    for J=2:1:13,      % step size of 15deg => 13 increments
        for I=2:1:NF,
            %
            delta_omega=abs(w(I-1)-w(I));
            delta_theta=beta_incr*pi/180;
            % SURGE
            S_surge_CAPED_sum = S_surge_CAPED(I,J) + S_surge_CAPED(I-1,J) +
S_surge_CAPED(I,J-1) + S_surge_CAPED(I-1,J-1);
            S_surge_CAPED_i  = S_surge_CAPED_i +
0.25*delta_omega*delta_theta*S_surge_CAPED_sum;
            S_surge_RRDF_sum  = S_surge_RRDF(I,J) + S_surge_RRDF(I-1,J) +
S_surge_RRDF(I,J-1) + S_surge_RRDF(I-1,J-1);
            S_surge_RRDF_i   = S_surge_RRDF_i +
0.25*delta_omega*delta_theta*S_surge_RRDF_sum;
            % HEAVE
            S_heave_CAPED_sum = S_heave_CAPED(I,J) + S_heave_CAPED(I-1,J) +
S_heave_CAPED(I,J-1) + S_heave_CAPED(I-1,J-1);
            S_heave_CAPED_i  = S_heave_CAPED_i +
0.25*delta_omega*delta_theta*S_heave_CAPED_sum;
            S_heave_RRDF_sum  = S_heave_RRDF(I,J) + S_heave_RRDF(I-1,J) +
S_heave_RRDF(I,J-1) + S_heave_RRDF(I-1,J-1);
            S_heave_RRDF_i   = S_heave_RRDF_i +
0.25*delta_omega*delta_theta*S_heave_RRDF_sum;
            % SWAY
            S_sway_CAPED_sum  = S_sway_CAPED(I,J) + S_sway_CAPED(I-1,J) +
S_sway_CAPED(I,J-1) + S_sway_CAPED(I-1,J-1);
            S_sway_CAPED_i   = S_sway_CAPED_i +
0.25*delta_omega*delta_theta*S_sway_CAPED_sum;
            S_sway_RRDF_sum   = S_sway_RRDF(I,J) + S_sway_RRDF(I-1,J) +
S_sway_RRDF(I,J-1) + S_sway_RRDF(I-1,J-1);
            S_sway_RRDF_i    = S_sway_RRDF_i +
0.25*delta_omega*delta_theta*S_sway_RRDF_sum;
            % ROLL
            S_roll_CAPED_sum  = S_roll_CAPED(I,J) + S_roll_CAPED(I-1,J) + S_roll_CAPED(I,J-
1) + S_roll_CAPED(I-1,J-1);
            S_roll_CAPED_i   = S_roll_CAPED_i +
0.25*delta_omega*delta_theta*S_roll_CAPED_sum;
            S_roll_RRDF_sum   = S_roll_RRDF(I,J) + S_roll_RRDF(I-1,J) + S_roll_RRDF(I,J-1) +
S_roll_RRDF(I-1,J-1);
            S_roll_RRDF_i    = S_roll_RRDF_i +
0.25*delta_omega*delta_theta*S_roll_RRDF_sum;
            % PITCH
            S_pitch_CAPED_sum = S_pitch_CAPED(I,J) + S_pitch_CAPED(I-1,J) +
S_pitch_CAPED(I,J-1) + S_pitch_CAPED(I-1,J-1);
            S_pitch_CAPED_i  = S_pitch_CAPED_i +
0.25*delta_omega*delta_theta*S_pitch_CAPED_sum;
```

```
        S_pitch_RRDF_sum  = S_pitch_RRDF(I,J) + S_pitch_RRDF(I-1,J) +
S_pitch_RRDF(I,J-1) + S_pitch_RRDF(I-1,J-1);
        S_pitch_RRDF_i   = S_pitch_RRDF_i +
0.25*delta_omega*delta_theta*S_pitch_RRDF_sum;
        % YAW
        S_yaw_CAPED_sum  = S_yaw_CAPED(I,J) + S_yaw_CAPED(I-1,J) +
S_yaw_CAPED(I,J-1) + S_yaw_CAPED(I-1,J-1);
        S_yaw_CAPED_i    = S_yaw_CAPED_i +
0.25*delta_omega*delta_theta*S_yaw_CAPED_sum;
        S_yaw_RRDF_sum   = S_yaw_RRDF(I,J) + S_yaw_RRDF(I-1,J) + S_yaw_RRDF(I,J-
1) + S_yaw_RRDF(I-1,J-1);
        S_yaw_RRDF_i     = S_yaw_RRDF_i +
0.25*delta_omega*delta_theta*S_yaw_RRDF_sum;


        %--------------------------------------------------------------------------------------
        % CALCULATIONS for POINT 1
        %--------------------------------------------------------------------------------------

        %Vertical Motion of CAPED
        S_m_t_CAPED_v_1_sum = S_m_t_CAPED_v_1(I,J) + S_m_t_CAPED_v_1(I-1,J) +
S_m_t_CAPED_v_1(I,J-1) + S_m_t_CAPED_v_1(I-1,J-1);
        S_m_t_CAPED_v_1_i  = S_m_t_CAPED_v_1_i +
0.25*delta_omega*delta_theta*S_m_t_CAPED_v_1_sum;
        %Horizontal Motion of CAPED
        S_m_t_CAPED_h_1_sum = S_m_t_CAPED_h_1(I,J) + S_m_t_CAPED_h_1(I-1,J) +
S_m_t_CAPED_h_1(I,J-1) + S_m_t_CAPED_h_1(I-1,J-1);
        S_m_t_CAPED_h_1_i  = S_m_t_CAPED_h_1_i +
0.25*delta_omega*delta_theta*S_m_t_CAPED_h_1_sum;
        %Vertical Velocity of CAPED
        S_v_t_CAPED_v_1_sum = S_v_t_CAPED_v_1(I,J) + S_v_t_CAPED_v_1(I-1,J) +
S_v_t_CAPED_v_1(I,J-1) + S_v_t_CAPED_v_1(I-1,J-1);
        S_v_t_CAPED_v_1_i  = S_v_t_CAPED_v_1_i +
0.25*delta_omega*delta_theta*S_v_t_CAPED_v_1_sum;
        %Horizontal Velocity of CAPED
        S_v_t_CAPED_h_1_sum = S_v_t_CAPED_h_1(I,J) + S_v_t_CAPED_h_1(I-1,J) +
S_v_t_CAPED_h_1(I,J-1) + S_v_t_CAPED_h_1(I-1,J-1);
        S_v_t_CAPED_h_1_i  = S_v_t_CAPED_h_1_i +
0.25*delta_omega*delta_theta*S_v_t_CAPED_h_1_sum;
        %Vertical Acceleration of CAPED
        S_a_t_CAPED_v_1_sum = S_a_t_CAPED_v_1(I,J) + S_a_t_CAPED_v_1(I-1,J) +
S_a_t_CAPED_v_1(I,J-1) + S_a_t_CAPED_v_1(I-1,J-1);
        S_a_t_CAPED_v_1_i  = S_a_t_CAPED_v_1_i +
0.25*delta_omega*delta_theta*S_a_t_CAPED_v_1_sum;
        %Horizontal Acceleration of CAPED
        S_a_t_CAPED_h_1_sum = S_a_t_CAPED_h_1(I,J) + S_a_t_CAPED_h_1(I-1,J) +
S_a_t_CAPED_h_1(I,J-1) + S_a_t_CAPED_h_1(I-1,J-1);
        S_a_t_CAPED_h_1_i  = S_a_t_CAPED_h_1_i +
0.25*delta_omega*delta_theta*S_a_t_CAPED_h_1_sum;
        %Vertical Motion of RRDF
        S_m_t_RRDF_v_1_sum = S_m_t_RRDF_v_1(I,J) + S_m_t_RRDF_v_1(I-1,J) +
S_m_t_RRDF_v_1(I,J-1) + S_m_t_RRDF_v_1(I-1,J-1);
        S_m_t_RRDF_v_1_i  = S_m_t_RRDF_v_1_i +
0.25*delta_omega*delta_theta*S_m_t_RRDF_v_1_sum;
        %Horizontal Motion of RRDF
```

S_m_t_RRDF_h_1_sum = S_m_t_RRDF_h_1(I,J) + S_m_t_RRDF_h_1(I-1,J) + S_m_t_RRDF_h_1(I,J-1) + S_m_t_RRDF_h_1(I-1,J-1);
S_m_t_RRDF_h_1_i   = S_m_t_RRDF_h_1_i + 0.25*delta_omega*delta_theta*S_m_t_RRDF_h_1_sum;
%Vertical Velocity of RRDF
S_v_t_RRDF_v_1_sum = S_v_t_RRDF_v_1(I,J) + S_v_t_RRDF_v_1(I-1,J) + S_v_t_RRDF_v_1(I,J-1) + S_v_t_RRDF_v_1(I-1,J-1);
S_v_t_RRDF_v_1_i   = S_v_t_RRDF_v_1_i + 0.25*delta_omega*delta_theta*S_v_t_RRDF_v_1_sum;
%Horizontal Velocity of RRDF
S_v_t_RRDF_h_1_sum = S_v_t_RRDF_h_1(I,J) + S_v_t_RRDF_h_1(I-1,J) + S_v_t_RRDF_h_1(I,J-1) + S_v_t_RRDF_h_1(I-1,J-1);
S_v_t_RRDF_h_1_i   = S_v_t_RRDF_h_1_i + 0.25*delta_omega*delta_theta*S_v_t_CAPED_h_1_sum;
%Vertical Acceleration of RRDF
S_a_t_RRDF_v_1_sum = S_a_t_RRDF_v_1(I,J) + S_a_t_RRDF_v_1(I-1,J) + S_a_t_RRDF_v_1(I,J-1) + S_a_t_RRDF_v_1(I-1,J-1);
S_a_t_RRDF_v_1_i   = S_a_t_RRDF_v_1_i + 0.25*delta_omega*delta_theta*S_a_t_RRDF_v_1_sum;
%Horizontal Acceleration of RRDF
S_a_t_RRDF_h_1_sum = S_a_t_RRDF_h_1(I,J) + S_a_t_RRDF_h_1(I-1,J) + S_a_t_RRDF_h_1(I,J-1) + S_a_t_RRDF_h_1(I-1,J-1);
S_a_t_RRDF_h_1_i   = S_a_t_RRDF_h_1_i + 0.25*delta_omega*delta_theta*S_a_t_RRDF_h_1_sum;
%Motion of Trolley Angle (Vertical Only)
S_m_trolley_angle_v_1_sum= S_m_trolley_angle_v_1(I,J) + S_m_trolley_angle_v_1(I-1,J) + S_m_trolley_angle_v_1(I,J-1) + S_m_trolley_angle_v_1(I-1,J-1);
S_m_trolley_angle_v_1_i = S_m_trolley_angle_v_1_i + 0.25*delta_omega*delta_theta*S_m_trolley_angle_v_1_sum;
%Motion of Trolley Horizontal Distance
S_m_trolley_distance_h_1_sum= S_m_trolley_distance_h_1(I,J) + S_m_trolley_distance_h_1(I-1,J) + S_m_trolley_distance_h_1(I,J-1) + S_m_trolley_distance_h_1(I-1,J-1);
S_m_trolley_distance_h_1_i = S_m_trolley_distance_h_1_i+ 0.25*delta_omega*delta_theta*S_m_trolley_distance_h_1_sum;
%S_v_trolley_angle_v_1_i
S_v_trolley_angle_v_1_sum= S_v_trolley_angle_v_1(I,J) + S_v_trolley_angle_v_1(I-1,J) + S_v_trolley_angle_v_1(I,J-1) + S_v_trolley_angle_v_1(I-1,J-1);
S_v_trolley_angle_v_1_i = S_v_trolley_angle_v_1_i+ 0.25*delta_omega*delta_theta*S_v_trolley_angle_v_1_sum;
%S_a_trolley_angle_v_1_i
S_a_trolley_angle_v_1_sum= S_a_trolley_angle_v_1(I,J) + S_a_trolley_angle_v_1(I-1,J) + S_a_trolley_angle_v_1(I,J-1) + S_a_trolley_angle_v_1(I-1,J-1);
S_a_trolley_angle_v_1_i = S_a_trolley_angle_v_1_i+ 0.25*delta_omega*delta_theta*S_a_trolley_angle_v_1_sum;
%S_v_trolley_distance_h_1_i
S_v_trolley_distance_h_1_sum= S_v_trolley_distance_h_1(I,J) + S_v_trolley_distance_h_1(I-1,J) + S_v_trolley_distance_h_1(I,J-1) + S_v_trolley_distance_h_1(I-1,J-1);
S_v_trolley_distance_h_1_i = S_v_trolley_distance_h_1_i+ 0.25*delta_omega*delta_theta*S_v_trolley_distance_h_1_sum;
%S_a_trolley_distance_h_1_i
S_a_trolley_distance_h_1_sum= S_a_trolley_distance_h_1(I,J) + S_a_trolley_distance_h_1(I-1,J) + S_a_trolley_distance_h_1(I,J-1) + S_a_trolley_distance_h_1(I-1,J-1);

S_a_trolley_distance_h_1_i = S_a_trolley_distance_h_1_i+
0.25*delta_omega*delta_theta*S_a_trolley_distance_h_1_sum;
%
%--
% CALCULATIONS for POINT 2
%--
%
%Vertical Motion of CAPED
S_m_t_CAPED_v_2_sum = S_m_t_CAPED_v_2(I,J) + S_m_t_CAPED_v_2(I-1,J) +
S_m_t_CAPED_v_2(I,J-1) + S_m_t_CAPED_v_2(I-1,J-1);
S_m_t_CAPED_v_2_i   = S_m_t_CAPED_v_2_i +
0.25*delta_omega*delta_theta*S_m_t_CAPED_v_2_sum;
%Horizontal Motion of CAPED
S_m_t_CAPED_h_2_sum = S_m_t_CAPED_h_2(I,J) + S_m_t_CAPED_h_1(I-1,J) +
S_m_t_CAPED_h_1(I,J-1) + S_m_t_CAPED_h_1(I-1,J-1);
S_m_t_CAPED_h_2_i   = S_m_t_CAPED_h_2_i +
0.25*delta_omega*delta_theta*S_m_t_CAPED_h_1_sum;
%Vertical Velocity of CAPED
S_v_t_CAPED_v_2_sum = S_v_t_CAPED_v_2(I,J) + S_v_t_CAPED_v_2(I-1,J) +
S_v_t_CAPED_v_2(I,J-1) + S_v_t_CAPED_v_2(I-1,J-1);
S_v_t_CAPED_v_2_i   = S_v_t_CAPED_v_2_i +
0.25*delta_omega*delta_theta*S_v_t_CAPED_v_2_sum;
%Horizontal Velocity of CAPED
S_v_t_CAPED_h_2_sum = S_v_t_CAPED_h_2(I,J) + S_v_t_CAPED_h_2(I-1,J) +
S_v_t_CAPED_h_2(I,J-1) + S_v_t_CAPED_h_2(I-1,J-1);
S_v_t_CAPED_h_2_i   = S_v_t_CAPED_h_2_i +
0.25*delta_omega*delta_theta*S_v_t_CAPED_h_2_sum;
%Vertical Acceleration of CAPED
S_a_t_CAPED_v_2_sum = S_a_t_CAPED_v_2(I,J) + S_a_t_CAPED_v_2(I-1,J) +
S_a_t_CAPED_v_2(I,J-1) + S_a_t_CAPED_v_2(I-1,J-1);
S_a_t_CAPED_v_2_i   = S_a_t_CAPED_v_2_i +
0.25*delta_omega*delta_theta*S_a_t_CAPED_v_2_sum;
%Horizontal Acceleration of CAPED
S_a_t_CAPED_h_2_sum = S_a_t_CAPED_h_2(I,J) + S_a_t_CAPED_h_2(I-1,J) +
S_a_t_CAPED_h_2(I,J-1) + S_a_t_CAPED_h_2(I-1,J-1);
S_a_t_CAPED_h_2_i   = S_a_t_CAPED_h_2_i +
0.25*delta_omega*delta_theta*S_a_t_CAPED_h_2_sum;
%Vertical Motion of RRDF
S_m_t_RRDF_v_2_sum = S_m_t_RRDF_v_2(I,J) + S_m_t_RRDF_v_2(I-1,J) +
S_m_t_RRDF_v_2(I,J-1) + S_m_t_RRDF_v_2(I-1,J-1);
S_m_t_RRDF_v_2_i   = S_m_t_RRDF_v_2_i +
0.25*delta_omega*delta_theta*S_m_t_RRDF_v_2_sum;
%Horizontal Motion of RRDF
S_m_t_RRDF_h_2_sum = S_m_t_RRDF_h_2(I,J) + S_m_t_RRDF_h_2(I-1,J) +
S_m_t_RRDF_h_2(I,J-1) + S_m_t_RRDF_h_2(I-1,J-1);
S_m_t_RRDF_h_2_i   = S_m_t_RRDF_h_2_i +
0.25*delta_omega*delta_theta*S_m_t_RRDF_h_2_sum;
%Vertical Velocity of RRDF
S_v_t_RRDF_v_2_sum = S_v_t_RRDF_v_2(I,J) + S_v_t_RRDF_v_2(I-1,J) +
S_v_t_RRDF_v_2(I,J-1) + S_v_t_RRDF_v_2(I-1,J-1);
S_v_t_RRDF_v_2_i   = S_v_t_RRDF_v_2_i +
0.25*delta_omega*delta_theta*S_v_t_RRDF_v_2_sum;
%Horizontal Velocity of RRDF
S_v_t_RRDF_h_2_sum = S_v_t_RRDF_h_2(I,J) + S_v_t_RRDF_h_2(I-1,J) +
S_v_t_RRDF_h_2(I,J-1) + S_v_t_RRDF_h_2(I-1,J-1);

S_v_t_RRDF_h_2_i = S_v_t_RRDF_h_2_i +
0.25*delta_omega*delta_theta*S_v_t_CAPED_h_2_sum;
        %Vertical Acceleration of RRDF
        S_a_t_RRDF_v_2_sum = S_a_t_RRDF_v_2(I,J) + S_a_t_RRDF_v_2(I-1,J) +
S_a_t_RRDF_v_2(I,J-1) + S_a_t_RRDF_v_2(I-1,J-1);
        S_a_t_RRDF_v_2_i = S_a_t_RRDF_v_2_i +
0.25*delta_omega*delta_theta*S_a_t_RRDF_v_2_sum;
        %Horizontal Acceleration of RRDF
        S_a_t_RRDF_h_2_sum = S_a_t_RRDF_h_2(I,J) + S_a_t_RRDF_h_2(I-1,J) +
S_a_t_RRDF_h_2(I,J-1) + S_a_t_RRDF_h_2(I-1,J-1);
        S_a_t_RRDF_h_2_i = S_a_t_RRDF_h_2_i +
0.25*delta_omega*delta_theta*S_a_t_RRDF_h_2_sum;
        %Motion of Trolley Angle (Vertical Only)
        S_m_trolley_angle_v_2_sum= S_m_trolley_angle_v_2(I,J) + S_m_trolley_angle_v_2(I-
1,J) + S_m_trolley_angle_v_2(I,J-1) + S_m_trolley_angle_v_2(I-1,J-1);
        S_m_trolley_angle_v_2_i = S_m_trolley_angle_v_2_i +
0.25*delta_omega*delta_theta*S_m_trolley_angle_v_2_sum;
        %Motion of Trolley Horizontal Distance
        S_m_trolley_distance_h_2_sum= S_m_trolley_distance_h_2(I,J) +
S_m_trolley_distance_h_2(I-1,J) + S_m_trolley_distance_h_2(I,J-1) +
S_m_trolley_distance_h_2(I-1,J-1);
        S_m_trolley_distance_h_2_i = S_m_trolley_distance_h_2_i+
0.25*delta_omega*delta_theta*S_m_trolley_distance_h_2_sum;
        %S_v_trolley_angle_v_2_i
        S_v_trolley_angle_v_2_sum= S_v_trolley_angle_v_2(I,J) + S_v_trolley_angle_v_2(I-
1,J) + S_v_trolley_angle_v_2(I,J-1) + S_v_trolley_angle_v_2(I-1,J-1);
        S_v_trolley_angle_v_2_i = S_v_trolley_angle_v_2_i+
0.25*delta_omega*delta_theta*S_v_trolley_angle_v_2_sum;
        %S_a_trolley_angle_v_2_i
        S_a_trolley_angle_v_2_sum= S_a_trolley_angle_v_2(I,J) + S_a_trolley_angle_v_2(I-
1,J) + S_a_trolley_angle_v_2(I,J-1) + S_a_trolley_angle_v_2(I-1,J-1);
        S_a_trolley_angle_v_2_i = S_a_trolley_angle_v_2_i+
0.25*delta_omega*delta_theta*S_a_trolley_angle_v_2_sum;
        %S_v_trolley_distance_h_2_i
        S_v_trolley_distance_h_2_sum= S_v_trolley_distance_h_2(I,J) +
S_v_trolley_distance_h_2(I-1,J) + S_v_trolley_distance_h_1(I,J-1) + S_v_trolley_distance_h_2(I-
1,J-1);
        S_v_trolley_distance_h_2_i = S_v_trolley_distance_h_2_i+
0.25*delta_omega*delta_theta*S_v_trolley_distance_h_2_sum;
        %S_a_trolley_distance_h_2_i
        S_a_trolley_distance_h_2_sum= S_a_trolley_distance_h_2(I,J) +
S_a_trolley_distance_h_2(I-1,J) + S_a_trolley_distance_h_1(I,J-1) + S_a_trolley_distance_h_2(I-
1,J-1);
        S_a_trolley_distance_h_2_i = S_a_trolley_distance_h_2_i+
0.25*delta_omega*delta_theta*S_a_trolley_distance_h_2_sum;
        %Motion of Trolley Angle-Twist
        S_m_trolley_angle_v_twist_sum= S_m_trolley_angle_v_twist(I,J) +
S_m_trolley_angle_v_twist(I-1,J) + S_m_trolley_angle_v_twist(I,J-1) +
S_m_trolley_angle_v_twist(I-1,J-1);
        S_m_trolley_angle_v_twist_i = S_m_trolley_angle_v_twist_i+
0.25*delta_omega*delta_theta*S_m_trolley_angle_v_twist_sum;
        %Motion of Trolley Angle Average
        S_m_trolley_angle_v_average_sum= S_m_trolley_angle_v_average(I,J) +
S_m_trolley_angle_v_average(I-1,J) + S_m_trolley_angle_v_average(I,J-1) +
S_m_trolley_angle_v_average(I-1,J-1);

```
        S_m_trolley_angle_v_average_i = S_m_trolley_angle_v_average_i+
0.25*delta_omega*delta_theta*S_m_trolley_angle_v_average_sum;
     end    % End of I Loop :
     end       % End of J Loop : % -----End Level 3b : Loop on Integral ----------------
     % -------------------------------------------------
     % CALCULATE the RMS values
     % -------------------------------------------------
     RMS_surge_CAPED(ibeta,iHS)   = sqrt(S_surge_CAPED_i);
     RMS_surge_RRDF(ibeta,iHS)    = sqrt(S_surge_RRDF_i);
     RMS_heave_CAPED(ibeta,iHS)   = sqrt(S_heave_CAPED_i);
     RMS_heave_RRDF(ibeta,iHS)    = sqrt(S_heave_RRDF_i);
     RMS_sway_CAPED(ibeta,iHS)    = sqrt(S_sway_CAPED_i);
     RMS_sway_RRDF(ibeta,iHS)     = sqrt(S_sway_RRDF_i);
     RMS_roll_CAPED(ibeta,iHS)    = sqrt(S_roll_CAPED_i);
     RMS_roll_RRDF(ibeta,iHS)     = sqrt(S_roll_RRDF_i);
     RMS_pitch_CAPED(ibeta,iHS)   = sqrt(S_pitch_CAPED_i);
     RMS_pitch_RRDF(ibeta,iHS)    = sqrt(S_pitch_RRDF_i);
     RMS_yaw_CAPED(ibeta,iHS)     = sqrt(S_yaw_CAPED_i);
     RMS_yaw_RRDF(ibeta,iHS)      = sqrt(S_yaw_RRDF_i);
     %Trolley Point 1
     RMS_m_t_CAPED_v_1(ibeta,iHS)  = sqrt(S_m_t_CAPED_v_1_i);
     RMS_m_t_CAPED_h_1(ibeta,iHS)  = sqrt(S_m_t_CAPED_h_1_i);
     RMS_v_t_CAPED_v_1(ibeta,iHS)  = sqrt(S_v_t_CAPED_v_1_i);
     RMS_v_t_CAPED_h_1(ibeta,iHS)  = sqrt(S_v_t_CAPED_h_1_i);
     RMS_a_t_CAPED_v_1(ibeta,iHS)  = sqrt(S_a_t_CAPED_v_1_i);
     RMS_a_t_CAPED_h_1(ibeta,iHS)  = sqrt(S_a_t_CAPED_h_1_i);
     RMS_m_t_RRDF_v_1(ibeta,iHS)   = sqrt(S_m_t_RRDF_v_1_i);
     RMS_m_t_RRDF_h_1(ibeta,iHS)   = sqrt(S_m_t_RRDF_h_1_i);
     RMS_v_t_RRDF_v_1(ibeta,iHS)   = sqrt(S_v_t_RRDF_v_1_i);
     RMS_v_t_RRDF_h_1(ibeta,iHS)   = sqrt(S_v_t_RRDF_h_1_i);
     RMS_a_t_RRDF_v_1(ibeta,iHS)   = sqrt(S_a_t_RRDF_v_1_i);
     RMS_a_t_RRDF_h_1(ibeta,iHS)   = sqrt(S_a_t_RRDF_h_1_i);
     RMS_m_trolley_angle_v_1(ibeta,iHS) = sqrt(S_m_trolley_angle_v_1_i);
     RMS_v_trolley_angle_v_1(ibeta,iHS) = sqrt(S_v_trolley_angle_v_1_i);
     RMS_a_trolley_angle_v_1(ibeta,iHS) = sqrt(S_a_trolley_angle_v_1_i);
     RMS_m_trolley_distance_h_1(ibeta,iHS) = sqrt(S_m_trolley_distance_h_1_i);
     RMS_v_trolley_distance_h_1(ibeta,iHS) = sqrt(S_v_trolley_distance_h_1_i);
     RMS_a_trolley_distance_h_1(ibeta,iHS) = sqrt(S_a_trolley_distance_h_1_i);
     %Trolley Point 2
     RMS_m_t_CAPED_v_2(ibeta,iHS)  = sqrt(S_m_t_CAPED_v_2_i);
     RMS_m_t_CAPED_h_2(ibeta,iHS)  = sqrt(S_m_t_CAPED_h_2_i);
     RMS_v_t_CAPED_v_2(ibeta,iHS)  = sqrt(S_v_t_CAPED_v_2_i);
     RMS_v_t_CAPED_h_2(ibeta,iHS)  = sqrt(S_v_t_CAPED_h_2_i);
     RMS_a_t_CAPED_v_2(ibeta,iHS)  = sqrt(S_a_t_CAPED_v_2_i);
     RMS_a_t_CAPED_h_2(ibeta,iHS)  = sqrt(S_a_t_CAPED_h_2_i);
     RMS_m_t_RRDF_v_2(ibeta,iHS)   = sqrt(S_m_t_RRDF_v_2_i);
     RMS_m_t_RRDF_h_2(ibeta,iHS)   = sqrt(S_m_t_RRDF_h_2_i);
     RMS_v_t_RRDF_v_2(ibeta,iHS)   = sqrt(S_v_t_RRDF_v_2_i);
     RMS_v_t_RRDF_h_2(ibeta,iHS)   = sqrt(S_v_t_RRDF_h_2_i);
     RMS_a_t_RRDF_v_2(ibeta,iHS)   = sqrt(S_a_t_RRDF_v_2_i);
     RMS_a_t_RRDF_h_2(ibeta,iHS)   = sqrt(S_a_t_RRDF_h_2_i);
     RMS_m_trolley_angle_v_2(ibeta,iHS) = sqrt(S_m_trolley_angle_v_2_i);
     RMS_v_trolley_angle_v_2(ibeta,iHS)    = sqrt(S_v_trolley_angle_v_2_i);
     RMS_a_trolley_angle_v_2(ibeta,iHS)    = sqrt(S_a_trolley_angle_v_2_i);
     RMS_m_trolley_distance_h_2(ibeta,iHS)  = sqrt(S_m_trolley_distance_h_2_i);
```

```
        RMS_v_trolley_distance_h_2(ibeta,iHS)     = sqrt(S_v_trolley_distance_h_2_i);
        RMS_a_trolley_distance_h_2(ibeta,iHS)     = sqrt(S_a_trolley_distance_h_2_i);
        RMS_m_trolley_angle_v_twist(ibeta,iHS)    = sqrt(S_m_trolley_angle_v_twist_i);
        RMS_m_trolley_angle_v_average(ibeta,iHS) = sqrt(S_m_trolley_angle_v_average_i);

    end % End of Level 2 : Main Wave direction Beta loop
end % End of Level 1 : of Significant Wave Ht(HS) Loop
% -------------------------------------------------------------------------
%   POLAR PLOTS
% -------------------------------------------------------------------------
theta=RMS_m_trolley_angle_v_average;
time=time_0*(sin(theta)+mu*cos(theta))/mu;
time_n=(sin(theta)+mu*cos(theta))/mu;
%


figure(1)
[th,r]=meshgrid((0:beta_incr:360)*pi/180,0.5:0.5:30);
[X,Y]=pol2cart(th,r);
h=polar(th,r);delete(h);
hold on
contour(X',Y',time),colorbar
title(['Transfer Time for Cosine^',int2str(i_cosine),' Spreading Function (mins)'])


%
%Transfer Rate Reduction Factor
figure(2)
[th,r]=meshgrid((0:beta_incr:360)*pi/180,0.5:0.5:30);
[X,Y]=pol2cart(th,r);
h=polar(th,r);delete(h);
hold on
c_p=[0:0.005:1.5];
contour(X',Y',time_n,c_p),colorbar
title(['Transfer Rate Reduction Factor Cosine^',int2str(i_cosine),' Spreading Function'])
%
%Average Vertical Trolley Angle
figure(3)
[th,r]=meshgrid((0:beta_incr:360)*pi/180,0.5:0.5:30);
[X,Y]=pol2cart(th,r);
h=polar(th,r);delete(h);
hold on
c_p=[0.0:0.1:2];
contour(X',Y',RMS_m_trolley_angle_v_average*180/pi,c_p),caxis([0 2]),colorbar
title(['Average Vertical Trolley Angle for Cosine^',int2str(i_cosine),' Spreading Function (deg)'])


%
figure(4)
[th,r]=meshgrid((0:beta_incr:360)*pi/180,0.5:0.5:30);
[X,Y]=pol2cart(th,r);
h=polar(th,r);delete(h);
hold on
c_p=[0.0:0.25:4];
contour(X',Y',RMS_m_trolley_angle_v_twist*180/pi,c_p),caxis([0 4]),colorbar
title(['Average Vertical Trolley Twist for Cosine^',int2str(i_cosine),' Spreading Function (deg)'])
```

THIS PAGE INTENTIONALLY LEFT BLANK

LIST OF REFERENCES

1. General C. C. Krulak U.S. Marine Corps, Commandant of the Marine Corps "Operational Maneuver From The Sea(OMFTS): A Concept for the Projection of Naval Power Ashore."

2. Higgins B. "Motion Analysis of a Trolley Interface for a Ship-to-Ship Cargo Transfer." Naval Postgraduate School. December 2002.

3. Holmes P. "Coastal Defense Systems I, Coastal Processes: Waves." Imperial College, England. July 2001

4. Constantine Memos. "Stochastic Description of Seaway." School of Civil Engineering, National Technical University of Athens.

5. HR Wallingford Limited. "FPSO Response in Long Crested and Short Crested Seas." Offshore Technology Report, 2002.

6. Ochi M.K. "Ocean Waves :A Stochastic Approach." Cambridge University Press, London. 1998.

7. Healey A.J and Reidel J.S. "Estimation of Directional Wave Spectra from an Autonomous Underwater Vehicle." Naval Postgraduate School, Center for AUV Research.

8. McCreight K.K. "A Note of Selection of Wave Spectra for Design Evaluation." Naval Surface Warfare Center, Carderock Division. January 1998.

6. Journée J.M.J. and Pinkster J. "Introduction In Ship Hydromechanics." Delft University of Technology. April 2002.

7. Beck R.F. and Reed A.M. "Modern Computational Methods for Ships in a Seaway." Twenty Third Symposium of Naval Hydrodynamics. August 2001

8. Naval Surface Warfare Center, Carderock Division. "Zero Speed Seakeeping Investigation of the New Roll-On/Roll-Off Discharge Facility (RRDF 2000) Aft of the CAPE H and CAPE D Sealift ships."

9. TECHET A. H. "Lecture Notes." www.mit.edu/afs/athena /course/13/13.42/spring01/handouts. 20 February 2003.

10. Glenn E.M. "Close-Proximity Vessel Towing In Six Degree-Of-Freedom Motions In Short Crested Seas." Naval Postgraduate School. September 2002.

INITIAL DISTRIBUTION LIST

1. Defense Technical Information Center
   Ft. Belvoir, VA

2. Dudley Knox Library
   Naval Postgraduate School
   Monterey, CA

3. Prof. Fotis Papoulias
   Mechanical Engineering Department
   Naval Postgraduate School
   Monterey, CA

4. Maj. Chong Keng Shin
   Republic of Singapore Navy
   Singapore